"I am the Lorax; I speak for the trees; I speak for the trees for the trees have no tongues; unless someone like you cares a whole awful lot, nothing is going to get better; it's not; it's not about what it is, it's about what it can become."— Dr. Seuss, The Lorax.

Promoters

       Prof. Dr. ir. Kathy Steppe

       Laboratory of Plant Ecology

       Faculty of Bioscience Engineering, Ghent University

       Prof. Dr. ir. Hans Verbeeck

       Computational and Applied Vegetation Ecology (CAVElab)

       Faculty of Bioscience Engineering, Ghent University

Local promoter in Uganda

       Prof. Dr. J.B.L. Okullo

       Department of Forestry, Biodiversity and Tourism

       College of Agriculture and Environmental sciences, Makerere University

Dean

       Prof. Dr. ir. Marc Van Meirvenne

Rector

       Prof. Dr. Anne De Paepe

Jackie EPILA

ECOPHYSIOLOGICAL ASSESSMENT
OF DROUGHT VULNERABILITY
OF THE AFRICAN TROPICAL TREE SPECIES
MAESOPSIS EMINII ENGL.

Dutch translation of the title: Ecofysiologische beoordeling van de vatbaarheid voor droogte van de Afrikaanse tropische boomsoort *Maesopsis eminii* Engl.

Acknowledgements

Beyond the formalities, I would like to extend my heartfelt gratitude to Kathy for throwing challenges my way that have helped panel beat me and allowed me to dream beyond the galaxies. Thank you also for pulling out all the stops hindering this doctorate achievement. Hans I am indebted to you for your uplifting words of encouragement and for always going ahead of me to straighten things out on my behalf. My co-workers past and present also played immense roles in moulding and shaping me. Bedankt Erik, Sruthi, Manfredo (ED2 guy), Marijn, Dr. S. Lewis, Dr. W. Hubau, Prof. C. Vanhove, Dr. B. Descamps, Stefan Vidts, Dr. I. Bauweraerts, Dr. L.L. Vergeynst, Dr. H. Beeckman, Thomas, Guy, Bart, Fran, Hans, Linus, Roberto, Dr. D. De Pauw, Kevin of the African Museum in Tervuren, Forest Department, Government of Uganda (1968) staff, the National Institute for Agronomy in Belgian Congo (INEAC) staff and the Uganda National Forestry Resources Research Institute staff. I am highly indebted to all of you in your respective stature. And of course not forgetting the "J's": Janne, Jens, Jonas, Jonas C., Jeroen and Jonathan. A lot of J's, thank you all not only having that special J bond with me but for being nice fellows.

There are also special individuals with whom I was more than blessed to have interacted with. Namely: Dr. E. Kearsley a.k.a Liz thanks a lot for being the encouraging and supportive friend you have been right from 2011 till now. Philip thanks for picking up my calls when I was stuck in Uganda and Belgium, and meticulously guiding me through what was required of me. Geert thanks for the times I was stuck you were always there to help even if it meant going out of your way to see to it that everything went smoothly on my part despite deterring your own program. Mama Ann, I always joke with my biological mum that I have a Belgian mom taking care of me in her absentia. Apwoyo tutwal (thank-you so much) for being my God sent beacon of hope. Pui Yi for always making me laugh and for just popping into the CAVE lab and saying hello, how are you doing? Those simple words touched me in ways you cannot fathom. My homeboy Hannes without your jokes and long talks gosh I would have collapsed from boredom and depression (jokes). Thanks especially for your help with R, the images were crappy but nevertheless, they did the job. When you are in Africa drop by Ug for a cup of chai and chapatti I will personally make them for you. Michiel the French guy who doesn't speak French, working with you has taught me that in life to cut the mustard you shouldn't judge a book by its cover nor dwell on crying over spilt milk. Michiel

*The more that you read,
the more things you will know. The
more that you learn, the more
places you'll go. Dr. Seuss.*

Gent December 22nd
2016

Jackie

Summary

Africa is endowed with the second largest block of nature-engineered machinery to sequester carbon: forests. Sadly, the functional traits and responses of this machinery are poorly understood, under non-drought, current drought and projected drought. Controversy surrounds the response of Africa's forest tree species to drought. Moreover, little is known on the mechanisms or strategies they evoke to cope with drought.

In this PhD study, the drought coping strategies and mechanisms of an African pioneer semi-deciduous tree species *Maesopsis eminii* Engl. (*M. eminii*) is investigated. A review of published and unpublished data provided insights in the species' associated functional traits, phenology and provenance. The species' occurrence niche was then characterized by combining this information and occurrence data of *M. eminii* in Africa with data on climate, soils and vegetation. It was found that *M. eminii* established itself in different ecosystems with diverse soil types and precipitation amounts. However, *M. eminii* mostly preferred the tropical rainforest region with fertile soils and annual precipitation exceeding 1000 mm yr^{-1}.

M. eminii's presence in areas with pronounced seasonal precipitation prompted ecophysiological studies under natural and greenhouse settings. The aim was to determine additional traits used by this species to cope with drought. Different from most other plants, *M. eminii* seedlings continued to grow for a few days after the onset of drought and were also found to have nocturnal sap flow, because of low transpirational control. On the one hand, this trait seemed useful during non-drought conditions, but accelerated dehydration during drought and the eventual death of the seedlings. Unexpectedly, fast growth of *M. eminii* was not linked to its photosynthetic rate, as this was rather low. Instead, autoradiographs indicated a leaf role partition with older leaves actively loading sugars into the phloem compared to the expected passive loading in younger ones. Regardless of the loading mechanism, severe drought halved *M. eminii*'s photosynthetic rate but increased relative leaf respiration compared to a non-drought situation. This might explain why its growth eventually declined after a few days into drought.

The hydraulic conduits of *M. eminii* were wide, which increased the likelihood of air-seeding and may make this species' xylem inherently vulnerable to drought-induced cavitation. But *M. eminii* was found to additionally have a considerable amount of water in its wood structure as evidenced by its low wood density, high volumetric water content and substantial hydraulic capacitance. This water probably contributed to the observed hydraulic redistribution between leaves, by which *M. eminii* could cope with drought for a couple of more days. During this hydraulic redistribution, a few leaves are shed while others remained hydrated, which reduced water loss but maintained limited carbon fixation. We also observed that *M. eminii* has low hydraulic conduits connection, which may limit the spread of drought-induced cavitation.

Summary

This research has revealed different novel mechanisms (i.e., nocturnal sap flow, active sugar loading into the phloem in adult leaves, and hydraulic redistribution in the leaves) that have substantially increased the knowledge on how *M. eminii* copes with drought. It also shows that more attention must be paid to understand how African trees and eventually forests will deal with drought, if we aspire to more accurately predict the impact of climate change on this terrestrial ecosystem.

Samenvatting

Afrika wordt geconfronteerd met toenemende droogte-events door het veranderende klimaat. Afrika heeft echter een belangrijke natuurlijke troef om koolstof op te slaan: bossen. Jammer genoeg is er nog altijd te weinig gekend over de functionele eigenschappen en responsen van deze bossen om in te kunnen schatten hoe zij met de voorspelde toenemende droogtestress zullen omgaan.

In dit doctoraat werden de strategieën en mechanismen onderzocht waarmee een Afrikaanse semi-bladverliezende pioniersoort, *Maesopsis eminii* Engl. (*M. eminii*) met droogte kan omgaan. Beschikbare gepubliceerde en niet-gepubliceerde gegevens leverden inzicht in de functionele eigenschappen, fenologie en herkomst van deze soort. De ecologische niche van voorkomen van de soort werd gedefinieerd aan de hand van deze informatie en verspreidingskaarten van *M. eminii* in combinatie met gegevens over klimaat, bodems en vegetatie. Hieruit bleek dat *M. eminii* voorkomt in een groot aantal ecosystemen met zeer uiteenlopend bodemtype en uiteenlopende jaarlijkse neerslag. Toch verkiest de soort tropische regenwouden met vruchtbare bodems en jaarlijkse neerslaghoeveelheden van meer dan 1000 mm per jaar.

De aanwezigheid van *M. eminii* in klimaten met een uitgesproken seizoenale neerslag lag aan de basis van ecofysiologische studies van zaailingen van deze soort, zowel in natuurlijke omstandigheden *in situ* als in serres. Het doel van deze studies was om te bepalen welke eigenschappen de plant gebruikt om met droogtestress om te gaan. Anders dan de meeste planten blijft *M. eminii* nog verschillende dagen groeien, zelfs nadat het vocht in de bodem sterk is gedaald. De plant vertoonde ook nachtelijke sapstroom, ten gevolge van een zwakke controle over transpiratieverliezen. Daardoor heeft de plant enkele voordelen wanneer er geen droogte heerst, maar anderzijds versnelt het de uitdroging van de bodem en leidde het uiteindelijk tot het afsterven van de planten. De snelle groei van de plant was niet veroorzaakt door de fotosynthesesnelheid, want deze lag aan de lage kant. Een andere verklaring voor de snelle groei ligt waarschijnlijk in de differentiatie van een specifieke bladfunctie. Zo toonden autoradiografie-beelden aan dat de bladeren naargelang de leeftijd een ander mechanisme van suikerlading vertoonden, waarbij oudere bladeren de suikers actief in het floëem laden vergeleken met jongere bladeren waar het laden passief gebeurde, zoals verwacht. Ongeacht het ladingsmechanisme, veroorzaakte ernstige droogte een halvering van *M. eminii*'s fotosynthesesnelheid, maar verhoogde de relatieve bladrespiratie vergeleken met een niet-stress situatie. Dit kan verklaren waarom groei uiteindelijk afnam na enkele droogtedagen.

De vaten van *M. eminii* waren groot, wat de kans op intrede van lucht normaal doet toenemen en dus het xyleem van deze boomsoort inherent vatbaar zou kunnen maken voor droogte-geïnduceerde cavitatie. Maar *M. eminii* bevatte ook een aanzienlijke hoeveelheid water in het hout wat bevestigd werd door de lage houtdensiteit, het hoge volumetrische watergehalte en de grote

hydraulische capaciteit. Dit water droeg waarschijnlijk bij tot de geobserveerde hydraulische redistributie tussen bladeren, waardoor *M. eminii* enkele dagen langer met droogte kon omgaan. Tijdens de hydraulische redistributie werd een deel van de bladeren afgeworpen, terwijl andere bladeren gehydrateerd bleven. Op die manier werd waterverlies tegengegaan, maar bleef er toch nog een beperkte fotosynthese plaatsvinden. We stelden ook vast dat *M. eminii* weinig connectie tussen vaten vertoonde, wat verspreiding van droogte-geïnduceerde cavitatie kan beperken.

Dit onderzoek heeft verschillende unieke mechanismen blootgelegd (nachtelijke sapstroom, actieve suikerlading in het floëem van volwassen bladeren en hydraulische redistributie tussen bladeren) waardoor onze kennis over hoe *M. eminii* met droogte omgaat sterk toegenomen is. Het toont ook aan dat meer onderzoek moet focussen op Afrikaanse soorten en hun waarschijnlijk unieke eigenschappen om met droogte om te gaan met het oog op accurate voorspellingen van de gevolgen van klimaatverandering voor de Afrikaanse bossen.

Table of contents

4 Capacitive water release and internal leaf water relocation delay drought-induced cavitation in African *Maesopsis eminii* ... 75

List of abbreviations and symbols

Abbreviations

AE	Acoustic emission
Cum AE	cumulative number of AE signals
ANOVA	Analysis of variance
C	Carbon
CCR	Cross correlation
CO_2	Carbon dioxide
DBH	Diameter at breast height
DM	Dry matter
DOY	Day of year
GIS	Geographical information system
H	Height
IPCC	Intergovernmental panel on climate change
KOH	Potassium hydroxide
LED	Light emitting diode
LVDT	Linear variable displacement transducer
MHz	Megahertz
NPKMg	Nitrogen, Phosphorous, Potassium and Magnesium
PAR	Photosynthetic active radiation (μmol m^{-2} s^{-1})
PEG	Polyethylene glycol
PET	Positron emission tomography
PLC	Percentage loss of hydraulic conductivity (%)
ppm CO_2	Parts per million of carbon dioxide
RH	Relative humidity (%)
RSFD	Relative sap flow dynamics (%)
SF	Sap flow (%)
SFD	Sap flow dynamics (-)
SWP	Soil water potential (MPa)
T	Air temperature (°C)
VC	Vulnerability curve
VPD	Vapour pressure deficit (kPa)
VPDB	Vienna Pee Dee Belemnite
VWC	Volumetric water content

List of symbols

g_s	Stomatal conductance (mmol m^{-2} s^{-1})
b	Conduit wall span (μm)
C	Hydraulic capacitance (kg m^{-3} MPa^{-1})
$C_{elastic}$	Hydraulic capacitance in the elastic phase (kg m^{-3} MPa^{-1})

$C_{inelastic}$	Hydraulic capacitance in the inelastic phase (kg m^{-3} MPa^{-1})
d_i	Initial diameter
dB	Decibel
E'_r	Apparent modulus of elasticity in the radial direction (MPa)
t	Conduit wall thickness (μm)
$(t/b)^2$	Conduit wall reinforcement (-)
V_G	Vessel grouping index (-)
V_S	Solitary vessel index (-)
W	Width
°C	Degrees centigrade
Ø	Diameter
ρ_b	Basic wood density (kg m^{-3})
Δd	Branch diameter shrinkage (μm)
$\Delta d/d_i$	Branch diameter strain (μm mm^{-1})
ψ_{xylem}	Xylem water potential (MPa)
ψ_{12}	Xylem water potential at 12% loss in hydraulic conductance (MPa) or the air entry point
ψ_{50}	Xylem water potential at 50 % loss in hydraulic conductance (MPa)
ψ_{88}	Xylem water potential at 88% loss in hydraulic conductance (MPa) or full embolism point
ψ_{100}	Xylem water potential at 100% loss in hydraulic conductance (MPa)
P_n	Net photosynthetic rate (μmol CO_2 m^{-2} s^{-1})
I_n	Light intensity (μmol PAR m^{-2} s^{-1})
α	Initial quantum efficiency (μmol CO_2/μmol PAR)
$P_{n,max}$	Maximum photosynthetic rate (μmol CO_2 m^{-2} s^{-1})
R_d	Dark respiration rate (μmol CO_2 m^{-2} s^{-1})
θ	Dimensionless or sharpness parameter
I_c	Light compensation point (μmol m^{-2} s^{-1})
L_s	Light saturation point (μmol m^{-2} s^{-1})
δ	P_n/P_{max}
$^{11}CO_2$	Gaseous carbon 11 isotope
$\delta^{13}C$	Carbon isotopic composition ($^{13}C/^{12}C$) (‰)
C_4	4-carbon molecule present in the first product of photosynthetic carbon fixation

Thesis introduction and outline

Africa's climate change

Climate change in Africa is a reality as shown by changing precipitation patterns and more frequent extreme weather events like floods, droughts and heat-waves (Shaw et al. 2009, Somorin 2010, Bishaw et al. 2013). Its non-homogeneity is predicted by climate models, indicating intensified dry seasons in the western Congo Basin, increased wetness for East Africa and severe water stress for Madagascar (James et al. 2013, Malhi et al. 2013a). Furthermore, these models agree that the African rainforest region will warm with a mean rate across models of 0.8-1.0°C per 1°C of global warming; hence, the realm is likely to warm by 3-4°C over this century under the most likely emissions scenario (Malhi et al. 2013a). This will result in an altered soil moisture profile (Figure 1). For Africa, the non-homogeneity is already in effect (Figure 2). Regardless of the climate change impact spectrum, national governments must make decisions now to mitigate or adapt (Box 1) to these impacts (GFEPAFCC 2009, Berry et al. 2014). The concluded (in 2012) Kyoto agreement and the recent Paris agreement (conference of parties (COP21, 2015) that has been ratified as of now by 113 parties of the 197 parties) were designed to mitigate climate change's effects. For Africa however, the existing mechanisms and resources under these agreements have all been directed at limiting future carbon emissions, rather than addressing the

---

Box 1

Adaptation is the adjustment in natural or human systems in response to actual or expected climatic stimuli or their effects, which moderates harm or exploits beneficial opportunities (GFEPAFCC 2009).

Mitigation is an anthropogenic intervention to reduce the sources or enhance the sinks of greenhouse gases (GHG) (Ravindranath 2007).

Vulnerability to climate change results from high exposure to climate impacts, low adaptive capacity or both. In the high exposure case, the opportunity cost, broadly defined, of expending resources to mitigate GHG emissions may be too high. In the case of low adaptive capacity, the factors responsible may also work to diminish mitigation capacity. And in the third case, both deleterious correlations could work to complement each other (Metz 2001).

Resilience has been popularly understood as the degree of elasticity in a system, its ability to rebound or bounce back after experiencing some stress or shock. It is indicated by the degree of flexibility and persistence of particular functions. Within the disaster risk community, resilience has been interpreted as the opposite of vulnerability (Pelling 2010).

region's vulnerability and lack of resilience (Box 1) to the impacts of climate change on its economies and populations (Shaw et al. 2009, Somorin 2010).
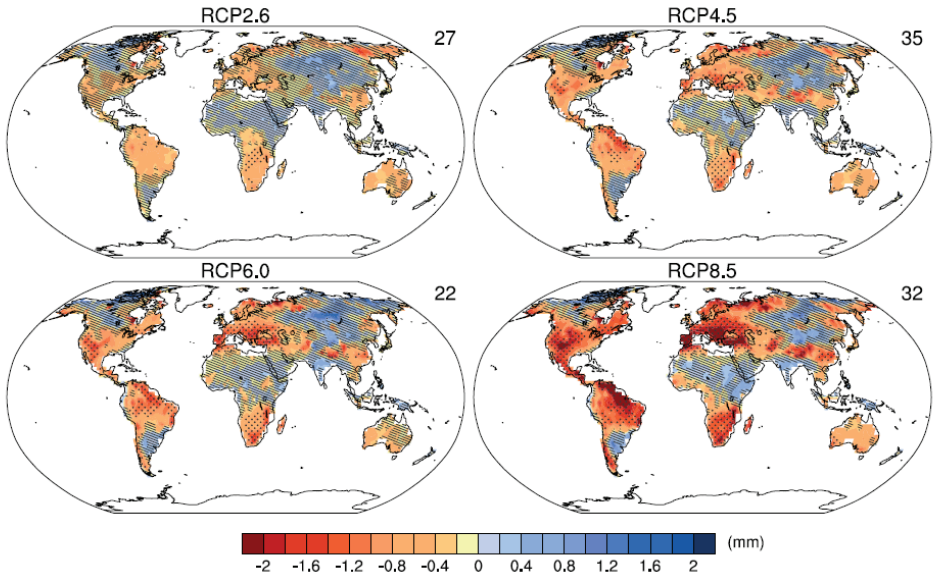
Figure 1 Change in annual mean soil moisture (mass of water in all phases in the uppermost 10 cm of the soil) (mm) relative to the reference period 1986–2005 projected for 2081–2100 from the Coupled Model Intercomparison Project Phase 5(CMIP5) ensemble. Hatching indicates regions where the multi-model mean change is less than one standard deviation of internal variability. Stippling indicates regions where the multi-model mean change is greater than two standard deviations of internal variability and where at least 90% of models agree on the sign of change. The number of CMIP5 models used is indicated in the upper right corner of each panel. RCPs imply Representative Concentration Pathways (IPCC report, Collins et al. 2013).

Figure 2 A shift in hydrological cycles as a result of climate change has resulted in a common regular occurrence of floods in some areas and droughts in other parts of Sub-Saharan Africa[1].

---

[1] www.redpepper.co.ug

Evidently, the eminent danger of climate change in Africa is obscured by the urgent needs for development to improve food security, reduce poverty and provide an adequate standard of living for the growing populations (Verchot et al. 2007). With agricultural land often being scarce, this leads to encroachment of crop farming on forests (Bishaw et al. 2013). The incidence of deforestation in Africa has however reduced. This is based on statistics from humid forests that show a declining rate (0.7 (1990) to 0.3 (2000) million ha yr^{-1}) (Achard et al. 2014). Additionally, Mayaux et al.'s (2013) statistics further show a declining trend from 0.28% yr[-1] (1990-2000) to 0.14% yr[-1] (2000-2010). Out of the various facets of climate change impacts, this PhD focuses on drought.

What is "drought"?

Considerable disagreement surrounds the concept of drought (Wilhite and Glantz 1985), and, hence, the six coined drought types (i.e., meteorological, climatological, atmospheric, agricultural, hydrologic, and water management), which evidently present a stumbling block for drought monitoring and analysis (Wilhite and Glantz 1985, McKee et al. 1993). Nonetheless, common to all types of drought is the fact that they originate from the deficiency of precipitation that result in water shortage for some functions (e.g., plant growth) or for some group (e.g., farmer) (Wilhite and Glantz 1985). Consequently, drought definitions are narrowed to either conceptual or operational (Wilhite and Glantz 1985). The conceptual definition is basically formulated in terms of identifying boundaries (e.g., "a long period with no precipitation") (Wilhite and Glantz 1985). Operational on the other hand attempts to identify the onset, severity and termination of drought episodes (e.g., "comparing daily precipitation values to evapotranspiration rates to determine the rate of soil moisture depletion, and express this relationships in terms of drought effects on plant behaviour at various stages of crop development") (Wilhite and Glantz 1985). Furthermore, operational definitions can be used to analyze drought frequency, severity, and duration for a given historical period as long as data on hourly, daily, monthly, or seasonal moisture deficiency or yield departures from "normal" (i.e., expected) exists for the purpose of identifying when drought occurred (Wilhite and Glantz 1985). Despite this broad overview, seldom are definitions transferable (Wilhite and Glantz 1985). In this PhD study, drought is considered as withholding the plants' water supply for a protracted period of time, and assessing the degree of stress the plants are undergoing during drought.

Why Africa's forest trees?

A simple and yet practical integrated adaptation and mitigation approach to address drought is to factor forests into the climate change response strategy equation, not only because they provide a host of ecosystem services such as support, provision, regulation and cultural services (Figure 3, Mayaux et al. 2013, GFEPAFCC 2009), but also because over two-thirds of Africa's 600 million people rely directly and indirectly on forests for livelihood and food security (Somorin 2010).

Figure 3 Left to right: Bwindi Impenetrable National Park, which is the home to ½ of the world's mountain Gorillas, dense rainforest and Batwa pygmies, beautifully displayed with low hanging clouds kissing the forest trees (source: Alamy). Trop of mountain Gorillas in Mgahinga Gorilla National Park (source: visituganda.com).

Forests have adapted to their local environments and evolved mechanisms to deal with hostile climatic conditions through a series of functional (Maharjan et al. 2011), phenological or biophysical traits, with interactions differing by region and social conditions (Parks and Bernier 2010). Functional response traits determine plant growth, survival and reproductive success, and as a result, they are expected to play an important role in shaping species' distribution patterns along environmental gradients (Maharjan et al. 2011). African forests have relatively low species richness compared to other tropical regions, but still host 4500-6000 tree species (Parmentier et al. 2007, Hardy et al. 2013, Slik et al. 2015). This functional diversity can be channeled as a tool to fight climate change in the sense that forests could address issues of adaptation, while their photosynthetic ability to sequester atmospheric CO_2 into biomass directly addresses mitigation of GHG emissions. Moreover, the use of indigenous tree species for planted forest is a pro-poor win-win solution if ground-rules are laid from project foundation. Use of locally sourced trees in plantations supposes less cost compared to if the seeds/seedlings are imported. This not only lowers the cost of producing planting materials, but invites transparent tree farming by involving people at community and grass root levels in the planning and execution of plantation projects (Shaw et al. 2009). Still, selection of the "right" species is cumbersome as there exist limited systematic regional studies of even the basic attributes of African forests such as biomass, species diversity and structure

compared to the American and Asian tropics (Malhi et al. 2013a). The cause of the lag in understanding Africa's forest biome is partly due to the current surge of interest in tropical forests research and policy attention being focused on the Amazon region, which is the world's largest tropical rainforest block, and to a lesser extent on Southeast Asia, which is the third largest (Malhi et al. 2013a). By contrast, the world's second largest tropical rainforest region in Central and West Africa (95% of African rainforests) with 30% global tropical rainforest cover (Malhi et al. 2013b) is relatively neglected (Malhi et al. 2013a). Other reasons are the local challenging and fragmented politics, civil conflicts, logistical and infrastructure challenges (Malhi et al. 2013a), insufficiently working meteorological stations or potential problems in reporting to international centres from different regions of Central and West Africa (Asefi-Najafabady and Saatchi 2013).

Drought-related studies on Africa's forests

Meta analyses from Anderegg et al. (2016) and Choat et al. (2012) indicate that very few drought-related studies have been performed in African forests. The study outcomes that do exist, are debatable. Asefi-Najafabady and Saatchi's (2013) satelite data indicates African forests as undisturbed by drought events, compared to the Amazon. Zhou et al. (2014) on the other hand paints a picture of large decrease in Congolese rainforest greenness as a result of short-term droughts, based on satelite observations over the past decade. Inventory studies mirror contrasting conclusions. Fauset et al. (2012) report increasing drought periods to favour deciduous, light-demanding species in Ghana. Ouédraogo et al. (2013) on the other hand find slow-growing, shade-tolerant species to be less sensitive to drought compared to fast-growing light-demanding species in M'Baïki, Central Africa's deciduous moist forest. Furthermore, the few available xylem-vulnerability to cavitation studies related to Africa (i.e., Tunisia, Madagascar and South Africa), based on the ψ_{50} values (Box 2), indicate that 92% of the studied African angiosperm species (exclusive of angiosperms: *Passerina obtusifolia* (ψ_{50}: -10.15 MPa; adult; South African woodland or shrubland (semi-arid; AI: 0.27)) and *Olea europaes* (ψ_{50}: -7.2 MPa; sapling; Tunisian

---

Box 2

Cavitation is an abrupt release of tension in the conduit lumen as liquid water at negative pressure is replaced by water vapour very near to vacuum pressure (Pockman et al. 1995).

ψ_{50} **value**, commonly known as the embolism resistance index, is the value extracted from the vulnerability curve (percentage loss of hydraulic conductivity (PLC, %) as a function of decreasing xylem pressure (ψ_x, MPa) at which 50% loss of hydraulic conductivity occurs below which the water transport function of the xylem is markedly impaired and the plant is exposed to considerable risk of accelerated embolism (Choat et al. 2012).

AI is the aridity index or the ratio of average annual precipitation to the potential evapotranspiration (Tsakiris and Vangelis 2005).

temperate seasonal forest (arid; AI: 0.17))) have vulnerable xylem (ψ_{50} < -4.29 MPa) when compared to species existent within Choat et al.'s (2012) global database. These skewed observations indicate that detailed ecophysiological studies are needed in Africa to understand species-specific drought responses. This PhD, focusing on a single tree species (*Maesopsis eminii* Engl.), demonstrates that indeed a complex array of technological marriages is required to answer the question: How does a tropical tree species respond to drought?

Why *Maesopsis eminii* Engl.?

African forests are more vulnerable to climate change compared to tropical forest in other continents because they sit close to a rainfall threshold that favours savannas over rainforest (Malhi et al. 2013a). The previous extensive contractions of rainforests in the Ice Age and the drier periods of the Holocene indicate that extensive climate-driven rainforest loss is clearly quite possible (Maley 1996, Malhi et al. 2013a). As such, it is fitting from socio-economic and environmental perspectives to not only identify forest trees that will cope under the drying scenario, but also understand mechanistically, physiologically and growth wise how they will cope (Sass-Klaassen et al. 2016). *Maesopsis eminii* Engl. that is a widely distributed tropical African tree species (Hall 1995, Orwa et al. 2009) belonging to the Rhamnaceae family (CABI 2016), which is known to include drought-tolerant species (Richardson et al. 2004), might be one such candidate. Comprehensive investigations using well-selected tree species growing under different environmental conditions foster a better understanding of projected large-scale forest response to changing climate (Sass-Klaassen et al. 2016). Furthermore, because the strength or frequency of external factors (e.g., extreme events) alone do not govern how a tree will respond, but because a tree's ability to tolerate and recover is equally relevant, intrinsic factors such as the tree's life stage, life history, and genetic characteristics need to be known (Sass-Klaassen et al. 2016). Inherently, *M. eminii* is part of a cosmopolitan family made up of trees, shrubs, climbers, and one herb consisting of *ca.* 50 genera and 900 species (Richardson et al. 2004). This family's current patterns in diversity and distribution (spanning both tropical and temperate regions) might be explained by migration and dispersal that occurred predominantly after the breakup of Gondwanaland (Richardson et al. 2004). The Rhamnaceae family's wide ecological amplitude however, makes it difficult to trace the family history (Raven and Axelrod 1974). Characteristically, this family has a tendency towards xeromorphism and prefers dry habitats (Richardson et al. 2004). Their effective seed dispersal brought about by a wide range of vectors (e.g., wind (Mori and Brown 1994) or birds (Hall 1995, Hampe and Bairlein 2000, Clark et al. 2004, Orwa et al. 2009)) justifies their wide distribution (Richardson et al. 2004).

Box 3

Drought avoidance for a plant is minimizing the impact of stress by spending the dry season in dormancy.

Delay is increasing water uptake and reducing water loss via high biomass investment in the roots, deep roots to enhance water uptake, early stomatal closure, low cuticular conductance, low transpiring leaf area, water storage in organs, osmotic adjustments and leaf shedding (Tyree et al. 2002, Tyree et al. 2003, Slot and Poorter 2007). Thick tap roots storing water is especially important in deciduous species as it permits evaporational water loss through the above-ground bark tissue, and maintains sufficiently high cell water content to maintain metabolic processes, and flush (Table 1) again at the onset of the rainy season (Poorter and Markesteijn 2008).

Physiological tolerance is the ability of a plant to physiologically be able to maintain plant functioning at low cell water content, including osmotic regulation, traits that permit continued water transport, gas exchange, or cell survival at low water content (w) and low water potentials (ψ), increased resistance of xylem to cavitation, the ability of cells (especially meristems) to remain alive at low w or ψ (Tyree et al. 2002, Tyree et al. 2003, Poorter and Markesteijn 2008).

For *M. eminii* to withstand xeric environments, it might be employing one of the three known strategies to cope with drought: drought avoidance, delay or physiological tolerance (Box 3; Tyree et al. 2003, Poorter and Markesteijn 2008). These mechanisms are assumed to be closely linked to the functional traits of a species (Poorter and Markesteijn 2008). To prove either, experimental assessments (Veenendaal et al. 1998, Engelbrecht et al. 2007) of *M. eminii*'s drought response are required. Further justification for the choice of *M. eminii*, aside from its multiple uses, availability, invasive nature, potential as reforestation or afforestation species, is its pioneer ecological strategy. This strategy makes it a particular suitable study system as pioneers usually respond rapidly in terms of growth and mortality to resource availability (Pearson et al. 2003b).

Why seedlings?

Soil water availability in the dry season, rather than in the wet season, is the likely driver for population dynamics and species distribution across moisture gradients in seasonal, un-inundated tropical forests (Comita and Engelbrecht 2009). This implies that the seedling stage might be the most important bottleneck for successful regeneration in dry areas, owed to their shallow root system that confers them naturally vulnerable to drought (Poorter and Markesteijn 2008). Comita and Engelbrecht's (2009) study findings from a semi-deciduous lowland moist forest in Panama's Barro Colorado Island substantiate the seedling-dry season theory. They found strong evidence indicating seasonal/temporal and spatial variation in soil water availability, particularly in dry years, as drivers for seedling dynamics and species distribution (Comita and Engelbrecht 2009). Therefore, in this PhD seedlings are used owed to the above

reasons, and due to the fact that they are easier to handle compared to adult trees especially when it comes to soil moisture manipulation experiments and most ecophysiological measurements.

Assessing a species' response to drought

Ecophysiological insights into a plant's strategies to cope with drought are undoubtedly the preferred way to assess and thus predict the consequences of climate change-induced drought on species performance (Slot and Poorter 2007, Poorter and Markesteijn 2008). However, to appreciate a species' drought response strategy, in addition to nullifying bias when interpreting a species' response to drought, generation of a species occurrence map is firstly required. Mapping gives one an idea of the geographic positioning of the species. Overlaying this distribution map on temperature, ecological and precipitation maps gives insights into a species' preferred ecological niche (De Frenne et al. 2013). Since the focus of this PhD is Africa, our boundaries for *M. eminii*'s occurrence or known cases of distribution are restricted to the said continent.

Secondly, sourcing published and unpublished rudimentary information on the species' functional traits provides an added advantage when it comes to species classification. Borchert (1994) proposed five groups of species classification based on plant information. Plant information includes structural traits (e.g., wood density, stem water storage capacity), phenology (e.g., deciduousness, flowering), plant-water relations (anisohydric (hydraulic failure) vs isohydric (carbon starvation); Figure 4), ecological strategy (e.g., light demanding pioneer), and timing of leaf flush.
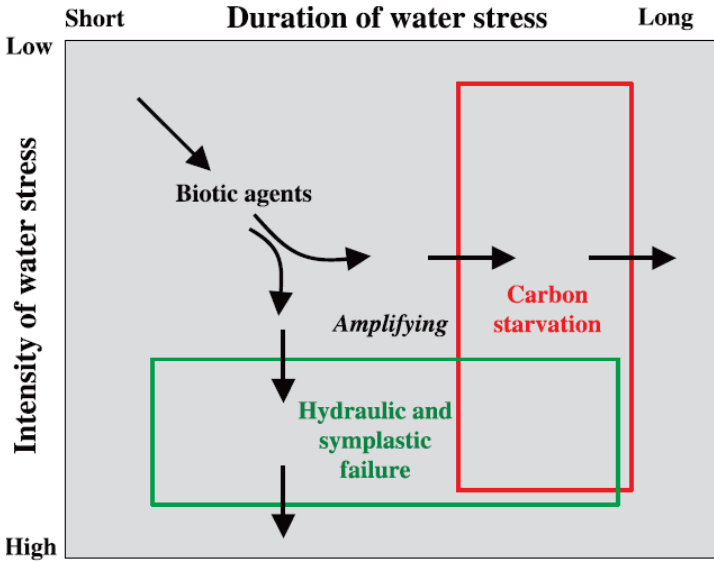
Figure 4 Theoretical relationship, based on the hydraulic framework, between the temporal length of drought (duration), the relative decrease in soil water availability (intensity), and the three hypothesized mechanisms (carbon starvation, hydraulic failure and biotic agents) underlying mortality (McDowell et al. 2008).

The five specified groups entail: (i) deciduous hardwood trees that desiccate strongly and remain bare to the end of the dry season (D_{hard}), (ii) deciduous light wood trees with low wood density and high stem water storage (D_{light}), (iii) deciduous softwood trees that rehydrate and flower after leaf shedding during drought (D_{soft}), (iv) evergreen softwood trees that exchange coriaceous leaves and flower during the dry season (EV_{soft}), and (v) evergreen water-storing lightwood trees (EV_{light}) (Borchert 1994). Based on the identified species group, ecophysiological assessments can then be used to validate hypothetic plant responses by linking the concept, mechanisms and drought (Table 1).

Table 1 Summary of phenology, morphology and plant processes used for plant drought stress assessment, related terminology and measurement methodologies used throughout this PhD.

Phenology, morphology and plant processes	Linked terminologies	Measurement methodologies used in this PhD
Phenology and morphological adaptations	**Evergreen** species retain a full canopy all year, and the decline in canopy fullness in the dry season is less than 10% (Eamus 1999). Leaves are costly produced but guarantee carbon fixation throughout the life of the leaf as opposed to deciduous leaves with relatively higher photosynthetic rates (Eamus 1999). **Deciduous** species lose all their leaves for at least one but usually two to four months of each year (Eamus 1999). This trait is linked to drought avoidance (Borchert 1994). During leafless periods cambial activity is usually dormant (Rao and Rajput 1999). **Semi-deciduous** species lose at least 50% of their leaves every year (Eamus 1999). **Leaf flushing** is the emergence and subsequent expansion of leaves from leaf buds. It occurs before the start of the wet season in Africa, Central America, India, Australia and Costa Rica (Eamus 1999). **Parahelionasty:** turgor loss of the petiole causing the leaf to position itself parallel to the incoming solar radiation. **Leaf shedding** is akin to **deciduous** species. **Rooting system: Tap roots** are observed to store substantial amount of water and aid in tapping deep seated water (Van den Bilcke et al. 2013). **Lateral roots** on the other hand are surface based, thus trap top soil water and form networking mats (Taylor 1989).	Phenology and morphology changes noted through leaf count and use of the naked eye or binoculars (Borchert 1994).
Plant growth and water use	**Absolute stem growth** is the maximum stem diameter of each day. **Sap flow** is root-extracted water that is conducted through the xylem and lost through the stomatal pores in a process known as transpiration. **Nocturnal sap flow** is sap conducted at night. **Stomatal conductance** estimates the rate of gas exchange (i.e., carbon dioxide uptake or photosynthesis and transpiration) through the leaf stomata as determined by the degree of stomatal aperture. It is therefore the physical resistance to the movement of gases between the air and the interior of the leaf. Hence, it is a function of the density, size and degree of opening of the stomata, with more open stomata allowing greater conductance, and consequently indicating that photosynthesis and transpiration rates are potentially higher (Pietragalla and Pask 2012). **Hysteresis loops** are caused by time shifts between diurnal patterns of radiation, vapour pressure deficit, temperature, stomatal conductance, transpiration and sap flow. Analysis of these patterns gives a better insight into the interactions between climate and the diurnal patterns of water flow in the tree (Saugier et al. 1997). **Isohydric** species control their stomatal conductance so that day-time leaf water potential values are unaffected by soil water deficits. They are thus more prone to carbon starvation (Lambers et al. 1998, McDowell et al. 2008). **Anisohydric** species usually succumb to hydraulic failure since both their leaf water potential and stomatal conductance (g_s) values decline with decreasing soil water potential hence encouraging	Growth parameters can be extracted from linear variable displacement transducers (LVDT) and dendrometers outputs (Steppe et al. 2006, De Swaef et al. 2015, Steppe et al. 2015). Sap flow values are mathematically extracted from sap flow sensor output (Steppe et al. 2010, Vandegehuchte & Steppe 2013). An AP4 porometer can be used to measure stomatal conductance (Bragg et al. 1991). Hysteresis can be determined by plotting transpiration, sap flow or stomatal conductance as a function of the vapour pressure deficit (VPD) (Saugier et al. 1997).

	continued sap loss (Lambers et al. 1998, McDowell et al. 2008). **Carbon starvation** occurs when drought duration is long enough to curtail photosynthesis longer than the equivalent storage of carbon reserves for maintenance of metabolism (McDowell et al. 2008). **Hydraulic failure** occurs if drought intensity is sufficient to push a plant past its threshold for irreversible desiccation before carbon starvation occurs. Biotic agents such as insects and pathogens can amplify or be amplified by **carbon starvation** or **hydraulic failure** (McDowell et al. 2008).	
Photosynthesis	**Photosynthesis** is a highly regulated, multistep process. It encompasses the harvest of solar energy, transfer of excitation energy, energy conversion, electron transfer from water to $NADP^+$, ATP generation and a series of enzymatic reactions that assimilate carbon dioxide and synthesize carbohydrate (Tanaka and Makino 2009). **Dark respiration rate (R_d)** is the rate of CO_2 evolution from the leaf in the dark (Lambers et al. 1998). **Light compensation point (I_c)** is achieved when the rate of CO_2 evolution is balanced by the uptake of CO_2 (Lambers et al. 1998). **Quantum efficiency (α)** is the slope of the light response curve and is the measure of CO_2 taken up per increase in light intensity (Lambers et al. 1998). **Light saturation point (L_s)** is the light intensity level above which net photosynthesis does not increase (Lambers et al. 1998). **Maximum photosynthetic rate (P_{max})** is the highest photosynthetic rate achieved by the plant (Lambers et al. 1998).	Photosynthesis measurements are done to gauge the carbon fixation rate of a plant and is usually determined using a gas exchange system. In this PhD, the LiCOR-6400 was used. Measuring per given light intensity the photosynthetic rate can generate light response curves. Use of the hyperbola model permits prediction of R_d, I_c, α and L_s.
Plant hydraulic functioning	**Cavitation (Box 2)** is a phenomenon that results in the rupture of the continuous water column in the xylem, which may lead to the introduction of **air bubbles** or **emboli** (Tyree and Sperry 1989). Cavitation is usually instigated by the interconduit pit of air seeding size (Zimmermann 1983), but this theory was recently updated by Schenk et al. (2015), who emphasized the formation of nano-bubbles prior to cavitation to account for the stability of gas bubbles under negative pressure. **Vulnerability curve (Box 2)** is a plot of percentage loss of hydraulic conductivity against the decreasing xylem water potential. From this plot the universal index (ψ_{50}) is obtained and is used to classify species vulnerability to drought-induced cavitation. A more negative value implies less vulnerable (Pammenter and Van der Willigen 1998, Meinzer et al. 2009, Choat et al. 2012). **Hydraulic capacitance (C)** is the ratio of change in tissue volumetric water content to change in xylem water potential (Vergeynst et al. 2015), or it's the amount of water released from the tissue per unit decrease in water potential (Edwards and Jarvis 1982, Steppe and Lemeur 2007) **Vessel elements and tracheids** when combined form the hydraulic conduit and play a crucial role in the transport of water from roots to leaves (Anfodillo et al. 2006, Scholz et al. 2013).	Several techniques exist to develop vulnerability curves, but the acoustic technique (Vergeynst et al. 2015) was preferred in this PhD. Gravimetric water loss was followed to determine C (Vergeynst et al. 2015).

Outline of the thesis and objectives

The overall aim of this PhD research was to perform an ecophysiological assessment of the drought vulnerability of *M. eminii* and to discern the morphological, phenological and physiological functional traits used by *M. eminii* to cope with drought and to use those traits to discuss its strategies. Seedlings were chosen as their response to drought is pivotal for species' extinction or survival.

Four main research topics were generated for this PhD dissertation:

1. Characterize *Maesopsis eminii*'s ecology and distribution in tropical Africa without distinguishing between invasive and native populations. This entailed the general synthesis of published and unpublished datasets of this species, and specifically the use of unpublished empirical data from a historical provenance trial in Uganda and a phenological study from the forest population of Yangambi, Democratic Republic of Congo (DR Congo) to functionally describe *M. eminii*. Finally, its functional description was linked with its occurrence data from multiple databases and the according environmental conditions, including climate and soil.

2. Deduce *M. eminii* drought-coping mechanisms by conducting a 4 month long ecophysiological study on seedlings in Uganda under non-atmospherically controlled conditions, following their diel sap flow, stomatal conductance and stem diameter variation patterns under three different drought treatments.

3. Assess the impact of drought on *M. eminii*'s leaf carbon balance by performing combined measurements of net photosynthesis, ^{11}C-labelling and ^{13}C stable isotope analyses on leaves of 3-year-old potted seedlings.

4. Quantify the vulnerability to drought-induced cavitation and the hydraulic capacitance of *M. eminii* seedlings using cumulative acoustic emissions and continuous weight measurements. Wood anatomical traits, including wood density, vessel area, diameter and wall thickness, vessel grouping index, solitary vessel index and conduit wall reinforcement are used to justify the observed physiological responses.

Chapter breakdown

This PhD thesis entails five main chapters exclusive of the thesis introduction: four research chapters (**Chapters 1-4**) and the general conclusion and future perspectives (**Chapter 5**). **Chapter 1** addresses the ecology and distribution of *Maesopsis eminii* in tropical Africa. This chapter highlights the functional traits and phenology of *M. eminii* that explain its wide distribution in different tropical African countries, soils, precipitation regimes and forest ecosystems. **Chapter 1**

established that water supply becomes crucial for *M. eminii* in places with strongly seasonal precipitation regimes including specific regions in Angola, Cameroon, DR Congo, Ghana, Tanzania and Uganda. The most pertinent question then was how *M. eminii* copes with the characteristic marginal soil moisture due to dry conditions which may last for up to 5-6 months. This question was addressed by investigating the physiological/morphological responses of soil-drought stressed *M. eminii* seedlings in Uganda (**Chapter 2**). The findings from **Chapter 2** indicated that *M. eminii* seedlings not only employed common plant delay (Poorter and Markesteijn 2008) and tolerance (Tyree et al. 2003) mechanisms (e.g. leaf shedding, stomatal control and leaf parahelionasty), but that they conducted nocturnal sap flow. Further investigation of its vulnerability to drought was split in two: (1) *M. eminii*'s leaf carbon relations (**Chapter 3**) and (2) *M. eminii*'s xylem vulnerability to drought-induced cavitation (**Chapter 4**). Fast growing pioneer species are usually characterised by high photosynthetic rates. We tested this hypothesis by conducting a combined leaf photosynthesis, ^{11}C radioactive isotope and ^{13}C stable isotope measurement campaign on *M. eminii* seedlings (**Chapter 3**). *M. eminii* not only had low photosynthetic rates compared to common tropical pioneers but autoradiographs showed that *M. eminii*'s adult leaves use active loading to transport carbon compared to the expected passive loading in juvenile leaves (**Chapter 3**). This interesting observation was used to explain its fast growth. Using a combination of techniques highlighted in objective 4 above portrayed *M. eminii* to rely on cavitation water and sap redistribution between leaves to cope with drought (**Chapter 4**). Totaling all the study findings during this PhD (**Chapter 5**), an *M. eminii* drought vulnerability characterization was made based on comparison with other tree species.

1 Ecology of *Maesopsis eminii* Engl. in tropical Africa

1.1 Abstract

Maesopsis eminii is referred to as one of the most widely distributed African tree species. However, its occurrence in Africa has never been mapped and little is known as to how this species can sustain in different environments. To get an insight into *M. eminii'*s ecology, we (i) made a synthesis of its functional trait data from literature, (ii) investigated phenological patterns using data on four *M. eminii* trees from Yangambi, Democratic Republic of Congo, (iii) assessed an empirical provenance trial from Uganda on 600 *M. eminii* trees, and (iv) synthesized geo-referenced point location maps of available occurrences of African *M. eminii*, entailing WorldClim precipitation and temperature, and FAO soils and ecological zones for Africa. We found *M. eminii* to straddle the equator equidistantly in terms of latitude (10.97N and 10.98S) covering five forest types where 20 soil types and variable rainfall regimes support complex plant biodiversity. *M. eminii* is however largely concentrated in the tropical rainforest ecosystem which contains fertile orthic ferralsol soils (26 % of the occurrences). More than 97 % of the point locations were found where annual precipitation was greater than 1000 mm, and 82 % of the occurrences were within an average annual temperature range of 22-28 °C. *M. eminii*'s functional traits and phenology further explained its occurrence in Africa. These traits include: (i) all year round seed production, (ii) conspicuous fleshy fruits encouraging easy seed dispersal, (iii) assumed high stem water storage, (iv) presence of different types of parenchyma cells within its wood, (v) fast growth, (vi) a rooting system that taps both surface and deep lying soil substrates, and (vii) drought avoidance through deciduous leaf loss.

1.2 Introduction

Maesopsis eminii Engl. (Figure 1.1) is an angiosperm that belongs to the Rhamnaceae family, which includes many extremely drought-tolerant species. *Maesopsis* is considered to be a complex of four subspecies: *berchemioides, eminii, stuhlmannii* and *tessmannii* native to tropical Africa (Hall 1995, CABI 2016, www.theplantlist.org). The subspecies *berchemioides* occurs from Sierra Leone to Congo Republic, while from DR Congo through Central African Republic further east and south to Angola and Zambia the subspecies *eminii* dominates (Hall 1995). Little is known about the specific distribution of subspecies *stuhlmannii* and *tessmannii*. The subspecies *tessmannii* is even indicated as a 'doubtful' species in the GBIF database (www.gbif.org). We will therefore not focus on the individual subspecies. At the species level, *M. eminii* is typically regarded as a Guineo-Congolian species (Hall 1995).

Figure 1.1 From top to bottom and left to right*: M. eminii* tree growing a forest in Sungai Buloh, Selangor, Malaysia © Ahmad Fuad Morad. Illustration of *M. eminii*'s tap and lateral rooting system and its leaves of seedlings of *M. eminii* thriving at ILVO (14th October 2014) © Jackie Epila. *M. eminii*'s immature (yellow) and mature (black) fruits as captured by Henry J. Ndangalasi.

Naturally, it grows in rainforests, riverine forests (Schabel and Latiff 1997), mixed swamp forests (Eggeling 1947, Jenkin et al. 1977), shrub dominated transition zones that separate forests from grasslands (Hall 1995), between high forests and savannah (Orwa et al. 2009), and lowland and submontane forests (Binggeli and Hamilton 1993; Dawson et al. 2011). In its natural occurrence, *M. eminii* has been characterized as a sub-climax forest species (Eggeling 1947, Hall 1995), being a long-lived pioneer species that can live for more than 150 years (Binggeli and Hamilton 1993). It tolerates drought for up to 2-6 months (Hall 1995, Jøker 2000, Ani and Aminah 2006). Commenting on soil type, Orwa et al. (2009) said that *M. eminii* tolerates a wide range of site conditions but grows best on deep, moist and fertile sandy loam soils with a neutral to acid pH. *M. eminii* is however quite susceptible to attacks by species of butterflies of the Lepidoptera order: *Hesperiidea* (e.g. *Eagris decastigma*) and *Nymphalidae* (e.g. *Charaxes achaemenes* and *Charaxes lactetinctus*) (Ferrer-Paris et al. 2014), beetles (*Monohammus scabiosus*), fungi (*Fusarium solani*, *Volutella* spp.), browsing animals (Orwa et al. 2009) such as elephants (Eggeling 1947), termites (Isoptera) (Eggeling 1947, Orwa et al. 2009) and spider mites (personal observation).

M. eminii provides excellent timber and crop shade services, and is often grown for these purposes (Engler 1906, Eggeling 1947, Struhsaker 1987, Binggeli and Hamilton 1993, Plumptre 1996, Owiunji and Plumptre 1998, Jøker 2000, Ani and Aminah 2006, Orwa et al. 2009, Buchholz et al. 2010a, Hall 2010). It has been reported to grow well on a range of altitudes and topographical ranges. Even though naturally it does not occur on steep slopes, when planted on such terrain it grows well (Eggeling 1947, Binggeli and Hamilton 1993, Hall 1995, Jøker 2000). Human introduction of *M. eminii*, e.g. in East Africa during the early 20th century for reforestation purposes (Binggeli et al. 1989, Hall 1995, Bosu et al. 2009), has brought *M. eminii* outside of its natural range. *M. eminii* has also been reported as a human-introduced species outside of Africa, namely in Australia, Philippines, Bangladesh, Brazil, Costa Rica, Fiji, India, Malaysia, Samoa, Solomon Islands, Hawaii, Puerto Rico and Indonesia (Buchholz et al. 2010a, Hall 2010, Slik et al. 2015, CABI 2016). Nevertheless, in this PhD we focus on the African continent. Through introduction of *M. eminii* in new regions within Africa, literature reports that it has become invasive in several areas: in disturbed forests (Binggeli and Hamilton 1993, Hall 1995, Bosu et al. 2009, Cordeiro et al. 2004, Dawson et al. 2011, 2015) with large gaps and with a high litter turnover rate (Hall 1995), and in areas where climate has shifted e.g. the case of the East Usambara, Tanzania where climate change has cause the vegetation composition of submontane forests to shift to a more lowland type (Binggeli and Hamilton 1993). Humair et al. (2014) defines such non-native invaders as species that spread spontaneously and rapidly, exerting negative impact on native species, ecosystem processes, the economy, or human health. Indeed, *M. eminii* in the East Usambara forest possesses these characteristics (see Binggeli and Hamilton 1993, Hall 1995). *M. eminii* has been recorded as invasive in East Africa e.g. Tanzania and Rwanda since the late 1970s (Binggeli 1989, Binggeli and Hamilton 1993, Bosu et al. 2009, CABI 2016).

Hall (1995), Orwa et al. (2009) and others state that *M. eminii* is one of the most widespread tree species in Africa's tropical forests. However, they do not provide a spatially explicit description of its distribution over Africa. This is what this PhD chapter attempt to address. We have in our study not considered the natural and introduced *M. eminii* populations separately, but rather have sought to understand its general ecology through a functional description of this species by synthesizing published and unpublished datasets. Next to literature, we specifically used unpublished empirical data from a historical provenance trial in Uganda and a phenological study from the forest population of Yangambi, Democratic Republic of Congo (DR Congo). Lastly, we link the functional description with occurrence data from multiple databases and the according environmental conditions (i.e. climate and soil). The main objective of this analysis is to increase our insight into the ecology and specifically the spatial distribution of *M. eminii* over the African continent.

1.3 Materials and Methods

1.3.1 Datasets used

Maesopsis eminii's functional traits and trait attributes were synthesized from reviewed published and unpublished data on the species. Unpublished data on its (1) phenology were extracted from a legacy dataset of the National Institute for Agronomy in Belgian Congo (INEAC) (1939-1956) in the DR Congo, and (2) provenance trials in Uganda (1964-1976) were obtained from the archives of the Forest Department, Government of Uganda (1968). Geo-referenced occurrence points (i.e., natural and introduced populations as distinction is not possible due to a lack of specification in the used data) of the species *M. eminii* were obtained from previous studies and data portals (www.gbif.org, www.afritron.org). Details of the sourced *M. eminii* occurrence data are presented in Table A1.1 (Appendix). Map sheets of Africa's long-term current (1960-1990) annual mean temperature and precipitation data of spatial resolution 30 arc-minutes were obtained from the www.worldclim.org (version 1.4) data portal or Hijmans et al. (2005) on the 28th of November 2016. Map sheets of Africa's dominant FAO soil types (FAO-UNESCO, 1971-81) and ecological zones were obtained from http://www.fao.org/geonetwork/srv/en/main.home on the 6th of April 2015.

1.3.2 Phenology of *M. eminii*

Scientists of the INEAC conducted a phenological study between 1938 and 1957 on more than 2000 individual trees of over 500 species (including eight individuals of *M. eminii*) in the rainforest reserve of Yangambi, DR Congo. The Yangambi reserve covers an area of 6297 km and is located just north above the Congo River about 100 km west of Kisangani, DR Congo. The region has an Af-type tropical rainforest climate and receives up to 1762 ± 295 mm of precipitation per year. Temperatures are high and constant throughout the year with a minimum of 24.4 ± 0.4 °C in July and a maximum of 25.5 ± 0.6°C in March. Soils on the Yangambi plateau are ferralsols. Vegetation in the

reserve is characterized by moist semideciduous rainforest, with fragments of moist evergreen rainforest, transition forest, agricultural land, fallow land and swamp forest (Kearsley et al. 2013). From this historical phenological study, annual patterns of fruit/seed dispersal, leaf shedding/defoliation, fruiting and flowering of eight *M. eminii* trees were scored as present (1) or absent (0) as in Couralet et al. (2013). Data collection occurred every 10 days. Information on how phenological stages were determined or how observations of crowns were made is not available in the INEAC archives, but the sampling must have been random e.g. species composition in Luki rainforest reserve has not changed (Couralet et al. 2013). For our study, four *M. eminii* trees were selected based on the fact that they were simultaneously and continuously followed for 9 years. Averages and standard deviations of the observed phenology frequencies were determined. This phenological data was also linked with climatological data from the same period (1948-1956) retrieved from the local meteorological station at Yangambi, in that period also operated by INEAC. The frequency of phenological observation for the complete 9 years for the four trees and the precipitation received for those years is plotted in Figure A1.1 (Appendix). Details for all eight *M. eminii* trees followed in Yangambi is shown Table A1.2 (Appendix).

1.3.3   Provenance trials

We synthesized unpublished data from a historical provenance trial that was conducted between 1964 and 1976 in Kibale rainforest, Uganda (located at 1280-1494 m a.s.l.; soils: Humic Nitosols and annual rainfall of 1346-1524 mm per annum) to assess the potential of using the species *M. eminii* for forest restoration. Trial seeds were sourced from two different locations in Uganda: Kalinzu (located at 1463 m a.s.l with annual rainfall of 795-1124 mm and containing Mollic andosols soil), and Busiro (located at 1158 m a.s.l with annual rainfall of 1124-1499 mm and containing Orthic ferralsols soil). The Kibale rainforest reserve is respectively ~236 km from Busiro, and ~116 km from Kalinzu. The distance between Busiro and Kalinzu is ~289 km. Seeds were sown in pots after which their seedlings were planted in 1965 in 0.1 acre plots replicated 12 times in randomized blocks. Each plot contained 25 trees planted at 20x20 m link spacing giving a total of 600 experimental trees. Throughout the study period annual assessments for survival, height and diameter at breast height (dbh) were made. Yearly means and standard deviations for the provenances were calculated.

1.3.4   Maps

Data of literature extracted 208 geo-referenced *M. eminii* occurrence point locations (coordinate reference system (CRS): WGS 1984 ellipsoid; Table 1.1A in Appendix), and Africa's precipitation, temperature, and soils and ecological zones (coordinate reference systems: WGS 1984 ellipsoid; in vector data model format) were used to study *M. eminii*'s ecological niche through mapping. Thematic maps for *M. eminii*'s preferred precipitation and temperature regime were generated through overlaying mapped geo-referenced *M. eminii* occurrence point locations with

Hijmans et al.'s (2005) (WorldClim) precipitation and temperature data (map sheets). Prior to the overlay, we set our study area extent to all land comprised between 20 °W (Atlantic Ocean) and 50° E (Indian Ocean), and 20°N (Sahara desert) and 20°S (Kalahari desert). Information extracted from the overlay using RStudio was used to generate a plot of *M. eminii*'s preferred precipitation as a function of temperature. This allowed the estimation of its ecological niche (De Frenne et al. 2013). To get an idea of soil exploited by *M. eminii* and in which forest ecosystem it thrives, *M. eminii*'s presence map (CRS: WGS84) was also overlaid on FAO's soils and ecological zones (CRS: WGS84) map sheets. This was done using Arc-GIS 10.3 software (ESRI, Redlands, Ca, USA). The intersect function of Arc-GIS 10.3 was used to determine in which soils and ecosystems *M. eminii* occurred.

1.4   Results

1.4.1   Functional traits

Based on our literature review on the functional traits of *M. eminii* (summarized in Table 1.1), we can state that it is a fast growing and light demanding pioneer tree species. Depending on the growth conditions and the geographical area, *M. eminii* can grow to various heights (up to 40 m) and has wood that is on average of low density (0.56 ± 0.27 g cm^{-3}). After an age of 10 years or less, *M. eminii* trees produce conspicuous flowers to attract insect pollinators which result into production of fleshy fruits. When these fruits ripen, based on observations from the East Usambaras in Tanzania, they attract arboreal animal dispersers (birds and mammals) that disperse the seeds to strategic niches to begin the cycle of tree life. The rapidly dispersed seeds have various useful attributes (Table 1.1). Furthermore, *M. eminii* that is known to be naturally semi-deciduous turns drought-deciduous under severe drought conditions (Eggeling 1947). *M. eminii* possesses a tap root combined with lateral roots allowing both horizontal and vertical resource uptake.

Table 1.1 Reviewed functional traits for the African tree species *Maesopsis eminii*

Functional traits	Trait attributes
Reproductive traits	
Flower colour	yellowish-green[1]
Flowering age	4-6 years (plantation); 10 years (natural regeneration)[1,2,3]
Reproductive mode	hermaphrodite and protogynous[1]
Pollination	Insects[1]
Fruit colour	purplish-black (mature)[1,4,5,6]
	green to yellow (immature)[1,4,5,6]
Fruit type	soft fleshy exocarp[1,3,4,5,6]
Fruit length (cm)	2-3[3]
Fruit ripening	2-4 months after flowering[7,16]
Seed dispersal	birds (*Tauraco fischeri*), hornbills (*Bycanistes bucinator, B. brevis, Ceratogymna brevis), fruit* bats (*Eidolon helvum),* blue monkey (*Cercopithecus mitis)* and chimpanzees[3, 22]
Seed traits	
Seed setting	1-2 seeds per endocarp[1,5,6]
Seed length (mm)	20-35[1,5,6]
Seed width (mm)	10-18[1,5,6]
Seed viability (%)	40-60[1,5,6]
Seed dormancy (days)	90-200[1,5,6]
Seed germination (days)	30[20] (seeds contained in a sisal bag were soaked in a basin of water at room temperature until roots broke through the seed wall, they were then immediately sown in pots in the greenhouse where eventually the first pair of leaves emerged)
Seed colour	Black[1]
Photosynthetic traits	
Leaf aging	Semi-deciduous (deciduous during serve drought)[4]
Leaf display	dorsiventral, hypostomatic and dentate simple alternate[1,9]
Leaf blade (cm)	6-15 x 2-5 (elliptic-lanceolate)[1]
Leaf sizes (cm^2)	small (2.25-20.25) and medium (20.25-182.25)[4,10]
Leaf stomata distribution	Irregular shaped stomata[9], *usually surrounded by four or more subsidiaries, variable in position, shape and size*[21].
Leaf carbon storage (%)	42.0±0.8[8]
Leaf dry matter (%)	35[1]
Wood traits	
Branch apparent modulus of elasticity (MPa)	15[8]
Wood density (g cm^{-3})	0.37-0.75[1,11,19]
Wood anatomy	Growth rings indistinct or absent, wood is diffuse porous, intervessel pits alternate and are of medium size: 7-10µm, mean tangential diameter of vessel of vessel lumina is >=200 µm, less than 5 vessels per square mm, mean vessel element length: 350-800 µm, contains different paratracheal axial parenchyma (e.g., vasicentric, aliform, lozenge-aliform, winged aliform and confluent)[19]
Site-specificity traits	
Diameter at breast height (mature, cm)	50-180[3,4,7,12,13,14,15]
Height (at maturity, m)	40 (Uganda and Tanzania (*eminii*))[16]
	35 (Democratic Republic of Congo (*eminii*))[16]
	25-30 (Angola (*eminii*) westwards (*berchemioides*))[16]
Branch aging (self-pruning, m)	10-35[1,3,4,7,12,13,14,15]
Rooting traits	Unbutressed[4,17]
	Lateral and deep tap roots[18]
Ecological strategy	Shade intolerant from 1 year[3,5,6]
	Fast growing light demanding pioneer[4,17]

Raunkier 1934[10], Eggeling 1947[4], Mugasha 1981[2], Taylor 1989[18], Binggeli 1989[5], Binggeli and Hamilton 1990[6], Binggeli and Hamilton 1993[3], Hall 1995[16], Ani and Aminah 2006[12], Chave et al. 2009[11], Orwa et al. 2009[1], Buchholz et al. 2010a[13], Buchholz et al. 2010b[14], Hall 2010[15], Tihurua 2012[9], Bulafu et al. 2013[17], CABI 2016[7], Epila et al. 2016[8], www.insidewood.lib.ncsu.edu[19], Personal observation[20], Prabhakar 2004[21], Cordeiro et al. 2004[22]

1.4.2   Phenology

From the onset, it is important to point out that capturing tree phenology data within the tropics is quite difficult. This is owed to limited visualization brought about by the sometimes dense canopy and tall trees that tower several meters above the ground. Particularly for this study, the 10-day window period for data collection presented a bias in that flowering that usually occurs for only three days might have been missed (explaining the peculiar pattern in Figure 1.2 discussed below). That said, of the four *Maesopsis* trees observed at Yangambi forest reserve, the average annual patterns in defoliation, flowering, fruiting and seed dispersal are found related to the seasonal precipitation pattern (Figure 1.2). Defoliation occurs at the start of the largest wet season (Aug-Sept), but only with low frequencies (< 10 % of the observations), suggesting that *M. eminii* is not deciduous in Yangambi. Flowering increases from October during the large wet season and peaks in January during the large dry season where more than 40 % of the observed trees had flowered (Figure 1.2). Fruiting is normally supposed to follow flowering, however our data shows otherwise. This piggybacks to the earlier mentioned difficulty in observing flowering, in addition to our 10-day frequency data collection window implying that the observers might have unintentionally missed *M. eminii* flowering that usually occurs for only three days. Nonetheless, fruiting is shown to increase from January, peaking in April (>80 % of the observations) towards the end of the short rainy season. Seed dispersal peaked more or less at the same time as fruiting (March-April).
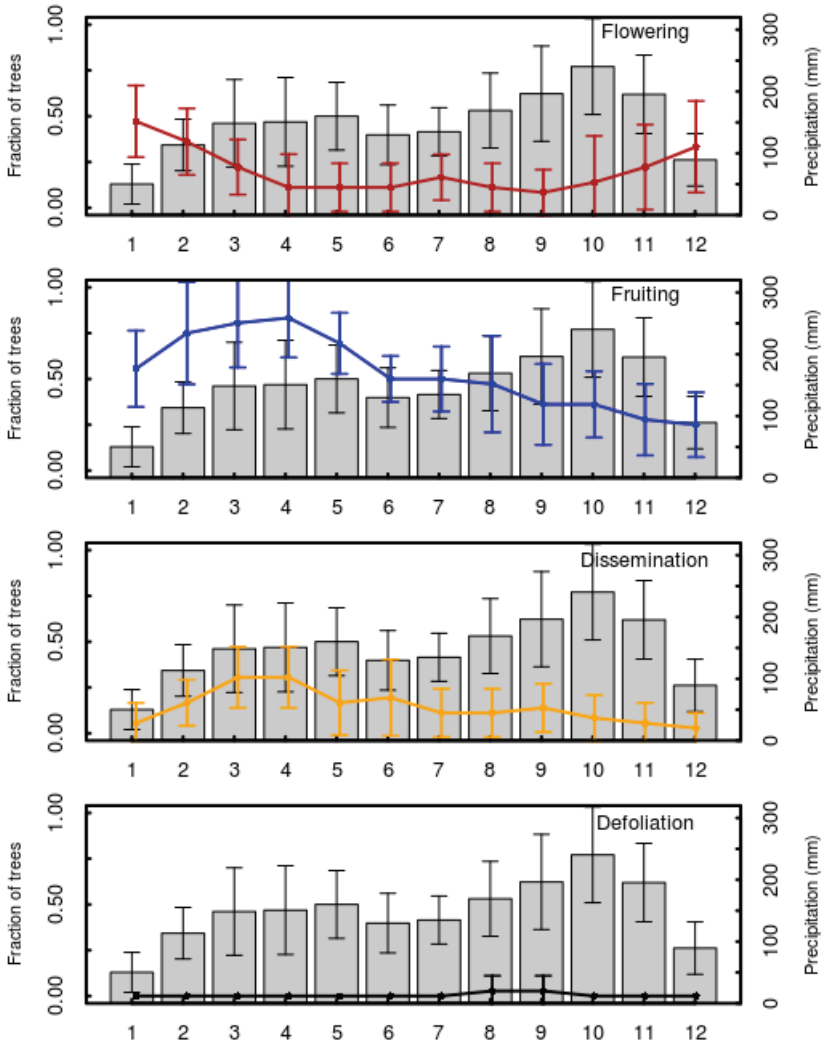
Figure 1.2 Phenology of four *M. eminii* trees in Yangambi, Democratic Republic of Congo followed for 9 years (see Appendix Table A1.2). The plot contains the mean frequencies and standard deviations of observed phenology of the four trees. The high observed fruiting and low flowering show how difficult it is to observe phenological changes in dense tropical forests.

1.4.3   Provenance trials

All the 600 test seedlings of the provenances survived the first year in Humic nitosols soil condition of Kibale. However, survival sharply declined to ~50% after a year and declined steadily to about 40 % at the age of 12 years (Figure 1.3A). Survival rates were low as a result of breakage of tops in Kibale due to arboricide treated trees falling on planted trees, animal browsing (e.g., bush bucks, elephants), neglected tending, line opening and climber cutting. Morphological characteristics

differences of the Busiro and Kalinzu provenances were not evident in sizes of leaves, crown sizes and in type of branching. Thus on average, tree growth performances for the two provenances were remarkably similar throughout the trial period as statistics graphed in Figure 1.3 show. The DBH (Figure 1.3B) and the vertical height (Figure 1.3D) of both provenances indicated an increasing pattern. Yearly increment in DBH (Figure 1.3C) and height (Figure 1.3E) illustrated a decreased incremental trend beyond 1973. This was attributed to poor overwood treatment that caused shading and might have affected growth.
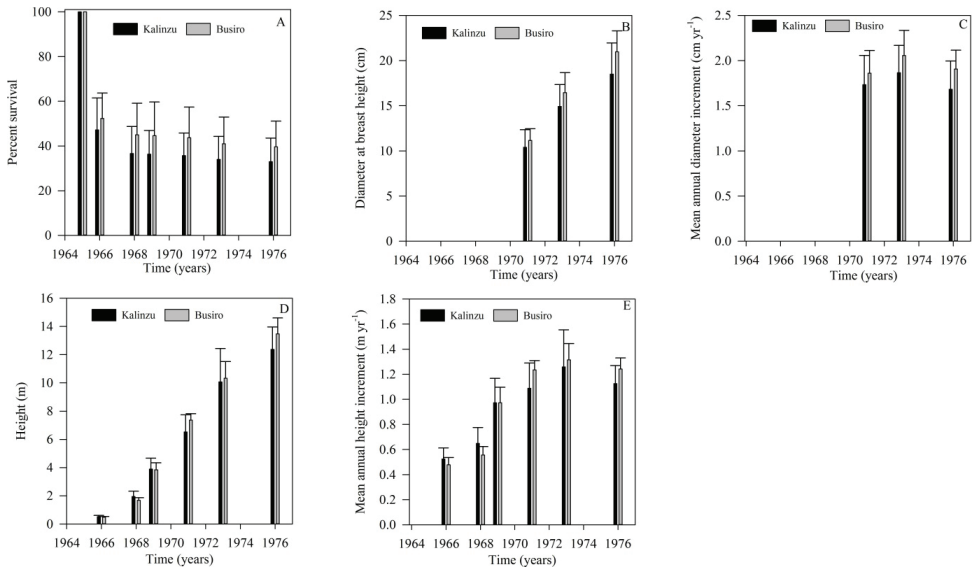
Figure 1.3 Performance variables for the two Ugandan provenances from Busiro and Kalinzu: Percent survival (A), diameter at breast height (DBH) (B), yearly increment of DBH (C), height (D) and yearly height increment (E) with their respective standard deviations followed during provenance trials in Kibale forest, Toro. Blank years portray situations where data was not collected or is missing.

1.4.4   *M. eminii'*s ecological niche

Equidistantly, the distribution of *M. eminii* straddles the equator to 10.97N, 3.14W in Burkina Faso and 10.98S, 26.73E in Likasi, DR Congo (Figure 1.4). *M. eminii* that is observed to occur in 19 different African countries concentrates most within the tropical rainforest realm (Uganda, DR Congo through to western coast of Africa). Nevertheless, it is also observed to occur in tropical shrub land of Burkina Faso and Tanzania, tropical moist deciduous forest in Angola, DR Congo, Zambia and Sudan, Tropical Mountain ecosystems in Cameroon, DR Congo, Uganda and Kenya, and in Burkina Faso and Tanzania in the tropical dry forest (Figure 1.4). The occurrences therein however cannot be distinguished (native or planted) due to lack of available information in the data that was used.
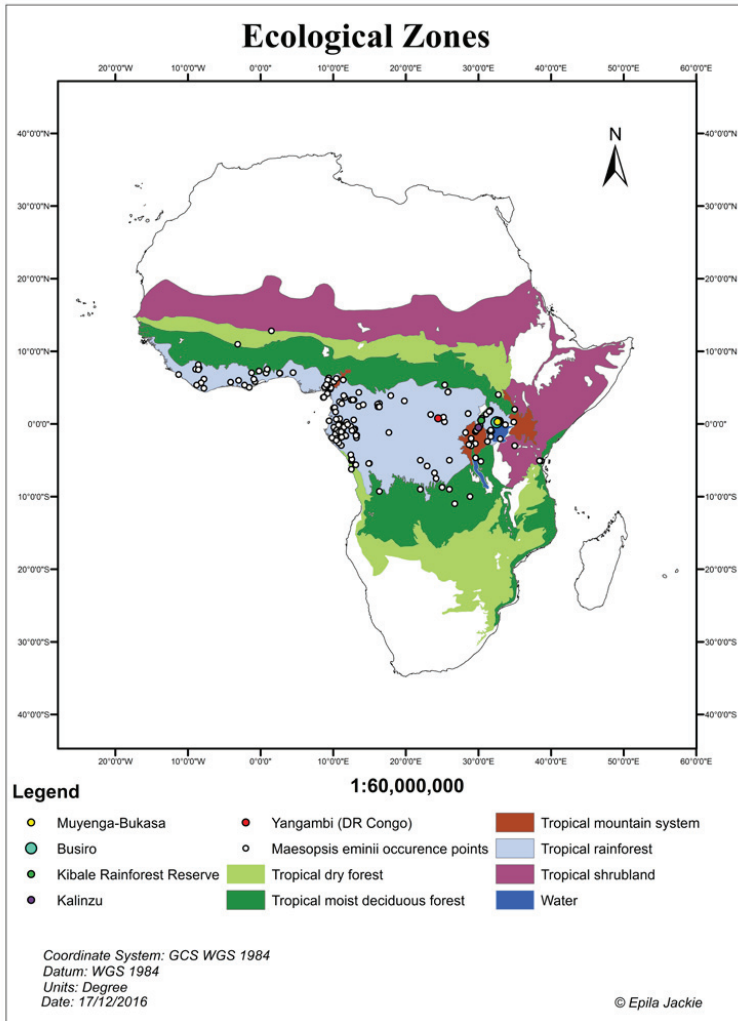
Figure 1.4 Map of Africa showing the geo-referenced occurrence positions of *M. eminii* within different ecological zones based on available datasets. The distinguished point locations (in colour) are where specific-studies (Uganda drought experiment (Chapter 2), provenances and phenology) were performed. The original map sheet was sourced from FAO.

Extracted information on *M. eminii*'s preferred precipitation (Table A1.1; Figure A1.2) and temperature (Table A1.1; Figure A1.3) regimes defined its ecological niche (Figure 1.5) as one requiring ample precipitation (1000-2000 mm yr-1; 97% of geo-referenced occurrence sites) and moderate temperatures (22-28 °C; 82 % of occurrences).
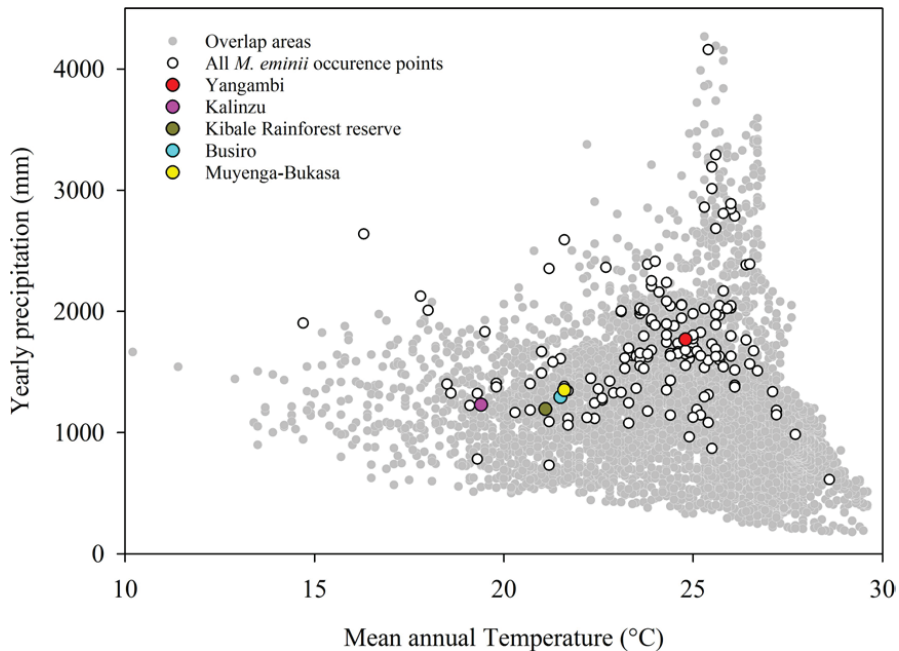
Figure 1.5 Plot of precipitation as a function of temperature gives an idea of *M. eminii*'s ecological niche based on occurrence data. The grey shaded region signifies the temperature and precipitation value within the latitudinal band that *M. eminii* is observed to occur in Africa. The different colour dots illustrate where more detailed studies (Uganda drought experiment (Chapter 2), provenances and phenology) on *M. eminii* were conducted.

1.4.5   Soils

The intersect function of ArcGIS allowed the determination of soils that *M. eminii* exploited. Because the attribute table born from the intersection between the soil map and the *M. eminii* occurrence points had country as one of the listed attributes, we made an overview per country of the soils *M. eminii* thrived in (Table A1.1). Based on the Land and Water Department Division, FAO soil codes, *M. eminii* has been found to grow on 20 different dominant soil types that constitute nine soil groups with differing physical and chemical qualities. The approximate percent breakdown of soil preference is, in order of importance: Orthic Ferralsols (Fo; 26%), Xanthic Ferralsols (Fx; 8%), Lithosols (I; 7%), Ferric Luvisols (Lf; 7%), Eutric Nitosols (Ne; 6%), Humic Nitosols (Nh; 6%), Ferralic Arenosols (Qf; 6%), Orthic Acrisols (Ao; 5%), Ferralic Cambisols (Bf; 5%), Dystric Nitosols (Nd; 5%), Ferric Acrisols (Af; 4%), Humic Gleysols (Gh; 4%), Humic Ferralsols (Fh; 2%), Dystric Gleysols (Gd; 2%), Pellic Vertisols (Vp; 2%), Eutric Cambisols (Be; 1%), Humic Cambisols (Bh; 1%), Calcic Cambisols (Bk; 1%), Rhodic Ferralsols (Fr; 1%), and Calcaric Gleysols (Ge; 1%) (Table A1.1).

1.5 Discussion

Our study objective was to enhance our understanding of the ecology and specifically the distribution of *M. eminii* in Africa. We achieved this by combining information from *M. eminii*: (i) functional trait attributes (Table 1.1), (ii) site-specific studies of tree phenology and growth (Figure 1.2 and Figure 1.3), and (iii) occurrence at sites with different forest types (Figure 1.4), precipitation (Figure A1.2) and temperature (Figure A1.3) regimes. This resulted in the establishment of *M. eminii*'s ecological niche (Figure 1.5). The ecological niche has only been described by plotting yearly precipitation as a function of time in comparison with more classical approaches of ecological niche modelling e.g., Huisman–Olff–Fresco (HOF) model, Gaussian responses as Generalized linear model (GLMs), and Generalized Additive Model (GAM) (Oksanen and Minchin 2002).

Firstly, it is clear that our mapping has improved our understanding of *M. eminii*'s ecology, occurrence distribution over Africa, and preferred ecological niche (based on presence data). We show that this tree species associates with growth conditions prevailing under numerous soil types, several precipitation (Figure A1.2) and temperature (Figure A1.3) regimes and variable ecological conditions in several forest types (Figure 1.4).

Our observation of *M. eminii*'s high occurrence in the rainforest region (Figure 1.4) supports Hall's (1995) technical report that states that *M. eminii*'s distribution range corresponds merely to the African rainforest zone. Observed *M. eminii* stands in forests outside this realm, especially within Tanzania's tropical dry and shrubland forest, are as a result of planting. We also illustrate that *M. eminii* occurs – at least – scantly at the centre of the Congo Basin (Figure 1.4), not previously observed by Hepper (1979), and where Hall (1995) attributed the absence of the species to swampy condition. Furthermore, we show that *M. eminii* based on its ecological niche (Figure 1.5) is unlikely to occur in very cool (<19 °C) temperature environments. *M. eminii*'s ecological strategy (Table 1.1) and our provenance trials support its non-preference of cool environments as overwood shading was observed to affect growth of the Ugandan provenances. Canopy induced shading has been observed by De Frenne et al. (2013) to lower understory microclimate (temperature). Nevertheless, such hump-shaped growth curves (Figures 1.3C & 1.3E) can also be linked to ontogenetic variation in growth rate (Herault et al. 2011).

Soils in Africa have been poorly mapped. However, for comparative purposes we show based on FAO's soil maps (FAO 1977, 1978, UNEP/ISSS/ISRIC/FAO 1993) that *M. eminii* prefers Orthic ferralsols. Hall (1995) notes that in localities with an extended (5-6 months) dry season where *M. eminii* occurs, fertile soils like Rhodic ferralsols in DR Congo, Eutric nitosols and Ferric luvisols of Tanzania and Sudan are present. Eggeling (1947) and Mugasha (1981) also attached great significance to soil quality in the establishment and growth of *M. eminii*. However, our empirical data from the provenance trial in Uganda (Figure 1.3) (although the provenance only covers a narrow habitat range) suggests that soil fertility is not a prerequisite for *M. eminii*'s establishment. Indeed, the

pioneer *M. eminii* within its preferred ecological niche (Figure 1.5) thrives under numerous soil types (Table A1.1, Figure 1.4). This supports the notions that *M. eminii* on the one hand has a broad ecological amplitude (Binggeli and Hamilton 1993, Schabel and Latiff 1997), but that on the other hand soils prone to drought stress seem unfavorable for *M. eminii* (Hall 1995). Limitation of water (Figure 1.5) might thus explain why the existing latitudinal expansion of *M. eminii* is less extensive within the tropical deciduous forest ecosystems and beyond where soil moisture is limiting (Figure 1.4 and Figure 1.5).

Another explanation for *M. eminii*'s latitudinal occurrence band could be linked to its arboreal dispersers that live in trees (Table 1.1). Furthermore, *M. eminii* does not invade and establish inside the fire-prone dense grass communities (Hafashimana, pers. comm., Hall 1995), suggesting that *M. eminii*'s presence is probably abated by non-conducive environments for both the species *M. eminii* and its arboreal seed dispersers.

Functional traits determine plant growth, survival and reproductive success, and as such play important roles in shaping species distribution pattern along environmental gradients (Maharjan et al. 2011). In harsh environmental conditions, the success of *M. eminii* can be related to its functional traits (Table 1.1). Firstly, *M. eminii*'s reproductive biology as indicated by our phenology data (Figure 1.2) shows an all year round seed production (Figure 1.2, Table 1.1). Indeed, also Hall (1995) stated that as long as large gaps exist, soil moisture is sufficient and seeds are produced frequently and copiously, *M. eminii*'s invasion is inescapable. A typical example of the invasion after introduction of *M. eminii* through planting is the Amani, Tanzania case. Here massive fruiting of *M. eminii* occurred in the Kwamkoro plantation which was readily dispersed by hornbills to Amani's natural forest leading to *M. eminii*'s invasion of Amani (see Hall 1995). Secondly, as a fast growing pioneer species, *M. eminii* possesses a trait ensemble favoring rapid resource acquisition and growth (e.g., wide long vessels with medium sized intervessel pits to facilitate efficient water movement; Table 1.1), increasing its survival potential in introduced areas given that drought is not pronounced as its hydraulic conduit based on size is vulnerable to cavitation (Holbrook 1995).

M. eminii's occurrence in several relatively dry sites (Table 1.1), plus the ability to survive and grow well in a new environment (provenance trials, Figure 1.3) indicate that *M. eminii*'s functional traits (Table 1.1) allow the species to establish in more marginal environments. Borchert (1994) classifies trees with similar functional traits as *M. eminii* (e.g. deciduousness and low wood density; Table 1.1) as species that have high stem water storage, allowing them to grow in moderately dry sites. Indeed this might be true for *M. eminii* with elastic cell walls based on its low apparent modulus of elasticity value (Table 1.1); a value which based on Bartlett (2012) and others' range of 5 - 80 MPa implies elastic cell walls. Such elastic walls have been found to store substantial amount of water (Bartlett et al. 2012). Observed vessel-associated parenchyma cells in *M. eminii*'s wood (Table 1.1) also suggest water storage. Another strategy to cope with dry events might be related to leaf

phenology. Although our phenological data (Figure 1.2) indicate that leaf defoliation was not really influenced by the dry-wet season cycles in DR Congo, we know that complete leaf shedding helps *M. eminii* in some cases to survive severe drought (Eggeling 1947). Finally, the root functional traits probably play an essential role in allowing *M. eminii* to grow under a wide range of site conditions. *M. eminii* has both deep tap roots and an intricate mat of lateral roots (Table 1.1) that permeate the subsoil, allowing the species to explore resources (nutrients and water) from both shallow and deep soil layers supporting its fast-growing and competitive habit.

Appendix

Tables

Table A1.1 Geo-referenced occurrence point locations of *M. eminii* with their respective identification numbers (ID), obtained from the different databases and datasets (Eggeling and Harris 1939[9], Exell and Mendonça 1954[1], Évrard 1960[6], Lawton 1969[12], Johnston 1972[7], Jenkin et al. 1977[8], Howard 1991[10], Hall 1995[2], Lewis et al. 2013[5], Slik et al. 2015[4], Forest Department, Government of Uganda (1968)[11], www.gbif.org[3].). These point locations (WGS84) were mapped and overlaid on www.worldclim.org or (Hijmans et al. 2005) data maps of average Temperature (T) ($T_{max}+T_{min}$) and yearly precipitation (precip.) of 30 minute arc resolution to obtain the mean Temperature (T) and Precipitation (mm yr^{-1}) at the different mapped occurrence point locations. The dominant soil types at the different point locations were obtained by overlaying *M. eminii*'s occurrence map with FAO's soil map of Africa (shape file). The soil map was prepared using the topographic map series of the American Geographical Society of New York as a base at a nominal scale of 1:5 000 000 (FAO 1977, 1978, UNEP/ISSS/ISRIC/FAO 1993). For Africa, the country boundaries are derived from the FAO Country Boundaries on the original FAO/UNESCO Soil Map of the World (FAO 1977, 1978, UNEP/ISSS/ISRIC/FAO 1993).

Country	ID	Lat. (Decimal degrees)	Long. (Decimal degrees)	T (°C)	Precip. (mm yr^{-1})	Dominant soil types
	AO1	-4.75[1,2]	12.53[1,2]	25.1	1189	
	AO2	-5.05[1,2]	12.50[1,2]	25.4	1082	
	AO3	-6.25[1,2]	12.50[1,2]	25.5	868	
	AO4	-9.28[3]	16.37[3]	21.7	1114	
ANGOLA	AO5	-4.88[3]	12.57[3]	25.2	1144	Qf, Fo
	AO6	6.97[3]	2.68[3]	27.2	1182	
	AO7	7.00[3]	2.64[3]	27.2	1145	
BENIN	AO8	6.99[3]	2.63[3]	27.2	1145	Nd
	AO9	10.97[4]	-3.14[4]	27.7	984	
BURKINA FASO	AO10	12.80[4]	1.50[4]	28.6	612	Be
	AO50	2.82[5]	16.35[5]	24.4	1652	
	AO51	5.37[3]	25.37[3]	25.3	1535	
	AO52	2.70[3]	16.12[3]	24.9	1609	
	AO53	2.35[3]	16.17[3]	24.8	1646	
	AO54	2.35[3]	16.18[3]	24.8	1646	
C.A.R	AO55	3.90[3]	17.93[3]	23.6	1654	Fo
	AO11	3.30[5]	12.48[5]	23.8	1623	
	AO12	3.31[5]	12.49[5]	23.8	1623	
	AO13	3.32[5]	12.87[5]	23.4	1633	
	AO14	3.30[5]	12.87[5]	23.4	1633	
	AO15	3.33[5]	12.72[5]	23.5	1629	
	AO16	2.43[5]	13.52[5]	23.2	1614	
	AO17	5.36[5]	9.55[5]	26.1	2786	
	AO18	2.64[5]	14.14[5]	23.6	1605	
	AO19	6.13[5]	9.41[5]	26.4	2383	
	AO20	6.33[5]	9.38[5]	23.9	2209	
	AO21	6.05[5]	9.27[5]	26.5	2390	
	AO22	3.03[4]	10.87[4]	23.6	1980	
	AO23	3.03[4]	10.87[4]	23.6	1980	
	AO24	3.03[4]	10.87[4]	23.6	1980	
	AO25	3.03[4]	10.87[4]	23.6	1980	
	AO26	3.03[4]	10.87[4]	23.6	1980	
	AO27	3.03[4]	10.87[4]	23.6	1980	
	AO28	3.03[4]	10.87[4]	23.6	1980	
	AO29	2.16[4]	10.03[4]	24.3	2239	
CAMEROON	AO30	2.24[4]	10.21[4]	23.9	2252	Fo, Fh, Ne, Bh, I, Ao

	AO31	5.08[4]	8.87[4]	25.3	2859	
	AO32	5.08[4]	8.87[4]	25.3	2859	
	AO33	5.08[4]	8.84[4]	25.3	2859	
	AO34	5.06[4]	8.83[4]	26.0	2844	
	AO35	5.04[4]	8.84[4]	25.3	2859	
	AO36	5.07[4]	8.85[4]	25.3	2859	
	AO37	5.06[3]	8.85[3]	25.3	2859	
	AO38	3.62[3]	11.61[3]	23.9	1678	
	AO39	5.82[3]	10.08[3]	17.8	2125	
	AO40	4.79[3]	9.60[3]	25.5	3012	
	AO41	4.98[3]	9.68[3]	21.6	2591	
	AO42	6.25[3]	10.43[3]	18.0	2008	
	AO43	5.28[3]	9.20[3]	25.3	2860	
	AO44	5.42[3]	9.07[3]	25.8	2808	
	AO45	2.80[3]	11.17[3]	23.7	1795	
	AO46	3.88[3]	11.45[3]	23.3	1695	
	AO47	4.33[3]	13.53[3]	23.6	1547	
	AO48	6.05[3]	11.38[3]	24.6	1736	
	AO49	4.17[3]	9.20[3]	16.3	2639	
CONGO	AO56	2.34[4]	16.35[4]	24.6	1666	Bf
	AO60	4.43[2,6]	25.85[2,6]	25.0	1665	
	AO61	3.17[2,6]	19.80[2,6]	25.0	1715	
	AO62	0.77[2,6]	24.45[2,6]	24.8	1767	
	AO63	-1.18[2,6]	17.67[2,6]	25.5	1729	
	AO64	-2.72[2,6]	29.58[2,6]	18.6	1324	
	AO65	-5.43[2,6]	14.98[2,6]	23.5	1363	
	AO66	-5.45[2,6]	14.90[2,6]	23.5	1363	
	AO67	-5.63[2,6]	13.07[2,6]	25.0	1125	
	AO68	-5.63[2,6]	13.12[2,6]	25.0	1125	
	AO69	-5.80[2,6]	22.93[2,6]	24.6	1650	
	AO70	-6.75[2,6]	23.95[2,6]	24.4	1429	
	AO71	-7.52[2,6]	24.18[2,6]	23.2	1527	
	AO72	-8.73[2,6]	25.00[2,6]	22.9	1326	
	AO73	-10.98[2,6]	26.73[2,6]	20.3	1164	
	AO74	0.29[5]	25.33[5]	25.0	1773	
	AO75	0.30[5]	25.33[5]	25.0	1773	
	AO76	-5.00[2]	22.00[2]	24.9	1658	
	AO77	-5.00[2]	26.00[2]	25.4	1312	
	AO78	-9.00[2]	26.00[2]	24.9	963	
	AO79	-9.00[2]	22.00[2]	22.8	1423	
	AO80	-2.00[2]	29.00[2]	18.5	1399	
	AO81	-3.00[2]	29.00[2]	22.6	1266	
	AO82	1.44[2]	28.58[2]	24.3	1745	
	AO83	-2.84[3]	28.68[3]	14.7	1902	
	AO84	1.29[3]	23.43[3]	25.2	1824	
	AO85	1.42[3]	28.58[3]	24.3	1745	
	AO86	-4.25[3]	12.42[3]	24.3	1350	
	AO87	0.77[3]	24.48[3]	24.8	1767	
	AO88	0.93[3]	25.20[3]	25.0	1803	
	AO89	-1.20[3]	28.22[3]	21.5	1608	
	AO90	0.77[3]	24.45[3]	24.8	1767	
CONGO, DEM. R.	AO91	4.38[3]	25.80[3]	24.9	1665	Fo, Fx, Gd, Nh, Nd, Vp, Ge, Fr, Fh

	AO92	1.65[3]	10.32[3]	21.2	2353	
	AO93	3.65[3]	8.64[3]	23.8	2388	
	AO94	3.70[3]	8.75[3]	24.0	2413	
EQUAT.GUINEA	AO95	3.67[3]	8.73[3]	24.0	2413	I, Fo
	AO96	0.72[5]	10.88[5]	23.6	2008	
	AO97	-1.90[5]	13.22[5]	23.9	1910	
	AO98	-1.81[5]	10.33[5]	25.3	2021	
	AO99	-1.79[4]	10.17[4]	25.3	2021	
	AO100	-1.79[4]	10.33[4]	25.3	2021	
	AO101	-0.82[3]	10.25[3]	26.0	2026	
	AO102	-1.92[3]	9.88[3]	25.7	1967	
	AO103	-0.45[3]	10.10[3]	25.8	2169	
	AO104	-1.67[3]	11.74[3]	23.1	1996	
	AO105	-0.81[3]	10.52[3]	26.0	2047	
	AO106	-2.97[3]	11.11[3]	24.8	1553	
	AO107	-1.43[3]	10.29[3]	25.8	2026	
	AO108	0.65[3]	10.41[3]	22.7	2363	
	AO109	-1.05[3]	11.18[3]	24.4	2045	
	AO110	-1.10[3]	11.31[3]	24.4	2045	
	AO111	-2.01[3]	10.43[3]	25.0	1980	
	AO112	-0.35[3]	12.43[3]	25.4	1594	
	AO113	0.55[3]	12.83[3]	23.8	1647	
	AO114	-2.60[3]	10.77[3]	25.6	1687	
	AO115	-0.12[3]	11.73[3]	25.7	1598	
	AO116	-0.03[3]	11.00[3]	25.6	1888	
	AO117	-0.42[3]	11.50[3]	24.3	1804	
	AO118	-0.25[3]	11.67[3]	25.7	1628	
	AO119	-0.42[3]	11.50[3]	24.3	1804	
	AO120	-0.08[3]	10.75[3]	25.7	2048	
	AO121	-0.08[3]	10.80[3]	25.7	2048	
	AO122	-0.14[3]	10.73[3]	25.7	2048	
	AO123	-0.70[3]	13.00[3]	25.1	1671	
	AO124	-0.80[3]	12.83[3]	24.8	1679	
	AO125	-0.92[3]	12.58[3]	25.2	1633	
	AO126	-1.63[3]	11.55[3]	23.6	2027	
	AO127	-1.68[3]	11.50[3]	23.7	2008	
	AO128	-1.07[3]	10.80[3]	25.9	2023	
	AO129	-1.60[3]	11.72[3]	23.1	2004	
	AO130	-1.92[3]	9.83[3]	25.6	1974	
	AO131	-2.27[3]	10.43[3]	24.7	1943	
	AO132	0.25[3]	11.83[3]	24.4	1631	
	AO133	-1.83[3]	11.17[3]	24.7	2056	
	AO134	-0.08[3]	11.98[3]	25.8	1541	
	AO135	-1.08[3]	11.10[3]	24.7	2052	
	AO136	-1.55[3]	13.25[3]	24.5	1879	
	AO137	-1.60[3]	13.15[3]	24.3	1894	
GABON	AO138	0.42[3]	9.45[3]	26.0	2888	Fo, Bf, Qf, Fx,
	AO139	5.99[5]	-3.02[5]	26.6	1674	
	AO140	5.86[5]	-0.80[5]	25.6	1626	
	AO141	5.83[5]	-0.78[5]	26.1	1514	
	AO142	6.15[5]	-0.92[5]	26.0	1629	
GHANA	AO143	5.03[3]	-1.56[3]	26.1	1390	lf, I, Ao, Fx

Country	Code	Col1	Col2	Col3	Col4	Habitat
	AO144	7.28[3]	-0.22[3]	27.1	1336	
	AO145	5.35[3]	-2.20[3]	26.4	1762	
	AO146	7.04[3]	-1.24[3]	25.3	1294	
	AO147	7.04[3]	-1.24[3]	25.3	1294	
	AO148	7.69[3]	-8.44[3]	23.9	1932	
	AO149	7.53[3]	-8.93[3]	24.3	2084	
GUINEA	AO150	8.14[3]	-8.57[3]	24.0	1885	Af, I
	AO57	6.17[3]	-7.79[3]	26.0	1797	
	AO58	4.90[3]	-7.79[3]	25.5	3191	
IVORY COAST	AO59	5.75[3]	-4.12[3]	26.5	1566	Af, Ao
KENYA	AO151	0.25[2,7]	34.87[2,7]	19.5	1831	Nh
	AO152	5.66[3]	-8.18[3]	25.6	2683	
	AO153	6.80[3]	-11.29[3]	25.4	4159	
	AO154	5.35[3]	-8.80[3]	25.6	3291	
LIBERIA	AO155	7.47[3]	-8.55[3]	24.1	2158	Fo, Fx, Bf
NIGERIA	AO156	7.06[4]	4.48[4]	26.7	1508	Lf
SUDAN	AO157	4.03[2,8]	32.75[2,8]	23.3	1244	Ne
	AO158	-1.00[2,9]	31.83[2,9]	21.0	1667	
	AO159	-1.07[2,9]	31.63[2,9]	20.7	1402	
	AO160	-2.05[2,7]	33.00[2,72,7]	22.5	1358	
	AO161	-2.42[2,7]	31.25[2,7]	21.7	1060	
	AO162	-5.17[2,7]	30.33[2,7]	21.2	1089	
	AO163	-5.10[5]	38.62[5]	22.3	1446	
	AO164	-5.11[5]	38.60[5]	22.3	1446	
	AO165	-5.10[5]	38.65[5]	22.3	1446	
	AO166	-3.00[2]	35.00[2]	19.3	781	
	AO167	-4.67[3]	29.62[3]	23.3	1076	
	AO168	-5.07[3]	38.41[3]	22.4	1243	
	AO169	-1.05[3]	31.57[3]	20.7	1402	
	AO170	-1.02[3]	31.58[3]	20.7	1402	
	AO171	-1.03[3]	31.62[3]	20.7	1402	
	AO172	-4.68[3]	29.63[3]	23.3	1076	
	AO173	-1.75[3]	31.70[3]	21.3	1581	Gh, Fo, Lf, Vp, Bk,
TANZANIA	AO174	-4.67[3]	29.62[3]	23.3	1076	Ne, Nh
	AO175	7.00[3]	0.75[3]	26.1	1373	
TOGO	AO176	7.53[3]	0.90[33]	23.7	1527	Lf, Nd
	AO177	1.78[2,9]	31.58[2,9]	23.1	1330	
	AO178	1.33[2,10]	31.08[2,10]	22.6	1282	
	AO179	0.80[2,10]	30.47[2,10]	19.8	1406	
	AO180	0.50[2,10]	32.95[2,10]	21.6	1380	
	AO181	0.40[2,7]	33.02[2,7]	21.7	1344	
	AO182	-0.12[2,7]	33.70[2,7]	22.4	1114	
	AO183	-0.25[2,10]	30.25[2,10]	20.7	1184	
	AO184	-0.50[2,10]	30.00[2,10]	19.4	1229	
	AO185	-0.85[2,9]	31.70[2,9]	21.0	1489	
	AO186	-1.08[2,10]	29.58[2,10]	19.3	1321	
	AO187	1.72[5]	31.50[5]	23.1	1330	
	AO188	0.55[5]	30.37[5]	19.8	1375	
	AO189	2.00[2]	35.00[2]	21.2	730	
	AO190	0.49[11]	30.39[11]	21.1	1193	
	AO191	0.22[11]	32.49[11]	21.5	1292	
UGANDA	AO192	0.29[11]	32.63[11]	21.6	1350	I, Fo, Af, Nh, Gh, Lf

	AO193	0.55[4]	30.38[4]	19.8	1375	
	AO194	1.73[4]	31.53[4]	23.1	1330	
	AO195	1.73[4]	31.53[4]	23.1	1330	
	AO196	1.72[4]	31.53[4]	23.1	1330	
	AO197	1.73[4]	31.53[4]	23.1	1330	
	AO198	1.73[4]	31.52[4]	23.1	1330	
	AO199	-0.91[4]	29.70[4]	19.1	1222	
	AO200	-0.91[4]	29.70[4]	19.1	1222	
	AO201	-0.89[4]	29.73[4]	19.1	1222	
	AO202	1.68[3]	31.54[3]	23.1	1330	
	AO203	1.80[3]	31.54[3]	23.1	1330	
	AO204	1.86[3]	31.65[3]	24.4	1143	
	AO205	1.71[3]	31.52[3]	23.1	1330	
	AO206	1.73[3]	31.54[3]	23.1	1330	
	AO207	1.71[3]	31.49[3]	23.8	1176	
	AO208	1.71[3]	31.49[3]	23.8	1176	
ZAMBIA	AO209	-10.00[2,12]	28.83[2,12]	22.2	1122	Fo

Table A1.2 Rudimentary data on 8 individuals of the species *M. eminii*'s yearly phenological (Flowering, Fruiting, Seed dispersal and Defoliation) observations extracted from the INEAC archives consisting of 500 species thriving within the tropical rainforest of Yangambi DR Congo between 1939-1956.

Individual	Flowering	Fruiting	Seed dispersal	Defoliation
Tree 1	1939: March 1940: February 1941:No 1942:December 1943: January-February 1944-1946: No	1938: January-June 1939: March-June 1940: January-April 1941: February-May 1942: January-August 1943: January-June 1944: January-October 1945: June-September	1938: March-June 1939: April-June 1940: No 1941: May 1942: No 1943: May-June 1944-1946: No	1939: October
Tree 2		1940: January-March	1940: Jan-March	
Tree 3	1948: December- 1949: January	1943: June 1949: March-June	1949: March-April	1948: October-November 1952: October-December
Tree 4	1941: September, November, December 1942: June	1941: September, November 1942: June	1941: September 1942: June	
Tree 5	1947: January-March, November-January (1948) 1949: January-February 1950: January-February, October-December 1951: December 1952: Dec-1953: April 1953: November-1954: March 1955: Dec-1956: January, March-April	1945: March, July 1946: March-August 1947: February-July 1948: January-May 1949: February-July 1950: January-May 1951: January-May, August-September 1952: January-October 1953: January-September 1954: March-May 1955: February-August 1956: April-August	1946: June-September 1947: March-June 1948: April-May 1949: May-June 1950: March-June 1951: March-April, June 1953: February-March 1955: August 1956: May-August	

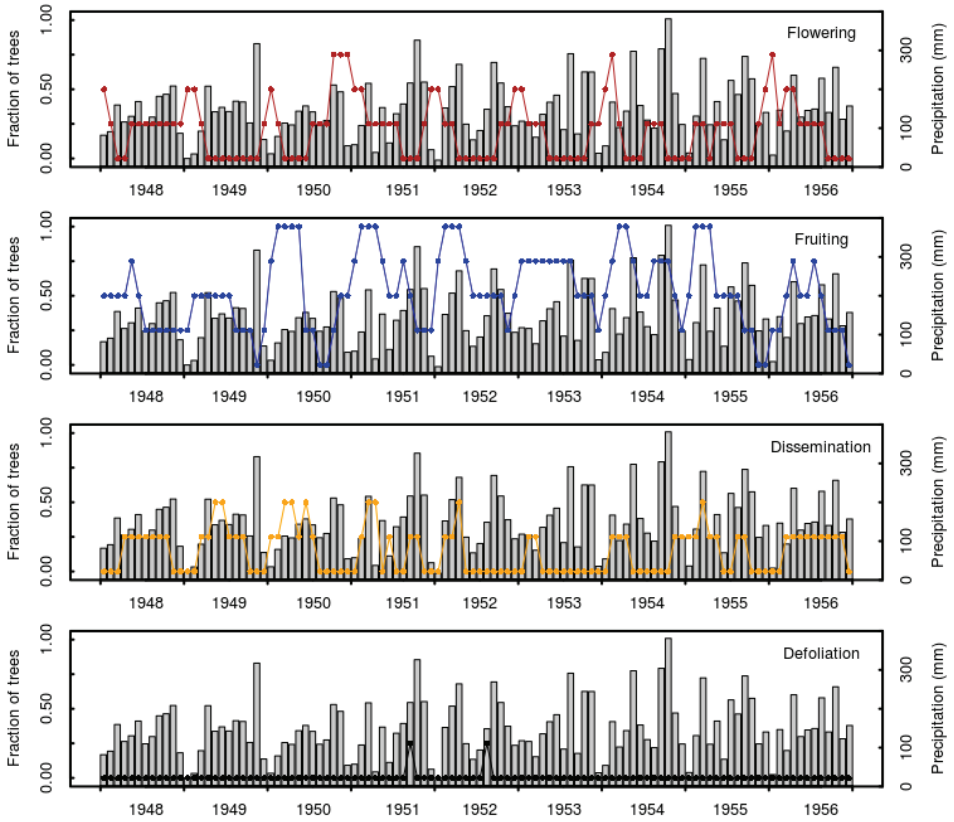| Individual	Flowering	Fruiting	Seed dispersal	Defoliation
Tree 6	1948: January-February	1947: January-March, May-September	1951: February-April, September-October	1948: July-1949: September
	1949: December- 1950: January, October-1951: January, November-January (1952)	1948: January-June	1952: February-April	1951:September
	1952: October-1953: January	1949: December-1950: May	1954: February, March-April, November-1955: April	1952: August
	1954: January-February, July-September	1950: November -1951: April, July-1952: May, December	1955: September	
	1955: February-March, May-July, November-1956: January, June-August	1954: January-April, August-1955: April, June-October	1956: March-April, September-November	
		1956: January-April, July-November		
Tree 7	1948: May-December	1948: May-1949: October	1948: June-October	
	1949: January- March	1950: January-July, October-1951: June	1949: March-September	
	1950: July-December	1952: February-1954: November	1950: January-July	
	1951: January-June	1955: February-April		
	1952: February-March	1956: March-July		
	1956: January-March			
Tree 8	1951: July	1950: February-May	1952: April	
	1952: January	1951: February-June, July-August	1955: March, May	
	1954: February	1952: January-April		
	1956: April-May	1953: January-August		
		1954: February-October		
		1955: January-May		

Figures

Figure A1.1 Phenological patterns of *M. eminii* (line plots) based on four trees that were followed consecutively for a window of 9 years in Yangambi Rainforest reserve DR Congo. The frequency of observation is computed per month based on presence (1) or absence (0) data. The monthly precipitation during the individual years is also displayed as bar graphs.
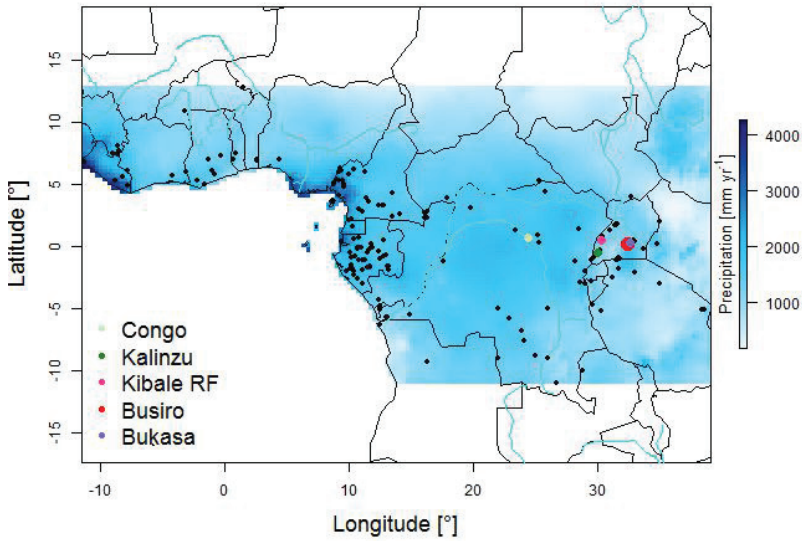
Figure A1.2 Map of Africa showing the geo-referenced occurrence positions of *M. eminii* based on occurrence data extracted from multiple databases under the different rainfall regimes. The different colour dots illustrate where more detailed studies (Uganda drought experiment (Chapter 2), provenances and phenology) on *M. eminii* were conducted. The original map sheet was sourced from the WorldClim database.

Figure A1.3 Map of Africa showing the geo-referenced occurrence positions of *M. eminii* under mean temperature regimes. The different colour dots illustrate where more detailed studies (Uganda drought experiment (Chapter 2), provenances and phenology) on *M. eminii* were conducted. The original map sheet was sourced from the WorldClim database.
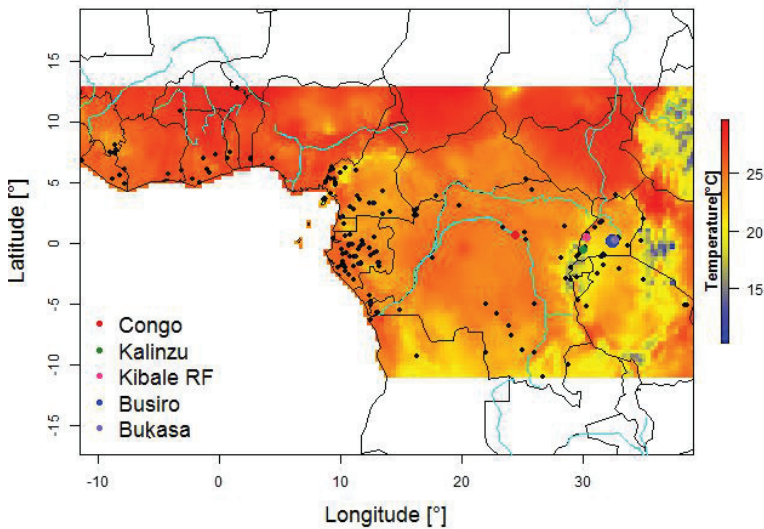
2   Response of tropical African *Maesopsis eminii* seedlings to drought stress

2.1 Abstract

Although studies in African evergreen and moist semi-deciduous forests show evidence of drought-induced forest composition shifts towards drought-tolerant, deciduous, light-demanding tree species, the mechanisms used by these species to cope with drought are hardly known. We subjected potted 15-month-old seedlings of a tropical deciduous and light demanding tree, *Maesopsis eminii* Engl. for ~4 months to three different drought treatments (control, rain-fed, and complete drought) and performed measurements of sap flow (SF), stem diameter variation (SDV) and stomatal conductance (g_s) to investigate the mechanisms. We observed that six days after drought stress establishments, sap flow of these pioneer seedlings declined, but radial stem growth continued for another five days. Clear SF-VPD and g_s-VPD hysteresis loops, generally low g_s rates (39 ± 30 mmol m^{-2} s^{-1}) at VPD (1.1 ± 0.5 kPa) during well watered conditions and leaf shedding regardless of soil moisture status show conservative stomatal control on water loss and indirect drought avoidance through leaf loss. But the seedlings were not able to fully control their stomata, and all treatments showed nocturnal sap flow, which accelerated soil moisture loss during drought. Recovery of internally stored stem water drastically declined below a soil water potential threshold value of -0.95 ± 0.03 MPa, signaling that once extraction of plant available water becomes difficult, reserve depletion and eventual death are inevitable. The small time lags between photosynthetic active radiation (PAR)-SDV, PAR-SF and SDV-SF indicated a limited but essential contribution of internally stored water in the bark to the transpiration stream to buffer sudden changes in water use. Taken together, it is a combination of these observed traits that may give this African tree cohort competitive advantages over other trees, allowing them cope better with drought.

2.2 Introduction

The increased frequency and severity of drought periods (IPCC, 2007) is placing forest ecosystems under increasing pressure around the globe (Anderegg et al., 2016), and is leading to dieback of less drought-tolerant species and to shifts in vegetation composition, with important long- and short-term impacts on ecosystem functioning (Anderegg et al., 2012; 2016; Avila et al., 2016; Berdanier and Clark, 2016; Bréda et al., 2006; Clark et al., 2016; Guada et al., 2016; Martin et al., 2015; Pellizzari et al., 2016). For African forests however, the impacts are not well understood. From the meta-analysis of Anderegg et al. (2016) on the link between drought and tree dieback, it is clear that very few studies have been performed in African forests. Furthermore, the few studies looking at the impact of drought on African forests disagree. Based on satellite data, Asefi-Najafabady and Saatchi (2013) found that African forests were remarkably undisturbed by drought events, unlike the Amazon. Zhou et al. (2014) on the other hand, reported a large decrease in Congolese rainforest greenness caused by short-term droughts. Similarly, inventory studies in African forests came to very different conclusions. Fauset et al. (2012) reported that increasing drought was causing a compositional shift in favour of deciduous, light-demanding species in Ghanaian wet evergreen, moist evergreen and moist semi-deciduous forests. Ouédraogo et al. (2013) on the other hand, found that slow growing shade tolerant species were less sensitive to drought compared to fast-growing light-demanding species in Central Africa's deciduous moist forest.

Based on these skewed observations, it is clear that we need to gain a better knowledge of how key African forest species will respond to drought in order to understand or predict the consequences of climate change-induced drought on African forest species. In particular, we need to assess species' functional traits and physiological responses and mechanisms that aid in coping with drought (Bazzaz and Pickett, 1980; Choat et al., 2012; Engelbrecht and Kursar, 2003; Gliniars et al., 2013; Lloret et al., 2012; Malhi et al., 2013a; Poorter and Markesteijn, 2008; Steppe et al., 2016).

In this study, we assess growth and water use of a light demanding deciduous pioneer species, *Maesopsis eminii* Engl. (*M. eminii*). This early successional species (Eggeling 1947) was chosen because of its economic and ecological importance in tropical Africa. It is used as timber, for crop shade (Eggeling 1947, Struhsaker 1987, Binggeli and Hamilton 1993), to limit erosion (Jøker 2000), as medicine, as medium for mushroom culture (Hall 2010), as source of edible oil, as a road-side ornament and as firewood and fodder (Jøker 2000). Moreover, as a pioneer species, it responds rapidly in terms of growth and mortality to resource availability, making it a suitable tree for this kind of research (Pearson et al. 2003b).

M. eminii that prefers annual precipitation of more than 1000 mm grows in tropical shrublands, tropical moist deciduous forests, tropical rainforests, tropical mountain systems and tropical dry forests, with its distribution most pronounced in the tropical rainforest region (Chapter 1). Within these forest ecosystems, *M. eminii* thrives as the dominant or transient species and can colonize new areas through seed rain from surrounding landscapes in forest gaps or clearings (Eggeling 1947, Hall 1995). Physiologically, *M. eminii* is both a tap and lateral rooted species (Taylor 1989) that is shade-intolerant from the age of one year (Eggeling 1947, Binggeli and Hamilton 1993). It has a low stem wood density of 0.37-0.48 g cm^{-3} (Chave et al. 2009) and has small to medium-sized (2.3-182.3 cm) palatable leaves (Raunkier 1934, Eggeling 1947). Adult trees of *M. eminii* are known to be semi-deciduous. However, during severe drought, they become deciduous, completely shedding all their leaves with flushing occuring just before the rains return (Eggeling 1947).

In a study of trees in Costa Rica in comparable climatic conditions, Borchert (1994) investigated the relationship between structural traits (wood density, stem water storage capacity), phenology and plant-water relations (anisohydric vs isohydric). He distinguished five different functional types, each with very different growth strategies and plant-water relations. These functional types have been proven relevant for species originating from other areas as well (e.g. Maes et al. 2009). The characteristics summed up in the previous paragraph would categorize *M. eminii* as a D$_{light}$ species, a deciduous lightwood tree with large stem water storage. Typically, such species are light-demanding pioneer species which can occupy dry, open and often rocky sites. Yet, these species possess isohydric characteristics, have mesomorphic leaves with little drought tolerance that are lost early in the dry season and, invoke stomatal control to regulate water loss (Borchert 1994). Similar traits have been observed for other Neotropical pioneer species with wood densities similar as those of *M. eminii* (Markesteijn et al. (2011a, 2011b), McCulloh et al. (2011, 2012).

Based on the plant-water relations of the D$_{light}$ species, we hypothesed that for *M. eminii* to tolerate protracted months of drought stress (i) being a pioneer species, it must rely on its assumed high stem water storage to support growth and to contribute water to the transpiration stream if demands arise, and (ii) regardless of soil water status, *M. eminii* will shed all its leaves during the dry season to delay drought stress effects. To test these hypotheses, two main questions guided our investigation: (i) What do the relationships between environmental variables like air temperature, relative humidity, vapour pressure deficit, photosynthetic active radiation and soil water potential and *M. eminii*'s sap flow, stomatal conductance and stem diameter variation during non-drought and drought conditions tell us about its water relations? (ii) Other than its assumed high stem water storage use and leaf shed, how else do *M. eminii* plants delay drought-stress effects?

We measured *M. eminii*'s diel sap flow and stem diameter variation patterns under different watering regimes. We also measured its stomatal conductance under well watered conditions. We opted to study seedlings for practical reasons and because they are a critical developmental stage (Tyree et al. 2003, Engelbrecht et al. 2005, Padilla and Pugnaire 2007) owed to their limited access to soil water due to their shallow roots (Tyree et al. 2003, McDowell et al. 2008, Brodribb et al. 2010), excessive competition for light and platable leaves liked by herbivores (Pearson et al. 2003a). In order to mimic the natural environment (Meir and Woodward 2010, Beier et al. 2012), we performed the measurements in open air and in its natural habitat in Uganda.

2.3   Materials and methods

2.3.1   Description of study site

The study was carried out at Muyenga-Bukasa (0°17'05.53"N, 32°37'53.55"E), a residential suburb of Kampala City, Uganda, located on the north-western shore of Lake Victoria. *M. eminii* seeds were collected on 7 February 2012 from mature trees of the Mabira Central Forest Reserve (0°23.357'N, 33°0.344'E), located on the northern shores of Lake Victoria. Seeds were germinated (see Table 1.1; Chapter 1) and newly germinated seedlings were placed into moist potting mix (forest soil mixed with clay loam soil) in plastic tubes on 9 March 2012, and raised for 12 months at the nursery of National Forestry Resources Research Institute (NaFORRI) located at 0°21'N, 32°46'E, approximately 1250 m a.s.l.. On 2 March 2013, fifteen seedlings were carefully transferred into moist potting mix in ten-litre plastic buckets whose bottom was perforated to allow drainage of excess water (Figure 2.1). These seedlings were allowed to grow and acclimatize in the buckets at the study site for two more months, and were watered to field capacity twice daily, early in the morning and in the evening.

Figure 2.1 Workers at NAFORRI transplanting fifteen randomly selected seedlings (A) into perforated buckets (B) and these were daily watered (C) before being transferred to the study site in Muyenga-Bukasa (D).

At this location, the tropical climate has a long rainfall season between March and May, and a highly variable shorter rainfall season between (August-) September and December (Black et al. 2003, Shongwe et al. 2011). Total annual rainfall is 1300 mm, ranging between 1000 and 1500 mm. Daily rainfall data were extracted from the Uganda National Meteorological Authority (UNMA) standard manual splayed-case copper rain gauge (aperture diameter: 127 mm and area 126.7 cm^2; Casella Monitor,UK), situated 3.6 km from our study site.

Air temperature (T) and relative humidity (RH) were measured with a ventilated sensor (SHT75, Sensirion Technology, Switzerland) and photosynthetically active radiation (PAR) was measured with a quantum sensor (model QS, Delta-T Devices, UK) installed at 0.93 m height in the middle of the study site.

2.3.2 Experimental treatments

On 8 May 2013, nine plants were randomly selected from the 15 plants and their mean height (44.4 ± 4.6 cm), root collar diameter (6.4 ± 0.6 mm) and number of leaves (89±13) were measured. The plants were then randomly assigned to one of three drought treatments. These drought treatments were (i) no irrigation at all (Drought), (ii) daily irrigation at 6 pm with 200 ml of tap water as control (Control), and (iii) rain-fed watering (Rain-fed), which only received water when it rained. All test plants were placed on wooden planks to prevent the possibility of the roots of seedlings out-growing through the holes at the bottom of the bucket and getting access to soil water. Drought and control seedlings were placed within an open wooden rain shelter (2.5 m length

× 1.5 m height × 1.5 m width) with a provision for placing a 3 × 6 m black plastic cover that could be anchored down to prevent rain from reaching the seedlings (Figure 2.2). The cover could be removed manually and was only installed when it rained and during the night (between 19:30-06:30 hours, when PAR was 0 µmol m^{-2} s^{-1}).

.

Figure 2.2 Set up at study site showing from extreme left, the drought followed by watered and on the extreme right, the rain-fed. The black plastic sheeting is the cover anchored down during rainy days and during the night

The microclimatic conditions and soil water potential of each treatment during the treatment period are given in Figure 2.3 and Table 2.1. Note that the first month, which should have covered the long rainy season (May), was relatively dry (daily rainfall in May was 1 ± 3 mm day^{-1}), indicating an abnormal rainy season
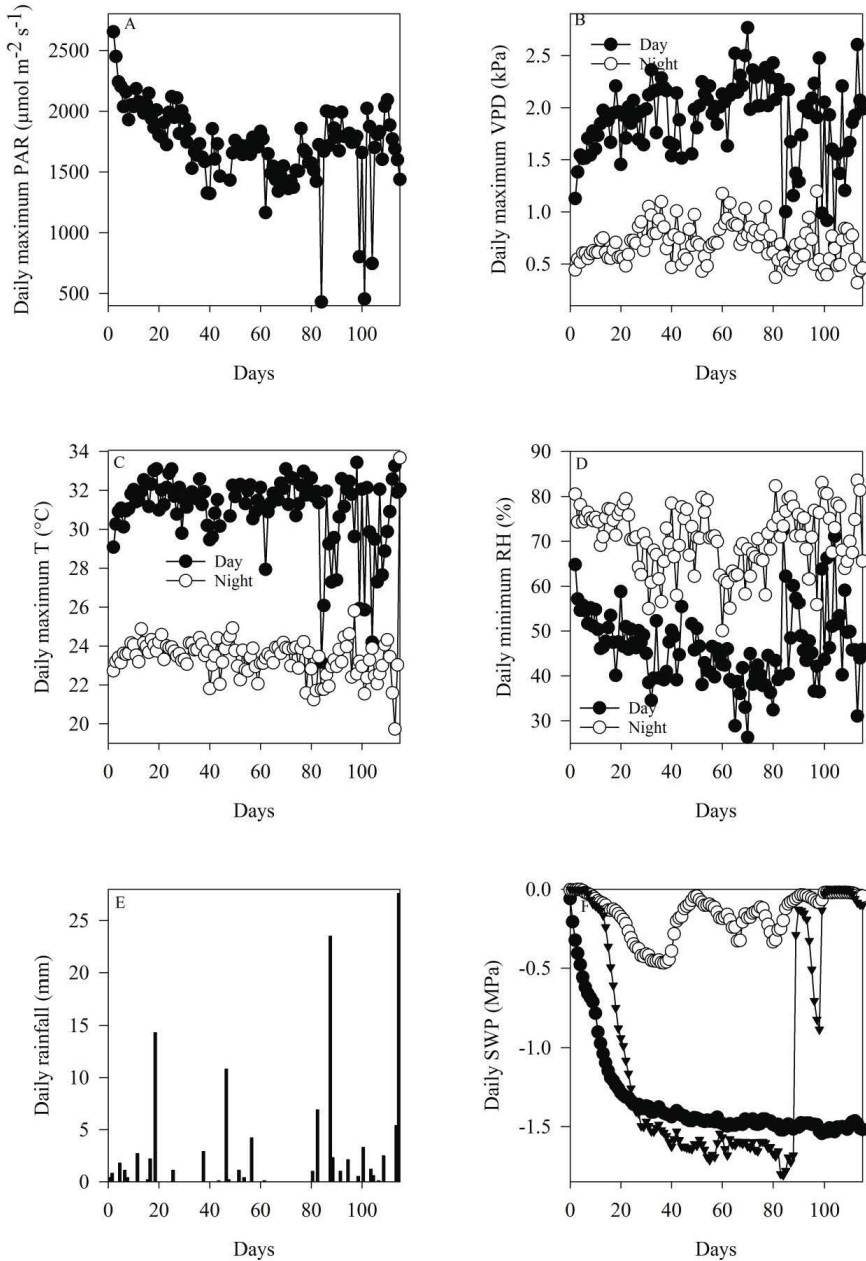
Figure 2.3 Daily values of environmental conditions experienced at the experimental site from day zero (8 May 2013) until day 115 (31 August 2013). (A) Maximum photosynthetic active radiation (PAR; ●), (B) maximum vapour pressure deficit (VPD) (day (●) and night (○)), (C) maximum air temperature (T) (day (●) and night (○)), (D) minimum relative humidity (RH) (day (●) and night (○)), (E) daily rainfall and (F) soil water potential (drought (●), control (○) and rain-fed (▼)). Blank spaces for all parameters except rainfall indicate regions with missing data.

Table 2.1 Average and standard deviation values for daily maximum photosynthetic active radiation (PAR), vapour pressure deficit (VPD), air temperature (T), daily soil water potential (SWP) and minimum relative humidity (RH). The SWP subscripts imply, drought for drought treatment, control for control treatment and rain-fed for rain-fed treatment.

Parameter	Units	Day	Night
PAR	(μmol m^{-2} s^{-1})	1727±330	0
VPD (kPa)	kPa	2.0±0.4	0.7±0.2
T	°C	31±2	23±1
RH	%	46±8	71±7
SWPdrought (MPa)	MPa	-1.3±0.3	
SWPcontrol (MPa)	MPa	-0.2±0.1	
SWPrain-fed (MPa)	MPa	-1.0±0.7	
Long rains (May)	mm day^{-1}	1±3	
Dry season (June-July)	mm day^{-1}	1±2	
Short rains (August)	mm day^{-1}	4±11	

2.3.3 Sap flow and stem diameter variation

All nine seedlings were equipped with sap flow and stem diameter variation sensors for a period of 115 full days, from the start of the drought treatment (9 May) until 31 August 2013. Sap flow dynamics were measured using a home-built non-invasive heat field deformation (mini HFD) sensor, following the design of Hanssens et al. (2013). Each sap flow sensor consisted of three thermocouples (type T copper constantan, Omega engineering limited, Netherlands) and a 100 Ω heater, which were sewn onto an insulating material (Class 0 Armaflex self-adhesive tape). More details on the principle of HFD can be found in Nadezhdina et al. (2012), Vandegehuchte and Steppe (2012) and Hanssens et al. (2013). Axially, two thermocouples (T$_1$ (above the heater) and T$_2$ (below the heater)) were placed 1 cm from the heater and the third thermocouple (T$_3$ (side of the heater)) was placed tangentially at 0.3 cm from the heater. The symmetric (T$_s$ or T$_1$-T$_2$) and asymmetric (T$_a$ or T$_3$-T$_2$) temperature differences were used to determine parameter K (Eq. 1) during zero sap flow (T$_s$=0) by plotting T$_s$-T$_a$ as a function of T$_s$/T$_a$ (Hanssens et al. 2013). K was derived as the intercept of the resulting linear fit. The R^2 values at which K was determined was 0.84±0.15. Once the parameter K was known, the sap flow dynamics (SFD) (-) were computed (Eq. 1) as in Hanssens et al. (2013).

$$SFDs = (K + (T_s - T_a))T_a^{-1} \qquad \text{(Eq. 1)}$$

The relative sap flow dynamic (RSFD) (%) was obtained by normalizing sap flow dynamic values using the highest value observed in the first full day of measurement (May 9) and the lowest value observed throughout the study period per individual to obtain percentages ranging between 0 and >100% (Eq. 2).

$$RSFD = \left(\frac{SFD_{measured} - SFD_{min}}{SFD_{maxDay1} - SFD_{min}}\right) 100 \qquad \text{(Eq. 2)}$$

From here on, RSFDs will be refered to as sap flow. Daily sap flow refers to diel sap flow. Day-time sap flow was observed when PAR was greater than 0 µmol m^{-2} s^{-1}, night-time sap flow when PAR was 0 µmol m^{-2} s^{-1}, running from the end of the current day into the next day before PAR became greater than 0 µmol m^{-2} s^{-1}. Day one refers to 9 May 2013. To highlight treatment differences in nocturnal sap flow, $SFD_{maxDay1}$ was replaced by nocturnal sap flow ($SFD_{maxnocDay1}$).

Stem diameter variations (SDV) of each monitored seedling were measured by a calibrated linear variable displacement transducer (LVDT; Solatron Metrology, DF/5.0, UK), secured about 3 cm above the root collar diameter using a home-built holder as described in Steppe et al. (2006). From the SDV data, two variables were calculated per seedling and for each day:

- **absolute growth**: the maximum stem diameter of each day, and
- **daily stem water recovery**: the difference between the following day's maximum stem diameter (wee hours of the morning peak value) and the minimum diameter of the previous day.

Equitensiometers (EQ2x, Delta-T Devices, UK) were used to measure soil water potential (SWP). One sensor per treatment was placed at a soil depth of 12 cm below root collar. SWP data, which were temperature sensitive, were normalized over a 24hr period. Data from all sensors were logged (CR1000, Campbell Scientific Inc., Logan, UT, USA) at 30 s intervals and averaged every 5 mins.

2.3.4 Stomatal conductance

Stomatal conductance (g_s) was measured at the end of July (23, 25 to 29 July 2013) and the beginning of August (4 to 7 August 2013) with a calibrated diffusion AP4 porometer (Delta-T Devices Ltd, Cambridge, UK). By then, only the control seedlings had leaves remaining, so stomatal conductance measurements were confined to the control treatment. Four leaves per seedling were measured in each measurement round. Daily measurement rounds were carried out between 06:34 hours and 21:38 hours ensuring night time g_s was captured, with night time occuring on average between 19:15-06:30 hours. Porometer resistance measurements (m s^{-1}) were converted to stomatal conductance (mmol m^{-2} s^{-1}) using the equations provided by Bragg et al. (1991).

2.3.5   **Statistical analysis**

For all statistical tests performed for this study, the significance level (α) was set at 5%. Repeated measures ANOVA with between-subject factor Drought (3 levels) and between-subject factor Time (115 levels) was performed on daily maximum day-time sap flow, daily maximum night-time sap flow, the ratio of daily maximum nocturnal to day-time sap flow, daily absolute growth and daily stem water recovery. If Mauchly's sphericity (ε) test statistic was significant ($\varepsilon > 0.75$), the Greenhouse-Geisser correction was used, else the Huynh-Feldt correction was preferred for the within subjects test. The Bonferroni procedure was used for confidence interval adjustment and post-hoc tests.

Cross correlation (CCR) analyses were performed to identify correlations and time lags between the environmental variables (x: T, RH, VPD, PAR and SWP) and the physiological responses (y: sap flow and stem diameter variations). The 5-minute dataset of the first 30 days of drought was used as input for all treatments as all treatment plants still had viable leaves. CCR analyses were performed individually per seedling and analyzed per treatment to determine the overall time lags and correlations. A one way ANOVA (univariate analysis) with the drought treatment as factor was performed on the CCR values to yield means and standard errors and to determine between which group means statistical differences arose. When group sizes were not equal the Scheffe test was used, otherwise the Tukey test was preferred. If Levene's test indicated the equal variance assumption was violated ($P<0.001$), between groups (ANOVA) and robust test of equality means (Welch and Brown-Forsythe) were checked. If they were significant ($P<0.001$) then the null hypothesis was rejected as there was a statistically significant difference among the group means. If these were not significant, the Tamhane's T2 test for unequal variance was used. The between subjects effects (treatment) was checked. If ($P<0.05$), the null hypothesis was rejected as there was a significant treatment effect. The Post Hoc test indicated where the statistical difference was ($P>0.05$; not significant; $P<0.05$ significant). Lower and upper bound 95% confidence intervals for estimated marginal means were checked for overlap.

Stomatal conductance (g_s) for the three control seedlings was split into day and night and correlated with PAR, RH, T and VPD using Spearman's correlation. A two-tailed test was performed and a 95 % confidence interval was chosen. All statistical tests were performed using SPSS 23.0 (SPSS, Inc. Chicago, IL, USA).

2.4   Results

2.4.1   Soil water potential

Soil water potential of the control treatment decreased slightly during the first 38 days, to -0.5 MPa and then recovered to the original 0 MPa value from day 100 onwards (Figure 2.4A).

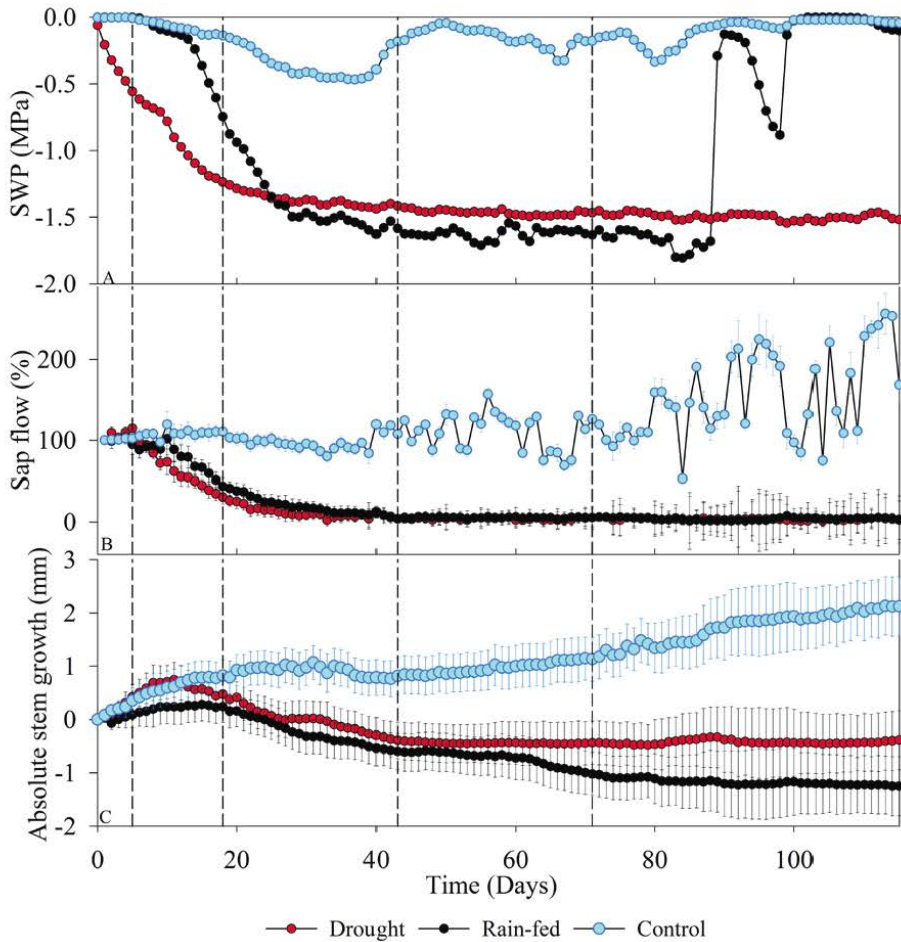**Figure 2.4** *M. eminii* seedlings' maximum day-time sap flow (B) and daily absolute stem growth (C), and their respective standard error bars per treatment during different soil moisture conditions (A). Control seedlings are coloured cyan, drought is red and the rain-fed is coloured black. The black vertical dashed lines indicate selected days (Days: 5, 18, 43 and 71), which are displayed in **Figure 2.5**.

Soil water potential dropped very rapidly after the onset of the drought treatment to reach -0.75 MPa after 10 days and then decreased further to -1.3 MPa after 24 days. Afterwards, it kept decreasing slightly. The limited amount of rain in the long rainy season caused the rain-fed treatment to be a treatment in between the control and the drought treatment. In the first 12 days, its SWP was the same as the control treatment, but then SWP dropped rapidly, reaching values of about -1.5 MPa after 28 days, after which SWP continued to decrease slowly. It peaked on day 88 when rains returned (Figure 2.3E) and then fluctuated as rain became periodical again.

2.4.2   Plant growth

At the end of the experiment, the recorded increase in seedling height was -0.03±0.84 cm for drought, 3.8±1.0 cm for rain-fed and 16.0±5.0 cm for the control treatment. At this point in time, drought and rain-fed plants had completely wilted leaves with the exception of one individual from the rain-fed treatment having five viable green leaves. The control seedlings had gained 55±17 leaves.

2.4.3   Sap flow

Repeated measures ANOVA revealed that there was a very significant interaction (all P< 0.001) between drought treatment and the time factor for daily maximum sap flow (Figure 2.4B) and absolute growth (Figure 2.4C).

In the first few days and despite the immediate drop in SWP of the drought treatment, sap flow of the three treatments was very similar. Sap flow for drought and rain-fed treatments declined respectively 6 (-0.6 MPa) and 10 (-0.1 MPa) days after the start of the treatment period (Figure 2.4B). Sap flow in the control treatment remained strongly coupled with atmospheric parameters (Figure 2.3 and Figure 2.4B). Figure 2.5 shows the diurnal and nocturnal sap flow pattern for four different days. The sap flow pattern was very similar for all treatments on day 5 (Figure 2.5A). However, the drought treatments had a strong and increasing impact on the sap flow patterns on days 18 (Figure 2.5B), 43 (Figure 2.5C) and 71 (Figure 2.5D) noted by decreased stem increment. For the first three selected days (5, 18 and 43), the relation between sap flow and VPD is plotted in Figure 2.6. This shows clockwise hysteresis loops, for all days and all treatments (Figure 2.6A-2.6B). Day 43 showed this similar loop for control (Figure 2.6C) with the relation for drought and rain-fed being highly obscured because of the very limited sap flow. For the control treatment, sap flow increases strongly until VPD is about 1 kPa and then levels off.

Based on the 5 minute-dataset, sap flow was highly correlated with all microclimatic variables, and most strongly with PAR. No significant time lag was observed between SF and any microclimatic variables, so the plants responded immediately to changes in environmental variables. Correlations between the microclimatic variables and the plants were highest for the

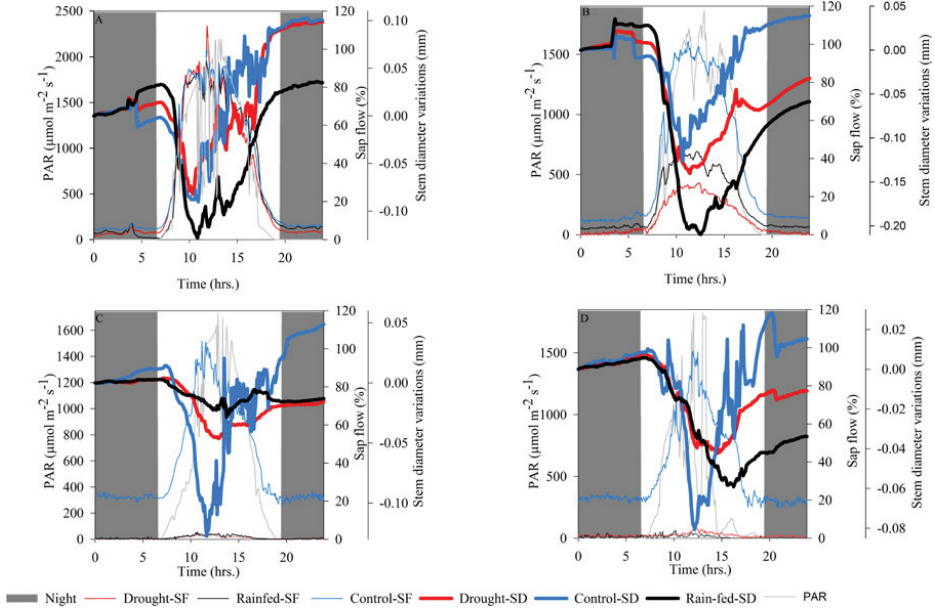control plants. The rain-fed and drought treatment plants were more strongly correlated to SWP (Table 2.2).

Figure 2.5 *M. eminii* mean sap flow and stem diameter variation patterns (shrinkage and swelling) for the three treatments as soil water potential declined on drought days (A) 5, (B) 18, (C) 43 and (D) 71. The photosynthetic active radiation (PAR) is the light grey line, sap flow is coloured lightly and stem diameter variations, darker. For the treatments, drought is red, control is blue and rain-fed is black. Night-time is shown by the dark grey shaded area; the white portion is day-time.
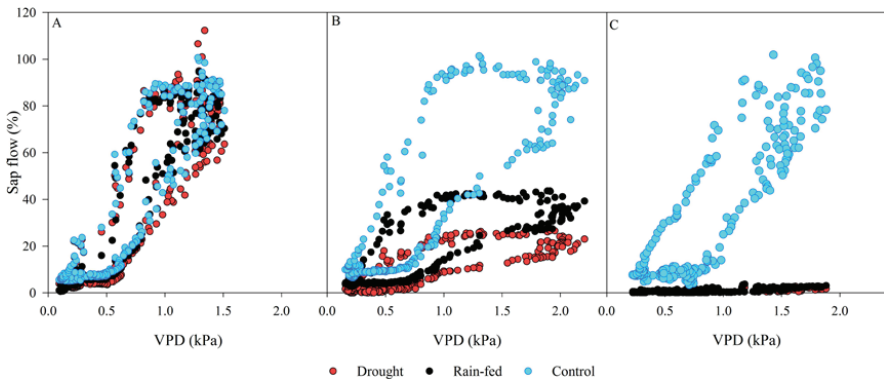

Figure 2.6 Clockwise hysteresis loops for *M. eminii* on day 5 (A), 18 (B) and 43 (C) showing that VPD strongly influenced *M. eminii* sap flow behaviour.

Table 2.2 Averages and standard error values of cross-correlation (CCR) output of 5 minute dataset values for the first 30 days of treatment when all seedlings still had leaves computed per seedling and treatment using a one way between groups ANOVA (univariate). The CCRs show how *M. eminii* seedling's sap flow (SF) and stem diameter variations (SDV) correlated between themselves as well as with environmental variables experienced at the study site and how the treatments influenced this correlation. The standard error of the CCR analysis was 0.009. Time lags are measured in minutes. Underlined values are the highest. A 95% confidence interval was used. PAR is photosynthetic active radiation, RH is relative humidity, T is air temperature, VPD is the vapour pressure deficit and SWP is the soil water potential. Letters in superscript indicate significant differences between the drought treatments with [a] being the highest and [b] the lowest.

Variable		**Sap flow** (SF)			Stem diameter variations (SDV)		
		Control	Rain-fed	Drought	Control	Rain-fed	Drought
PAR	R-value	0.9±0.0[a]	0.7±0.1[ab]	0.6±0.0[b]	-0.4±0.1	-0.6±0.1	-0.3±0.1
	Lag	1.5±0.7	2.2±0.0	2.2±0.0	3±2	20±13	7±2
RH	R-value	-0.8±0.0[b]	-0.4±0.1[a]	-0.3±0.0[a]	0.4±0.1	0.6±0.1	0.3±0.1
	Lag	0±0	0±0	0±0	0±4	7±4	0±4
T	R-value	0.9±0.0[a]	0.6±0.0[ab]	0.5±0.1[b]	-0.4±0.1	-0.7±0.1	-0.4±0.1
	Lag	0±0	0±0	0±0	0±4	7±4	0±4
VPD	R-value	0.8±0.0[a]	0.5±0.1[b]	0.4±0.0[b]	-0.4±0.1	-0.6±0.1	-0.3±0.2
	Lag	0±0	0±0	0±0	0±3	5±3	0±3
SWP	R-value	0.0±0.1[b]	0.5±0.1[a]	0.5±0.1[a]	0.2±0.1	0.0±0.1	0.1±0.1
	Lag	0±0	0±0	0±0	0±0	0±0	0±0
SDV	R-value	-0.5±0.1	-0.5±0.2	-0.3±0.1			
	Lag	3±4	8±4	7±4			

Nocturnal sap flow (Figure 2.7A) was not zero and was strongly influenced by atmospheric conditions. Nocturnal sap flow pattern for drought (day 6; SWP = -0.6 MPa) and rain-fed (day 10; SWP = -0.1 MPa) plants started declining a day after and on the same day as the diurnal sap flow started decreasing. For the control, there is an increasing trend of nocturnal sap flow from the onset with the highest value recorded on day 110. The nocturnal sap flow trend in the control treatment closely followed atmospheric conditions. The ratio of nocturnal and diurnal sap flow (Figure 2.7B) indicates the highest ratio (approximately 1) was presented by the rain-fed treatment, followed by drought (approximately 0.5) and then the control (<0.5) treatment, indicating that more stressed trees lose relatively more water at night.

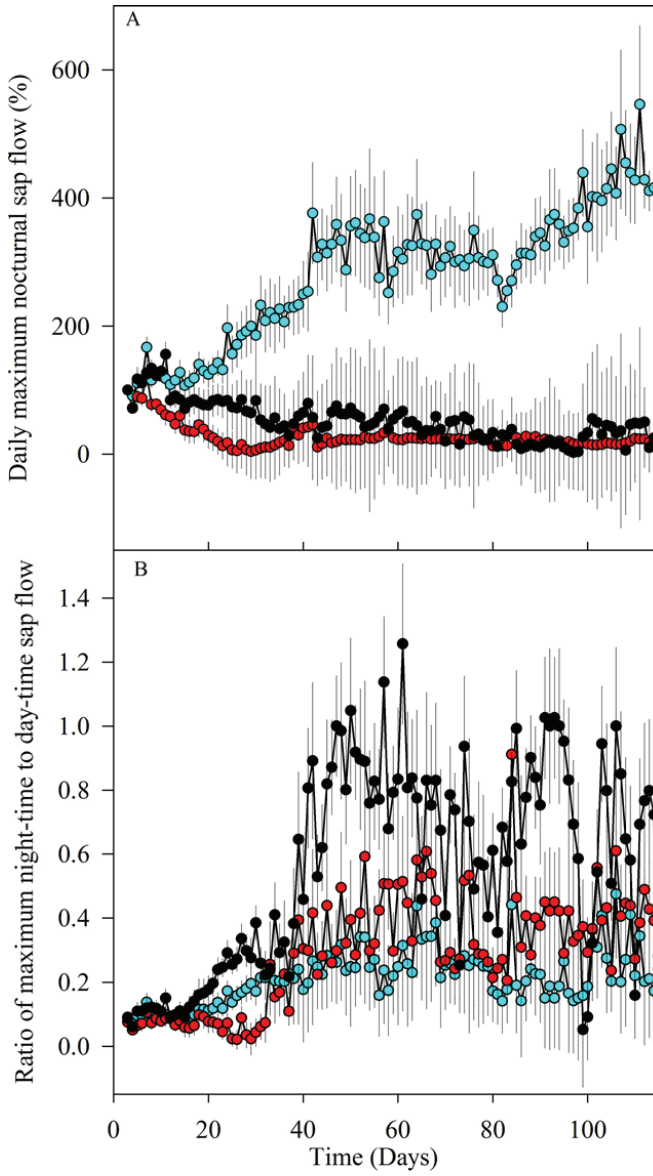**Figure 2.7** *M. eminii* seedlings nocturnal sap flow pattern (A) and ratios (B) with standard error values for the three different treatments; control (cyan), drought (red) and rain-fed (black). These values (in A) have been renormalized using the first day highest nocturnal sap flow value setting it to 100% and the rest were relative to it. The ratios (in B) were computed from non-normalized values.

2.4.4   Stem diameter variations

Initially, all treatments had a positive absolute growth trend, although this growth tended was lower for the rain-fed seedlings than for the control and drought ones (Figure 2.4C). The absolute stem growth declined for the drought treatment on day 11 (at SWP of -0.9 MPa), 11 days after the initial decrease in SWP and 5 days after SF started declining. Absolute stem growth of the rain-fed trees started decreasing on day 15 at SWP of -0.4 MPa, also 5 days after the initial decline in SF (Figure 2.4C). Diameter growth of the controls increased the first 18 days and continued regardless of SWP fluctuation, but then stabilized and became more coupled to SWP.

The stem diameter patterns did not differ between the treatments on day 5 (Figure 2.5A), with a strong decrease when sap flow starts flowing, and a recovery after the sap flow peak was reached. On the three other days, differences in the profiles between the treatments were evident (Figure 2.5B-2.5D). Stem shrinkage was more pronounced in the rain-fed and drought treatments compared to the control on day 18 (Figure 2.5). However, later in the experiment, the shrinkage and swelling was highest in control (Figure 2.5C-2.5D). After 115 days into drought stress (data not shown), drought-stressed and rain-fed seedlings continued to shrink and still had some sap flow recorded despite not having any viable leaves. This is confirmed in the analysis of the daily stem water recovery (Figure 2.8).
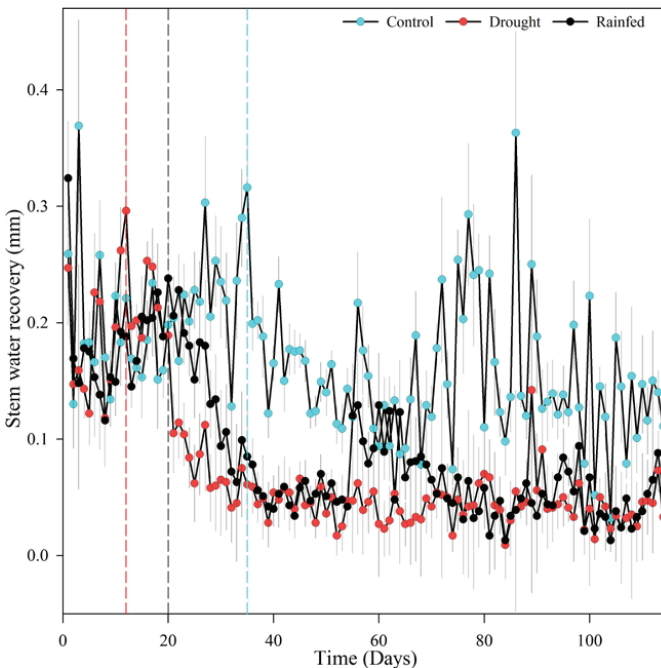

Figure 2.8 *M. eminii* seedlings' stem water recovery and standard error values for the control (cyan), drought (red) and rain-fed (black) treatment. The red vertical dashed line indicates when the drought treatment recovery started declining, the black is for the rain-fed and the cyan is for the control.

The daily stem water recovery of all treatments had an initial incremental profile but sharply declined beyond day 35 for control (SWP = -0.45 MPa), day 12 for drought (SWP = -0.97 MPa) and day 20 for rain-fed (SWP = -0.93 MPa) seedlings (Figure 2.8). The deviation profile exhibited by the rain-fed plants immediately before and after day 60 was due to rain water contribution (Figure 2.3 and Figure 2.8). The recovery of the control treatment remained rather irregular for the rest of the study period also following atmospheric conditions (Figure 2.3).

Like the SF data, SDV data were closely correlated to the environmental variables when looking at the 5 min dataset (Table 2.2), although correlations were lower than for the SF data. There were also small time lags between PAR and SDV for all treatments, and also between SF and SDV responses. Correlations between SDV and SWP were very low.

2.4.5 Stomatal conductance

M. eminii's stomatal conductance (g_s) as illustrated for a single day (Figure 2.9A) had a general incremental profile from predawn up to around 10:50 am after which it reduced as VPD increased. The mean day time g_s value for the selected day was 33 ± 24 mmol m^{-2} s^{-1} at VPD of 1.2 ± 0.6 kPa. The mean daily day time value for the entire campaign window of July and August was low: 39 ± 30 mmol m^{-2} s^{-1} at VPD of 1.1 ± 0.5 kPa.
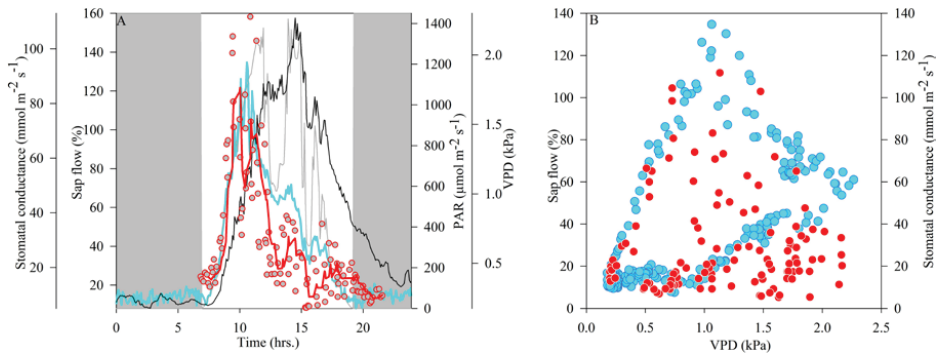
Figure 2.9 (A) Representation of a selected sunny day of the control treatment with non-pronounced fluctuating PAR (light grey line; 29 July (82 drought days)) depicting the 5 minute sap flow (thick cyan line) and 3 minute averaged stomatal conductance (g_s; grey circles with red edging) patterns to follow PAR. Vapour pressure deficit (VPD; black line) is noted to lag behind. A 5 point moving average forecast curve (thick red line) was fitted through the g_s point values. The dark grey portion represents night and the white, day time. (B) Hysteresis loops of 5 minute sap flow (cyan dots) and 3 minute averaged g_s (red dots) plotted as functions of VPD show coherence in *M. eminii* physiological responses to VPD.

Stomatal conductance measurements show that the earlier observed hysteresis loop for all treatments (Figure 2.6) was due to stomatal closure (Figure 2.9B). Nocturnal stomatal conductance was confirmed (Figure 2.5 and Figure 2.9A). The g_s were much lower during the night (11 ± 4 mmol

m^{-2} s^{-1} for a VPD range of 0.5±0.2 kPa) than the day (39±30 mmol m^{-2} s^{-1} for a VPD range of 1.1±0.5 kPa).

Statistical correlations revealed that day-time g_s were most strongly coupled to PAR followed by T. An exemplified illustration of how g_s closely followed PAR is depicted by Figure 2.9. In the night, g_s weakly coupled to RH, T and VPD (Table 2.3).

Table 2.3 *M. eminii* control seedlings' day and night stomatal conductance (g_s) values correlated with climatic variable of T (temperature), RH (relative humidity), VPD (vapour pressure deficit) and PAR (photosynthetically active radiation) using Spearman's bivariate correlation. Flagged values indicate: ** correlation is significant at the 0.01 level (2-tailed) and * correlation is significant at the 0.0 level (2-tailed).

	RH (%)	T (°C)	VPD (kPa)	PAR (μmol m^{-2} s^{-1})	N
Day					
g_s (mol s^{-1} m^{-2})	-0.037	0.076**	0.047*	0.307**	2709
Night					
g_s (mol s^{-1} m^{-2})	-0.051	0.173**	0.081	-	411

The typical clockwise hysteresis loops between g_s and VPD and, SF and VPD (Figure 2.9B) explain the relatively low correlation during the day compared to night as VPD increase provoked a decline in g_s and SF beyond VPD ranges of 0.9-1.13 kPa.

2.5   Discussion

When sap flow started decreasing as a consequence of reduced soil water availability, drought-stressed and rain-fed seedlings kept growing at high rates for five more days (Figure 2.4). This indicates that pioneer *M. eminii* seedlings prioritise growth despite decreases in soil moisture and the coupled down-regulation of sap flow (Figure 2.4). Control seedling's stem diameter growth was accompanied by fast height growth, which is characteristic of tropical pioneer species (Croat 1978, McCulloh et al. 2012). Fast vertical growth is a strategy to quickly outgrow competitors and escape herbivores (Pearson et al. 2003b, Pearson et al. 2003a), but may come at a cost as rapid growth is often associated with softer, less durable wood, as is the case in *M. eminii*. Less thick conduit walls might govern a hydraulic system that is more vulnerable to cavitation (Tyree et al. 1994, Hacke et al. 2006, McCulloh et al. 2011, McCulloh et al. 2012).

The observed hysteresis in both sap flow and stomatal conductance (g_s) (Figure 2.6 and Figure 2.9B) for drought and control treatments and the low g_s rates imply that even if water is available, *M. eminii* does not maximize its water use, but instead strictly controls its stomatal conductance, exhibiting a conservative water use strategy. Throughout all days, we observed that *M. eminii* on average started to close their stomata at a VPD threshold of about 1 kPa. This agrees with the general isohydric features of other trees of the D_{light} type, which generally close their

stomata at a VPD threshold to maintain leaf water potential at high levels and avoid cavitation risk (Borchert 1994, Maes et al. 2009). We observed that *M. eminii* responded to dry conditions by adjusting the leaf angle (parahelionasty) and curling, an effective measure to prevent leaf overheating when g_s is reduced when atmospheric conditions are demanding (Maes et al. 2011).

Despite stomatal control, *M. eminii* was not able to avoid water losses through transpiration. As long as there were leaves left on the plant, sap flow rates of rain-fed and drought-stressed seedlings were still significantly different from zero, even after soil water potential values dropped to very low values. Moreover, all treatments showed nocturnal sap flow. This was not caused by incorrect calculation of sap flow rates (parameter K setting; see M&M), because *i*) the nocturnal sap flow was significantly correlated to climatic conditions, and *ii*) it was confirmed by nocturnal g_s measurements of the control treatment seedlings. As such, it is clear that the plants were still 'leaking' water when they had leaves, not uncommon in mesomorphic leaves (Borchert 1994). The control seedlings had increasing nocturnal sap flow (Figure 2.7A), despite the fact that microclimatic conditions at night did not systematically become more demanding throughout the experiment (Figure 2.3). We believe the most likely reason for this observed increase is leaf area. Due to the moderate night-time g_s and VPD correlation (Table 2.3) we can assume that the observed nocturnal sap flow is a mere consequence of *M. eminii* not being able to fully control its stomatal conductance or lose water through the cuticular layer. The combination of this uncontrolled sap loss and water evaporation from the soil surface without replenishment, orchestrated an accelerated soil moisture loss. Once the soil water potential fell below -0.95±0.03 MPa (16±4 drought days), stem water recovery sharply declined (Figure 2.8). This indicates a depleted internal stem water reserve as the recovery deviation profile was comparably similar to shrinkage deviations observed by De Swaef et al. (2009) for their apple cultivars after approximately 3 days of drought stress linked to exhausted internal water reserves.

Species thriving within seasonally dry forests have a suit of traits that help them avoid or tolerate drought stress (Slot and Poorter 2007). Low wood densities, as observed in adult *M. eminii* trees (Chave et al. 2009), are indicative of high stem water content (Borchert 1994). In several tropical pioneer species (Markesteijn et al. (2011a, 2011b), McCulloh et al. 2012), high internal stem water storage may play an important role in coping with drought stress by contributing water to the transpiration stream when demand is high (Tyree and Yang 1990, Borchert 1994, Holbrook 1995). For our 15 month-old seedlings, the potential contribution of stored stem water in the bark at peak shrinkage is minimal. The data of our seedlings indicated that the daily shrinkage of the control seedlings was about 6.2% of its total volume (calculated as V = 0.5 H π r), amounting to only 0.44 cm of contribution water.

This very limited role of stem water for balancing tree water use was further reflected by small time lags between sap flow and environmental conditions (Table 2.2), where larger time lags

have been related to larger stem water storage (Goldstein et al. 1998, O'Grady et al. 1999, Phillips et al. 2003, Ford et al. 2004, Steppe and Lemeur 2004). Our findings of limited contribution of the stem water to buffering water use are in line with findings by Maes et al. (2009) in *Jatropha curcas* and by Chapotin et al. (2006) and Van den Bilcke et al. (2013) in Baobab (*Adansonia* sp). Nevertheless, we observed that most of the shrinkage occurred in the first two-three hours after sunrise and coincides with the sudden increase in sap flow (Figure 2.5). During this short period, internally stored stem water might still play a buffering role.

M. eminii seedlings periodically shed some but not all their foliage regardless of soil moisture, conferring drought avoidance and survival (Borchert 1994, Eamus 1999, Engelbrecht and Kursar 2003, Poorter and Markesteijn 2008, Tomlinson et al. 2013). Thin, soft leaves are relatively cheap to produce and shedding them avoids maintenance costs during the dry season (Eamus 1999). However, when leaves are shed, no carbon can be fixed (Eamus 1999, Pearson et al. 2003a) leaving the plant to rely on reserves to support root and shoot respiration (Eamus 1999) and for the flushing of new leaves in the next wet season. Flushing is possible because just before the rains return, new leaves are formed.

In conclusion, this study demonstrates that interplay of mechanisms are invoked by *M. eminii* to cope with drought stress. While as a pioneer species, it is adapted to fast growth and fast response to favorable growth conditions, strict stomatal control, leaf shedding and tension buffering via internally stored bark water allows the seedlings to also cope with drought stress periods.

3 Photosynthesis and photoassimilate distribution in ^{11}C-labeled leaves reveal an unexpected carbon strategy in the African tropical tree species *Maesopsis eminii*

3.1 Abstract

With carbon stocks expected to change under forecasted climate change and its potential feedbacks, it is now more than ever important to better understand tropical forests carbon balances. Strategies for carbon phloem loading and transport in the tropical African terrestrial biome are however heavily understudied. We combined measurements of net photosynthesis with ^{11}C-labelling and ^{13}C stable isotope analyses on leaves of 3-year-old potted *Maesopsis eminii* Engl. trees in order to understand its leaf carbon strategy. Surprisingly, this fast-growing pioneer tree species showed low photosynthetic rates during well-watered reference conditions (5.0 ± 2.2 μmol m^{-2} s^{-1}), which further decreased in response to soil-drought. *M. eminii* is C$_3$ in nature (δ^{13}C analysis), but the leaves showed interesting ^{11}C distribution patterns, pointing to putative C$_4$-like bundle sheath cells around the veins. Improved leaf carbon export rate and enhanced hydraulic integrity were therefore proposed to explain this pioneer species' capacity to rapidly grow despite its low photosynthesis rates. Given this unexpected leaf carbon strategy, we recommend more studies like this one for African tree species, especially if we aspire to make more reliable predictions with our dynamic vegetation models.

3.2 Introduction

There have been quite a few climate change impact studies on tropical African forests (Fauset et al. 2012, Asefi-Najafabady and Saatchi 2013, James et al. 2013, Malhi et al. 2013a, Oslisly et al. 2013, Otto et al. 2013, Ouédraogo et al. 2013, Willis et al. 2013, Zhou et al. 2014, Schippers et al. 2015). But only seldom do these studies include measurements of photosynthesis (dosAnjos et al. 2015), respiration (Atkin et al. 2015) or carbon fluxes (Cao et al. 2001, Williams et al. 2007, Ciais et al. 2009, Hiernaux et al. 2009, Ciais et al. 2011, Washington et al. 2013). And even if incorporated, most of the reported values are model-based (Williams et al. 2007, Fauset et al. 2012). And yet, evidence is increasing that correctly assessing tropical carbon stocks faces many challenges (Kearsley et al. 2013, Chave et al. 2014, Picard et al. 2015), and a lively debate exists on how to correctly implement tropical biomass models (Saatchi et al. 2015). This points to the relevance of increasing our knowledge on the ecophysiological mechanisms underlying carbon assimilation.

Photosynthesis, respiration, carbon transport and allocation are not only linked (Flexas et al. 2005, Flexas et al. 2006, Fatichi et al. 2014, Kolari et al. 2014, Malhi et al. 2015, Varone and Gratani 2015), but are the quickest avenues for assessing terrestrial carbon balances (Lewis et al. 2011). Moreover, the impact of water status on the aforementioned processes is manifold (De Schepper et al. 2013, Fatichi et al. 2014, Mencuccini 2014, Sevanto 2014, Hubeau and Steppe 2015, Steppe et al. 2015). A combination of (i) light response curves to characterise plant species photosynthetic behaviour (Wang et al. 1995, Cannell and Thornley 1998, Thornley 1998, Ye 2007, Greer and Weedon 2012, Ye et al. 2013, Kolari et al. 2014, Xu et al. 2014, Fang et al. 2015), (ii) ^{13}C stable isotope analysis to determine the plant's metabolic pathway for carbon fixation (Epron et al. 2012, Zuidema et al. 2013), and (iii) positron autoradiography, which yields high-resolution distribution images of the radioactive ^{11}C isotope (Bloemen et al. 2015), and allows studying carbon allocation (Kiser et al. 2008), were used to better understand the leaf carbon strategies in a common tropical tree species.

Undoubtedly, such measurements for Africa are necessary as this continent dominates global inter-annual variability in terrestrial carbon cycling (Cao et al. 2001, McGuire et al. 2001, Williams et al. 2007, Fisher et al. 2013), and net CO_2 fluxes in tropical forests are not well understood (Doughty et al. 2015, Malhi et al. 2015). Furthermore, droughts make it difficult to understand carbon fluxes in forests as water deficit may lead to both hydraulic failure and carbon starvation, with the interpretation being further hampered by the different time scales involved (van der Molen et al. 2011, Sala et al. 2012, Sevanto et al. 2014, Doughty et al. 2015, Hubeau and Steppe 2015). It is therefore crucial to acknowledge the limitations of an exclusively large-scale modeling approach to map carbon fluxes, and support the need for ecophysiological studies and the

comparison of scaled chamber measurements with ecosystem-scale flux measurement to validate these models (Ryan et al. 1996, van der Molen et al. 2011, Gustafson et al. 2015).

Because seedlings and saplings due to their shallow roots are pivotal for a tree species survival or death (Tyree et al. 2003, Engelbrecht et al. 2005, Padilla and Pugnaire 2007, McDowell et al. 2008, Markesteijn and Poorter 2009, Brodribb et al. 2010, Niinemets 2010, Matías et al. 2012), 3-year old tropical trees of a multipurpose pioneer drought-deciduous tree species *Maesopsis eminii* Engl. were used. The aim of our study was to (i) determine *M. eminii*'s leaf carbon strategies during soil-drought and well-watered reference conditions, (ii) determine the impacts of soil-drought on *M. eminii*'s leaf carbon fluxes and carbon balance estimates, and (iii) reflect on the impact of our study on general predictions made with dynamic global vegetation models.

3.3   Materials and Methods

3.3.1   Site description

The study was conducted between May and October 2015 in a tropical greenhouse (6.4 m wide, 9.6 m long and 4.75 m high) of Ghent University, Belgium (50°59.58'N, 3°47.04'E). Light within the greenhouse was supplied by natural solar radiation in combination with nine Philips bulbs of 200 W. A 14-h photoperiod was used, with lights turned on between 0700 h and 2100 h. Air temperature ranged between 18°C and 35°C and relative humidity of the air was set at 70 %. A HortiMaX MT/MTV sensor unit measured the interior microclimate.

3.3.2   Experimental set-up

Fifteen 3-year-old *Maesopsis eminii* Engl. trees were used. At the start of the experiment, the trees were 2.3 ± 0.4 m tall and had a stem diameter of 21 ± 5 mm, measured at 40 cm above root collar. The trees were grown in 35-L bottom perforated pots containing peat soil, and were germinated from randomly picked seeds of unselected parent plants thriving in Mabira forest, Uganda (0°23.357'N, 33°0.344'E). Trees were randomly distributed on tables raised to a height of 0.75 m above ground and were irrigated three times a day for four minutes using an automatic flood-table irrigation system to ensure unstressed reference conditions with ample soil water. Irrigation water consisted of a mix of rainwater and soluble fertilizer (NPKMg ratio: 19:8:16:4, boron (0.02 %), copper (0.03 %), iron (0.038 %), manganese (0.05 %), molybdenum (0.02 %) and zinc (0.01 %)) with a solution pH of 5.7.

For the first 13 days (~2 weeks) of the experiment, all trees were subjected to soil-drought by completely turning off daily irrigation. Black round plastic plant pot trays were used to prevent potted seedlings tapping stagnant water on the tables. Subsequently, for the remainder of the

experiment, all young trees were well-watered with the same irrigation scheme as before the drought treatment, three times a day for four minutes.

3.3.3   Photosynthesis measurements

It should already be noted from the onset that our measurements commenced with a drought treatment. The control measurement is taken 16 weeks after drought treatment. This is a valid alternative when control measurements prior to drought are not possible. Also, photosynthesis measurements were always performed on new leaves and not old ones that might have been damaged or influenced by drought. Net photosynthesis was measured three times during the experiment. Characterization of the drought response was done after two weeks of soil-drought (T_0), followed by the recovery response after three (T_3) weeks of rewatering. In this study, well-watered reference conditions were measured sixteen (T_{16}) weeks after the drought treatment, when trees were fully recovered and unstressed. Net photosynthesis (P_n) was measured on the upper most sun leaf of all fifteen trees with a portable photosynthesis system (LI-6400; LiCor Biosciences, Lincoln, NE, USA) (Figure 3.1). As illustrated in Fang et al. (2015), irradiance was gradually increased from 0 to 2000 µmol m^{-2} s^{-1} in five steps (0, 50, 100, 1250 and 2000 µmol m^{-2} s^{-1}), each lasting 3 minutes, and leaf gas exchange was determined, while keeping the atmospheric CO_2 concentration at 400 µmol CO_2 m^{-2} s^{-1} and block temperature at 24°C. All light response curves were measured between 10h and 16h.

Figure 3.1 Photosynthetic measurements being done on an *M. eminii* seedling using a LICOR in the tropical greenhouse at ILVO

3.3.4 From light response curves to carbon fluxes

A light response curve (LRC) per measurement day was fitted using the non-rectangular hyperbola (NRH) model (Fang et al. 2015; Eq. 1):

$$P_n(I) = \frac{\alpha I + P_{n,max} - \sqrt{\left(\alpha I + P_{n,max}\right)^2 - 4 I \alpha \theta P_{n,max}}}{2\theta} - R_d \qquad \text{(Eq. 1)}$$

with $P_n(I)$ (μmol CO_2 m^{-2} s^{-1}) the net photosynthetic rate, I the light intensity (μmol PAR m^{-2} s^{-1}), α the initial quantum efficiency (μmol CO_2 (μmol PAR)$^{-1}$), $P_{n,max}$ the maximum photosynthetic rate (μmol CO_2 m^{-2} s^{-1}), R_d the dark respiration rate (μmol CO_2 m^{-2} s^{-1}), and θ the dimensionless or sharpness parameter fixed to a value of 0.5 (Lieth and Reynolds 1987, Thornley 1998, Calama et al. 2013). Important to note is that in the original equation presented by Fang et al. (2015) $P_{n,max}$ does not yield maximum net photosynthetic rate, but maximum gross photosynthetic rate as can be deduced from the limit calculation of P_n for an infinite light intensity (Eq. 2).

$$\lim_{I\to\infty} P_n(I) = P_{n,max} - R_d = P_{max} \qquad\qquad \text{(Eq. 2)}$$

To avoid any confusion, we will henceforth use P_{max} ($\mu mol\ CO_2\ m^{-2}\ s^{-1}$) to indicate maximum net photosynthetic rate.

In addition, the light compensation point (I_c) (Eq. 3; Fang et al., 2015) and the light saturation point (L_s) at 70 % P_{max} ($\delta = P_n/P_{max} = 0.7$) (Eq. 4; Wang et al. 1995) were calculated per measurement day:

$$I_c = \frac{R_d P_{n,max} - \theta R_d{}^2}{\alpha(P_{n,max} - R_d)} \qquad\qquad \text{(Eq. 3)}$$

$$L_s = \frac{\delta P_{max}}{\alpha}\left(\frac{\delta-\theta}{1-\delta} + \theta(1+\delta)\right) + I_c \qquad\qquad \text{(Eq. 4)}$$

Next, a 7-day reference period of diel PAR was used to calculate net photosynthetic rates with the three developed LRCs (one per measurement day). Simulated courses were integrated to obtain day- and nighttime carbon fluxes.

$^{11}CO_2$ leaf labeling

Following a promising preliminary experiment on *M. eminii* leaves in December 2014, an unstressed reference tree (T_{16}) was transferred to INFINITY in October 2015, the pre-clinical imaging lab of Ghent University, Belgium, to carry out ^{11}C-labeling and autoradiography. Just before labeling, a primary branch was excised under water to avoid cavitation, and was kept in a sealed container with water. Its secondary branch with both old and young leaves was secured, while still being attached to the primary branch, in an air-tight custom-made transparent cylindrical chamber (20 cm length and 15 cm diameter). A series of red and blue light emitting diodes (LEDs) where placed on top of the cuvette yielding 250 $\mu mol\ m^{-2}\ s^{-1}$ PAR at leaf surface. The cuvette was tubed (inner diameter 4.0 mm and outer diameter 5.6 mm) to a LI-6400 (LiCor Biosciences, Lincoln, NE, USA), which provided an inflow ($\pm$ 0.8 L min^{-1}) with constant humidity and a 400 ppm CO_2 concentration, and the outflow was directed to a container with KOH base to trap all $^{11}CO_2$ exiting the cuvette. The set-up was checked for leakages by ensuring an equal in- and outflow rate.

The chamber also had a thin inlet tube (inner diameter 0.9 mm and outer diameter 1.5 mm) for administering radioactive $^{11}CO_2$ isotope tracer gas, with a half-life of 20.4 minutes, into the cuvette. This inlet tube was lead-shielded to reduce exposure during gas injection. About 10 mCu initial label activity was transferred into the leaf chamber. During injection, air flow was switched off and the leaves were exposed to the tracer for 10 minutes. Thereafter, the air flow was switched on again to remove all $^{11}CO_2$ from the air surrounding the leaves. The leaves were left in the chamber for an additional hour before excision and autoradiograph imaging (Figure 3.2).

Figure 3.2 Left to right: An excised *M. eminii* branch with secondary branch placed in chamber and inserted into a radiation shield chamber

3.3.5 Positron autoradiography

Distribution of the labeled carbon was imaged by cutting the exposed leaves, and putting them on a multisensitive imaging phosphor screen (Perkin Elmer, Waltham, MA), which is sensitive for high-energy radiation. The screen was digitally scanned after 10 min exposure using a Cyclone Plus Phosphor imager (Perkin Elmer, Waltham, MA) and the autoradiograph was quantified using OptiQuant software (Perkin Elmer, Waltham, MA) (Bloemen et al. 2015). These images were further processed with Fiji, an image processing software (Schindelin et al. 2012). Leaf autoradiography was repeated on three branches.

3.3.6 Stable δ^{13}C isotope analysis

To determine *M. eminii*'s metabolic pathway for carbon fixation, leaf stable carbon isotope analysis (δ^{13}C) was performed on a sample of thirty randomly selected old and young T_{16} leaves. These were pre-weighed and oven-dried at 80°C for five days until constant dry weight was achieved. Thereafter, they were ground to fine powder using a ball mill (ZM200, Retsch, Germany). δ^{13}C was determined using an Elemental Analyzer (ANCA-SL, SerCon, Crew, UK) coupled to an Isotope Ratio Mass Spectrometer (20-20, SerCon, Crew, UK) (EA-IRMS). Baking flour with a δ^{13}C value of −27.01‰ (certified by IsoAnalytical, UK) was used as a laboratory reference, and all δ^{13}C are expressed relative to Vienna Pee Dee Belemnite (VPDB).

3.3.7 Data analysis and statistics

For each set of measuring points a light response curve (LRC) was fitted according to the NRH model. The R^2 was determined and modeled curves with a $R^2 < 0.9$ were removed from the analysis. This resulted in at least ten LRCs per measurement day used in the analysis. Parameter

values were estimated for each individual LRC and averaged per measurement day. Because the distribution of the model values was not normal, a non-parametric Kruskal-Wallis test was performed (Kruskal and Wallis 1952), followed by the Dunn's post-hoc multiple comparison test (Dunn 1964) with a Bonferroni adjustment used to generate significance levels for differences between the three measurement days.

3.4 Results

3.4.1 *M. eminii*'s photosynthesis during soil-drought

Overall, *M. eminii* showed low P_n values: during drought (T_0) when the combined weight of pot and tree was on average 35% lower compared to T_3 and T_{16}, three weeks after re-watering (T_3) when new leaves were resprouting, and also when trees were in unstressed conditions with ample soil water reserves (T_{16}). Under soil-drought, measured P_{2000} was only 2.0 ± 1.0 µmol m^{-2} s^{-1}, which more than doubled to 5.0 ± 2.2 µmol m^{-2} s^{-1} under reference conditions (T_{16}) (Figure 3.3, Table 3.1).
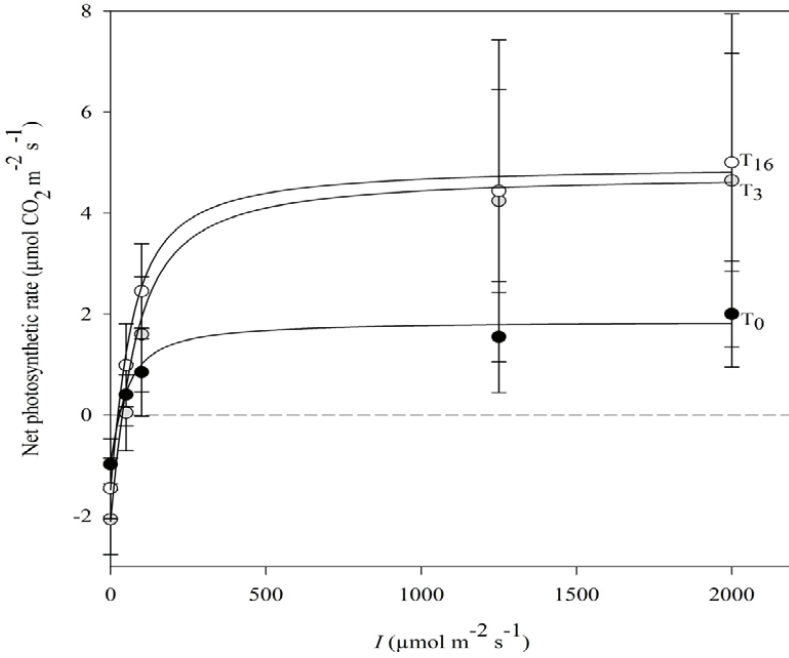
Figure 3.3 Measured light response curves per potted *Maesopsis eminii* leaf were individually run in the NRH model (Fang et al. 2015) to obtain average model parameters from which an average light response curve per measurement day was developed. Net photosynthesis (P_n, µmol CO_2 m^{-2} s^{-1}) increases with increasing light intensity (I, µmol m^{-2} s^{-1}). Points were obtained by averaging all measurement points of the same measurement day exposed to the same amount of light. Error bars are standard deviation of the average values. T_0 (drought), T_3 and T16 (resp. 3 and 16 weeks after rewatering) are depicted with black circles, grey circles and open circles, respectively.

Table 3.1 Averages of measured and modeled light response curve (LRC) values per measurement day with standard deviations based on n LRCs depicting measured net photosynthetic rate P_{2000} (µmol CO_2 m^{-2} s^{-1}) at a light intensity of 2000 µmol m^{-2} s^{-1} and dark respiration rate R_d (µmol CO_2 m^{-2} s^{-1}) values, in addition to non-rectangular hyperbolic (NRH) model predicted values of P_{2000}, R_d, maximum net photosynthetic rates P_{max} (µmol CO_2 m^{-2} s^{-1}), photosynthetic efficiency or slope (α) (µmol CO_2 (µmol PAR)$^{-1}$), light saturation point L_s (µmol m^{-2} s^{-1}), light compensation point I_c (µmol m^{-2} s^{-1}), and R^2 values describing the correlation coefficient between measured points and their individually fitted light response curves.

	Measurement day	T_0	T_3	T_{16}
	n	10	12	10
Measured values	P_{2000}	2.0 ± 1.0	4.6 ± 3.3	5.0 ± 2.2
	R_d	1.0 ± 0.5	2.1 ± 0.7	1.5 ± 0.6
	P_{2000}	1.8 ± 1.1	4.5 ± 3.3	4.8 ± 2.1
	R_d	1.0 ± 0.5	2.1 ± 0.7	1.5 ± 0.6
	P_{max}	1.9 ± 1.1	4.8 ± 3.6	4.9 ± 2.2
NRH model predicted values	α	0.04 ± 0.02	0.07 ± 0.02	0.07 ± 0.03
	L_s at 70% P_{max}	80 ± 64	71 ± 49	27 ± 21
	I_c	50 ± 42	33 ± 20	27 ± 13
P_n (Measured vs. NRH)	R^2	0.983	0.997	0.994

Despite the large natural variability, a clear difference existed between soil-drought and unstressed trees, with measured averaged P_{2000} and R_d both lowest during soil-drought (T_0) (Table 3.1). From the simulated LRCs important photosynthetic parameters were derived. Soil-drought P_{max} significantly differed from P_{max} after re-watering and P_{max} obtained under reference conditions ($T_0 < T_3 \approx T_{16}$; T_0-T_3 ($P < 0.01$), T_0-T_{16} ($P < 0.01$), T_3-T_{16} ($P > 0.05$)). R_d values only significantly differed between soil-drought and 3 weeks after rewatering (T_0-T_3 ($P < 0.00$), T_0-T_{16} ($P > 0.05$), T_3-T_{16} ($P > 0.05$)). The initial quantum efficiency (α) reduced under soil-drought (T_0-T_3 ($P < 0.01$), T_0-T_{16} ($P < 0.05$), T_3-T_{16} ($P > 0.05$)). Other photosynthetic parameters were not significantly affected by drought. Differences in LRC (Figure 3.3) showed that soil-drought significantly reduced *M. eminii*'s photosynthetic behaviour. In general, measured LRCs retained for analysis corresponded very well with their individually fitted NRH model (T_0; R = 0.983, T_3; R = 0.997, T_{16}; R = 0.994).

3.4.2 Estimated diel carbon fluxes and leaf carbon balances

Illustratively, diel carbon flux dynamics of *M. eminii* trees were projected for drought-stressed, recovered and reference conditions (Figure 3.4A).
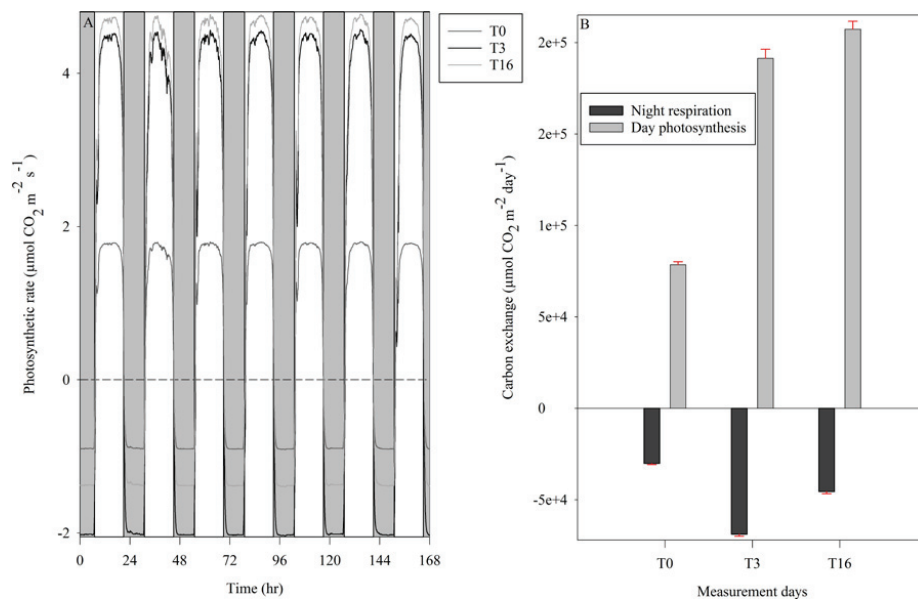
Figure 3.4 (A) Simulated photosynthetic rates (μmol CO_2 m^{-2} s^{-1}) for a 7-day reference week using the average NRH model per measurement day. Daytime was 0700 h – 2100 h and nighttime 2100 h – 0700 h. (B) Photosynthetic rates (μmol CO_2 m^{-2} day^{-1}) were converted to carbon exchanges represented as night respiration and daytime photosynthesis. Bars higher than 0 μmol CO_2 m^{-2} day^{-1} indicate net photosynthesis, and lower net respiration. Error bars were obtained as standard deviation (coloured red) from the average values for the reference week.

Integrated day and nighttime carbon exchange showed that nighttime CO_2 release was always less than daytime net CO_2 fixation (Figure 3.4B), but total net carbon accumulation (T_0: 48 ± 2 x 10^3 µmol CO_2 m^{-2} day^{-1}, T_3: 122 ± 5 x 10^3 µmol CO_2 m^{-2} day^{-1}, T_{16}: 162 ± 4 x 10^3 µmol CO_2 m^{-2} day^{-1}) significantly decreased with soil-drought (T_0-T_3 ($P \approx 0.05$), T_0-T_{16} ($P < 0.00$) and T_3-T_{16} ($P \approx 0.05$)). These values of CO_2 uptake can be converted (according to Larcher (2003); 1 g $CO_2 \approx 0.285$ g C ≈ 0.625 g organic DM) in carbon assimilation (T_0: 0.61 ± 0.02 g C m^{-2} day^{-1}, T_3: 1.54 ± 0.06 g C m^{-2} day^{-1}, T_{16}: 2.03 ± 0.05 g C m^{-2} day^{-1}) or gain in dry organic matter (T_0: 1.33 ± 0.04 g org. DM m^{-2} day^{-1}, T_3: 3.37 ± 0.12 g org. DM m^{-2} day^{-1}, T_{16}: 4.45 ± 0.11 g org. DM m^{-2} day^{-1}). During days with soil-drought (T_0), 38 ± 1 % of daily fixed carbon was respired and lost at night. After three weeks, the trees were not yet fully recovered because still 36 ± 1 % was respired during the night. After 16 weeks, nighttime respiration of the unstressed trees was lower being only 22.0 ± 0.6 % of the daily fixed carbon, which implies that more carbon was available for growth, storage and defense processes (Figure 3.4).

3.4.3 ^{11}C autoradiographs and ^{13}C stable isotope

Autoradiographs displayed a high correspondence of absorbed gaseous $^{11}CO_2$ isotope tracer with venation (Figure 3.5).
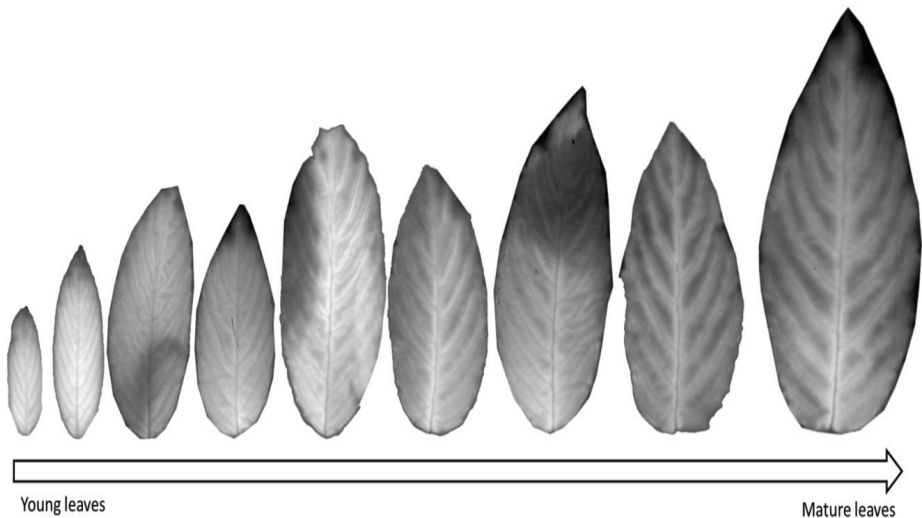
Figure 3.5 Typical example of positron autoradiographs arranged from younger to older *Maesopsis eminii* leaves showing the distribution of ^{11}C, 1 h after $^{11}CO_2$ was administered to an excised branch. Brighter regions reflect higher ^{11}C accumulation. Younger leaves have a uniform carbon distribution across the leaf blade, while the older leaves show a higher accumulation around the primary and secondary veins, suggesting a C_4-like bundle sheath mechanism.

In younger leaves, the signal is nearly equally distributed across the leaf blade, whereas in the older leaves the signal concentrated more around, but not inside, the primary and secondary veins. Interestingly, in all leaves, signal strength was lower inside primary and secondary veins. While the higher carbon label in the area around the veins might suggest a CO_2 concentration mechanism related to bundle sheath cells associated with C_4-metabolism, *M. eminii*'s stable carbon isotope signature ($\delta^{13}C$) was -26.81 ± 1.04 ‰, pointing to a C_3-metabolism (O'Leary 1988).

3.5 Discussion

Scarcity of studies within the field of leaf carbon uptake and fluxes, and their drought responses for the African terrestrial biome raises uncertainty about its contribution to the global carbon budget, especially in this drought-prone-era. We address these issues by investigating the leaf carbon metabolism of the African tree species *M. eminii* during soil-drought stress, during recovery and in unstressed reference conditions. The study aim was not only to try to bridge this knowledge gap, but also assess *M. eminii*'s leaf strategies for carbon assimilation and highlight that African tree species need to be explored to increase prediction certainty of dynamic global vegetation models, as these models are based on plant functional type traits (Scheiter et al. 2013).

Photosynthetic derived measurements showed that two weeks of soil-drought significantly reduces *M. eminii*'s P_n, an expected consequence of stomatal response to a depleting soil water status observed in trees and crops (Loustalot 1945, Upchurch et al. 1955, Hsiao 1973, Filella et al. 1998, Porporato et al. 2001, Flexas et al. 2005, Flexas et al. 2006, Gallé et al. 2007, De Swaef et al. 2009, Pantin et al. 2012, Koller et al. 2013). Full recovery was not yet attained after three weeks as pointed out by a higher R_d at T_3 compared with the reference condition (T_{16}) (Figure 3.3, Table 3.1). Interestingly, this is not shown in carbon assimilation during the day but is clearly visible in nighttime respiration (Figure 3.4) and the net daily carbon assimilation. Average P_{max} was reduced with 60 % by soil-drought (Figure 3.3, Table 3.1). Koller et al. (2013) reported a similar reduction in photosynthesis of about 60 % after three weeks of withholding water in three evergreen *Quercus* spp., comparable in height with our study. Varone et al. (2012) investigated several Mediterranean species, and observed a photosynthetic reduction of 50 % in less than a week.

The impact of a reduction in photosynthetic rate on a species' drought tolerance is not straightforward. On one hand, a species that keeps high photosynthetic rates under drought stress will grow faster, having a competitive advantage, and reduces as such the risk to suffer from carbon starvation (McDowell and Sevanto 2010, van der Molen et al. 2011, Sevanto 2014, Sevanto et al. 2014, Roman et al. 2015). But on the other hand, such a species will continue to have a higher water use during drought, eventually emptying its internal water reserves, which may ultimately lead to hydraulic failure (McDowell et al. 2008, van der Molen et al. 2011, Sevanto et al. 2014). In

contrast, a species with a more conservative water use will close its stomata during drought stress, and reduce its water loss, but also its carbon gain (McDowell et al. 2008, van der Molen et al. 2011, Sevanto et al. 2014). Being able to disentangle and understand which of both strategies are being used in an ecosystem is of utmost importance to project how this ecosystem will respond to drought episodes and in which timeframe (van der Molen et al. 2011, Roman et al. 2015, Steppe et al. 2015).

M. eminii is a known pioneer species characterised by fast growth (Eggeling 1947, Binggeli and Hamilton 1993, Viisteensaari et al. 2000, Hulme et al. 2013). This seems to contradict its relatively low measured P_{2000} values under well-watered conditions and modeled P_{max} (resp. 5.0 ± 2.2 μmol CO_2 m^{-2} s^{-1} and 4.9 ± 2.2 μmol CO_2 m^{-2} s^{-1} (Figure 3.3, Table 3.1)). Meir et al. (2007) conducted a study on several tree species in Cameroon's lowland tropical rainforest with P_{max} values in the range of 6 – 13 μmol CO_2 m^{-2} s^{-1}, with the pioneer species having the highest values. In Panama, Ellis et al. (2000) conducted photosynthetic measurements on a wide range of tropical trees to conclude that pioneer species had significant higher P_{max} values compared to non-pioneer species with an average P_{max} of 16.1 μmol CO_2 m^{-2} s^{-1}, which is well above the values presented in our study. In their study, Domingues et al. (2010) looked at photosynthesis in African savanna and semi-deciduous dry forest and all their reported values (> 7 μmol CO_2 m^{-2} s^{-1}) were higher than our P_{max} values for *M. eminii*.

Surpringsingly, we are thus dealing with a tree species with a seemingly low photosynthetic capacity, capable of pioneering forest gaps, attaining fast growth and outcompeting other species (Eggeling 1947, Binggeli and Hamilton 1993, Viisteensaari et al. 2000, Hulme et al. 2013). One important advantage of *M. eminii* is its large seeds which enables its freshly germinated seedlings to quickly grow to a considerable height without requiring much light (Binggeli and Hamilton 1993). After seeds reserves are being depleted, it typically has grown larger than other seedlings, populating the forest gap, and at this stage *M. eminii* becomes a light-demanding plant (Binggeli and Hamilton 1993). But then still, how does *M. eminii* prevent that it is being overtaken by other species with higher photosynthetic rates after the large-seed advantage has spent its force?

To acquire a better understanding of the carbon assimilation of *M. eminii*, we visualised carbon distribution in the leaves with ^{11}C-autoradiographs. Remarkably, the autoradiographs showed an unusual carbon distribution inside the leaf (Figure 3.5). In ^{11}C-analysis, differences in carbon distribution are used to explain prevailing sugar gradients (Turgeon 2010, Fu et al. 2011). Fu et al. (2011) used this analysis on many species to categorize whether the species utilized an active or passive phloem loading mechanism. Trees typically have a passive loading strategy, characterized by a higher concentration in the mesophyll and a lower concentration in the veins. Herbaceous species are typically active loaders, showing a higher concentration of sugars in their veins. In our study, the younger leaves showed the expected carbon distribution, indicating passive sugar loading into phloem vessels (Figure 3.5, Fu et al. 2011, Turgeon 2010). The higher sugar concentration in

the mesophyll creates a concentration gradient, which passively directs sugars from the mesophyll into the phloem. In mature *M. eminii* leaves however, the distribution changed with higher carbon accumulation close to primary and secondary veins compared to the mesophyll (Figure 3.5) and again lower concentrations within the veins, which points to a passive loading into the phloem, but an active concentration step near the veins. An up-concentration of carbon close to the veins suggests the presence of C_4-like bundle sheaths (Griffiths et al. 2013). Measured $\delta^{13}C$ clearly demonstrated that *M. eminii* uses a C_3 fixation pathway, based on the distribution reported by O'Leary (1988). C_3 have a $\delta^{13}C$ range of -21 to -35‰, and C_4 from -9 to -20‰ (O'Leary 1988). These C_4-like bundle sheath structures in *M. eminii* leaves introduce a myriad of benefits that could explain its fast growth despite low photosynthesis rates. The up-concentration of sugars in cells near the veins causes a high carbon concentration gradient between these cells and the phloem, possibly (i) increasing carbon export from leaves to sinks (e.g. shoots and roots) (Slewinski and Braun 2010, Turgeon 2010, De Schepper et al. 2013), (ii) improving efficiency of sugar transport (Jensen et al. 2013), and (iii) increasing growth potential (Turgeon 2010). Additionally, the rapid transport of assimilated carbon to the bundle sheath structures close to the primary veins also ensures a low mesophyll concentration, which reduces the chance of a negative feedback to the photosynthetic machinery (Turgeon 2010, De Schepper et al. 2013). This sugar loading strategy would still be defined as passive, but needs active loading in the bundle sheaths to maintain a higher sugar concentration. Such an active loading strategy is a trait typically ascribed to herbaceous species (Fu et al. 2011), which invest in growth across the year. Bundle sheaths also contribute to a safer hydraulic system, because there is a water potential barrier between leaf mesophyll and leaf veins, and its high sugars amount might contribute to carbon-assisted cavitation repair (Leegood 2008, Zwieniecki and Holbrook 2009, Griffiths et al. 2013).

The observed discrepancy between low P_n values in an established fast-growing pioneer species reveals how difficult it might be to accurately predict a species' behaviour without a minimum set of measured species-specific plant traits. This potential mismatch has previously been acknowledged by Fatichi et al. (2014), and highlights the need for thorough measurements, which will lay the ground for a better understanding of the ecophysiology of tropical trees, and their used strategies to cope with drought. This is a necessity if we aspire to predict the future of tropical ecosystems as important drivers of global carbon and water cycling.

The fact that we discovered these interesting leaf carbon strategies in *M. eminii* that may support drought delay and subsequently resilience draws us to the question: are current dynamic global vegetation model projections reliable for Africa? The answer is very uncertain because there remains a lack of studies on measured process-based traits in African tree species, such as LRCs or carbon distribution strategies, especially under drought stress. And yet, it is on these plant functional types (PFT) traits that dynamic global vegetation models are based. In order to resolve issues with dynamic global vegetation models we support the call of van der Molen et al. (2011) to

evolve from PFT-based models towards plant strategical properties (PSP) in which drought response strategies are better described. Much work remains to be done in the field of mapping PSPs of species worldwide, but we hope that studies like ours entice other researchers to study ecological strategies of tropical species.

Our study reports on the complexity of a tropical tree species' carbon assimilation and distribution strategy, and shows that measuring too few plant functional parameters can easily lead to wrong conclusions. But more importantly, it showed that the scarcity of data for Africa may lead to erroneous predictions based on plant functional traits. We believe that there is an urgent need for more plant strategical properties studies in tropical regions, such as leaf carbon studies, to further increase model certainty, particularly if we aspire to predict more accurately the impacts of climate change associated droughts in tropical regions.

4 Capacitive water release and internal leaf water relocation delay drought-induced cavitation in African *Maesopsis eminii*

4.1 Abstract

Paucity of xylem cavitation vulnerability studies of African tropical forest species translates into increased uncertainty of how its tree species will cope with increased drought frequency and severity. We investigated the hydraulic functioning of whole-branch segments of a widely distributed tropical, fast-growing timber tree species *Maesopsis eminii* Engl. during bench-top dehydration. Cumulative acoustic emissions and continuous weight measurements were used to quantify *M. eminii*'s vulnerability to drought-induced cavitation and hydraulic capacitance. Wood anatomical traits, including wood density, vessel area, diameter and wall thickness, vessel grouping index, solitary vessel index and conduit wall reinforcement were used to further underpin the observed physiological responses. On average, the water potential at which 50% loss of conductivity occurred (ψ_{50}) was -2.1±0.1 MPa, portraying *M. eminii*'s xylem as vulnerable to drought-induced cavitation, just as one would expect for a common tropical pioneer. However, *M. eminii* additionally employed an interesting desiccation delay strategy, fuelled by internal relocation of leaf-water, hydraulic capacitance, and the presence of parenchyma around the xylem conduits. Our findings suggest that sole reliance on ψ_{50} might be limiting and sometimes misleading when assessing drought stress behaviour and vulnerability of plants. Hydraulic capacitance linked to anatomy and leaf-water relocation behaviour was equally important to better understand the drought survival strategies employed by *M. eminii* when coping with drought stress.

4.2 Introduction

Trees are able to extract water from the soil and transfer it tens of meters upwards along their vessel elements and tracheids, collectively known as conduits (Anfodillo et al. 2006, Scholz et al. 2013), where it is evaporated by the foliage into the atmosphere (Cochard et al. 2013). This is a passive process driven by very negative water potentials in the air and puts the xylem under negative pressure gradients, resulting in a metastable condition of the transported water (Dixon and Joly 1895). Drought stress can further increase the tension within the xylem to the extent where continuous water columns break or cavitate, creating embolisms or air-filled conduits (Tyree and Sperry 1989). According to the hypothesis postulated by Zimmermann (1983), cavitation is induced by air-seeding through the pore of an inter-conduit membrane. This theory is widely accepted (Shen et al. 2002, De Roo et al. 2016), but was recently updated by Schenk et al. (2015), who emphasized the formation of nano-bubbles prior to cavitation to account for the stability of gas bubbles under negative pressure.

Essentially there is a trade-off between hydraulic efficiency and hydraulic safety (Sperry et al. 2008). Higher efficiency is associated with greater conduit dimensions, higher vessel connectivity and a higher degree of vessel grouping (Carlquist 1984, Loepfe et al. 2007). The more efficient the xylem network, the higher the hydraulic conductivity, photosynthetic capacity and plant growth (Loepfe et al. 2007). Additionally, high efficiency permits lower xylem construction and maintenance cost per unit transpiration (Gleason et al. 2016). Contrastingly, the more resistant the xylem network, the better the plant performance will be under higher xylem tension, allowing plants to operate in dry soils and enabling them to keep transpiring for longer periods during the day or year (Gleason et al. 2016). Hydraulic safety is typically associated with a smaller size of the pit aperture (Bouche et al. 2014). The reverse is true for hydraulic efficiency: according to the rare pit hypothesis, conduits with larger pit size are more susceptible to air entry as they are likely to possess "rare" pores of air-seeding size (Christman et al. 2009). In addition to pit size, the hydraulic capacitance (C) might play an important role in guaranteeing hydraulic safety even in dry habitats (Gleason et al. 2016). The hydraulic capacitance is theoretically defined as the ratio of change in tissue volumetric water content to change in xylem water potential (Vergeynst et al. 2015a), and can be measured as the amount of water released from the tissue per unit decrease in water potential (Edwards and Jarvis 1982, Steppe and Lemeur 2007). Indeed, plants with a high C can temporarily ward off cavitation by releasing stored water into the transpiration stream from different organs and tissue types (Sperry et al. 2008, Meinzer et al. 2009, Steppe et al. 2012, Vergeynst et al. 2015a).

To characterize the sensitivity of a plant species to drought stress, a vulnerability curve (VC) is usually developed (Pammenter and Van der Willigen 1998, Meinzer et al. 2009) from which the universal index, ψ_{50}, is determined. This value represents the tension at which 50% loss

of xylem hydraulic conductivity occurs (Choat et al. 2012). The ψ_{50}-values enlisted by Choat et al. (2012) capture multiple species from different continents, but African tree species drought vulnerability was only reflected by Tunisian and South African tree species. This entails increased uncertainty for the general African tree species response, especially now that the intensity and frequency of drought events are more pronounced because of climatic change (Asefi-Najafabady and Saatchi 2013).

Although ψ_{50} is often used as a single index of plant's sensitivity to drought stress, a suit of physiological, allometric and anatomical traits that reduce the risk of potential xylem dysfunction (Barnard et al. 2011) can be equally important. Such traits can be either physiomorphological – e.g. deep rooting, strict stomatal control, and control of leaf area, e.g. through leaf shedding (Pineda-Garcia et al. 2013) – or structural and anatomical traits, which determine the functionality during low plant and soil water conditions (Pineda-Garcia et al. 2013). Examples of such structural or anatomical traits are low wood density (Borchert 1994), high hydraulic capacitance, narrow inter-conduit pit pores, low degree of vessel connectivity and high conduit wall reinforcement (Hacke and Sperry 2001, McCulloh et al. 2012, Scholz et al. 2013). The latter is expressed as $(t/b)^2$ with t the thickness of the double wall between two conduits and b the span or conduit diameter (Hacke and Sperry 2001).

To address Africa's forest trees' drought response uncertainty, and to increase our general knowledge of how tropical tree species respond to drought intensification, we examined the vulnerability to drought of whole-branch segments of 3-year old seedlings of *Maesopsis eminii* Engl.. *M. eminii* is an economically important tropical pioneer tree species (Eggeling 1947) that occupies a wide ecological amplitude within tropical Africa, localized between latitude 10.97°N and 10.98°S in areas receiving an annual mean rainfall range of 657-3217 mm yr^{-1} and experiencing up to 6 dry months (Chapter 1). Its wide ecological amplitude makes it a particularly suitable study tree as it most likely possesses functional traits that allow it to cope with drought-induced cavitation.

The main objective of our study was to assess the hydraulic functioning of *M. eminii* trees and to determine which physiological and anatomical characteristics contribute to the species' drought-coping ability. Because experience has demonstrated that it requires several weeks of drought stress to induce cavitation in intact trees (Cochard et al. 2013), bench-top dehydration of long leafy branch segments was applied to induce cavitation. Vulnerability curve development was performed with acoustic emission (AE) sensors using the cumulative number of AE signals (Rosner et al. 2009, Vergeynst et al. 2015a) and leaf and stem water potential (ψ_{leaf} and ψ_{xylem}) measurements were performed with the pressure bomb (Begg and Turner 1970). We also assessed wood anatomy of *M. eminii* branches to understand the role of the structural and anatomical traits in cavitation impairment. We used relative radial xylem diameter shrinkage as an additional indicator

for water tension, and branch gravimetrical water loss was monitored to gain insights into the consecutive phases of dehydration and to quantify hydraulic capacitance (Irvine and Grace 1997, Vergeynst et al. 2015a). Lastly, wood density was quantified as an indirect method for cavitation vulnerability (Borchert 1994, Rosner et al. 2013).

4.3 Materials and methods

4.3.1 Experimental set-up

Maesopsis eminii Engl. seeds from unselected parent plants were randomly picked from Uganda's Mabira forest floor in October 2012 (0°23.357'N, 33°0.344'E) and were grown in the tropical greenhouse facility of Ghent University, Belgium (50°59.58'N, 3°47.04'E) in 5-L pots and later transplanted into 35-L pots containing peat soils (Figure 4.1).

Figure 4.1 Left to right: Germinated *M. eminii* seedlings in January 2013 thriving in a tropical greenhouse in Belgium. Same seedlings in June 2015 on tables and on floor to emphasize their height versus mine.

The seedlings were well-watered and fertilized throughout the entire period and were harvested at the age of 3 years. Chemistry of the irrigation water consisted of a mix of rainwater and soluble fertilizer with an NPKMg ratio of 19:8:16:4, boron (0.02%), copper (0.03%), iron (0.038%), manganese (0.05%), molybdenum (0.02%) and zinc (0.01%), resulting in a solution of pH 5.7. Climatic conditions were automatically controlled by a HortiMaX MT/MTV sensor Unit. Greenhouse air temperature (T) ranged between 18 and 36 °C, daily photosynthetic active radiation (PAR) ranged between 0 and 2044 μmol m^{-2} s^{-1} and relative humidity (RH) between 24 and 96 %. Each day, lights were turned on at 8 am and off at 8 pm. At the time of sampling, the seedlings had an average height of 2.3 ± 0.4 m and an average stem diameter of 28.3 ± 5.4 mm, measured approximately 2 m below the apex.

4.3.2 Sampling procedure

A total of five seedlings were used for the percentage loss of hydraulic conductivity and the volumetric water content experiments. Experiments were performed using two alternating branches excised from each of these five *M. eminii* trees; 10 branches in total. Branch selection and preconditioning occurred a day prior to the start of the experiment, and was based on the length (~ 70 cm), diameter (~ 7 mm), positioning on the stem and growth vigour. The positioning on the stem meant that the selected branches per tree had to be opposite or alternate to each other. Growth vigour meant that the branches essentially had to look healthy and have sufficient number of leaves (~ 100 leaves). Leaves of the five branches dedicated to drought vulnerability characterization (henceforth referred to as set 1) were wrapped with aluminium foil and were additionally covered with double-packed black polythene bags (Figure 4.2) to ensure equilibrium between leaves and stem water potential (Begg and Turner 1970).

Figure 4.2 Left-Right: The wrapping of leaves, excision of branches and packaging for transportation to lab for analysis.

A similar procedure was followed for the second set of five branches used for hydraulic capacitance determination (henceforth referred to as set 2) with exception of the individual leaf-foil wrapping. The five selected trees were watered to runoff to ensure complete hydration 15 hours before branch excision. Aside from this pre-watering, overnight watering was repeated twice (8 pm and 11 pm) to guarantee complete plant hydration. Sampling was done predawn and branches of both sets were cut under water followed by two additional re-cuts of ~3 cm to avoid artifacts due to possible air entry (Cochard et al. 2013, Wheeler et al. 2013) (Figure 4.2). The exposed parts of the branches were covered with wet cloth to keep the ends moist and to avoid dehydration during transport (Figure 4.2). The first measured water potential values for all branches were 0 MPa and no AE signals were registered during the first 30 minutes of dehydration, so we conclude that this wet cloth technique successfully avoided the occurrence of native emboli.

4.3.3   Measurements during dehydration

Excised branches were transported to the Laboratory of Plant Ecology, Ghent University (51°3.204'N, 3°42.511°E). The experimental room was darkened and equipped with an artificial green light to limit photosynthesis and transpiration when the black polythene bags were removed. After two separate sections of bark (1.5 x 0.5 cm) were removed with a scalpel to expose branch xylem, the five branches of set 1 were equipped with a broadband point-contact acoustic emission (AE) sensor (KRNBB-PC, KRN Services, Richland, WA, USA) and a dendrometer (DD-S, Ecomatik, Dachau, Germany) (Figure 4.3). The branches were also fixed in a custom-built holder to ensure a stable mount of both sensors, and an unbiased link between AE and diameter shrinkage.

Figure 4.3 Left to right: An excise *M. eminii* branch with leaves wrapped with foil (set 1) and onto which an acoustic and dendrometer have been attached. The branches stripped of their leaves (set 2) can be seen placed on black plastic plates. The pressure bomb used in xylem water potential measurements.

The AE sensor was pressed to the exposed xylem via a compression spring (D22050, Tevema, Amsterdam, The Netherlands) in a small PVC tube (Figure 4.3). To ensure good acoustic contact, a droplet of vacuum grease was added between sensor tip and xylem, after which installation was validated via the pencil lead break test according to Vergeynst et al. (2015a). Petroleum jelly was also applied between dendrometer sensor tip and xylem to prevent evaporation from the exposed wound.

The five branches of set 2 (Figure 4.3) were stripped of all their leaves and petal wounds were covered with petroleum jelly to prevent loss of sap through the wound (Vergeynst et al. 2015a). These branches were placed on continuous weight balances (4x DK 6200 with 0.01g accuracy and 2x PS 4500/C/1 with 0.1 g accuracy, Henk Maas, Veen, The Netherlands). Because the leaves of the set 1 branches were completely covered with aluminium foil and those of set 2 completely removed, it could be assumed that both sets of branches dehydrated in a similar way (Vergeynst et al. 2015a). Once both sets of branches were installed, wet clothes were removed and normal lights turned on.

Dendrometer and balance read-outs were registered every minute via custom-built acquisition boards. AE signals were amplified by 35.6 dB (AMP-1BB-J, KRN Services, Richland, WA, USA) after which waveforms of 7168 sample length were acquired at 10 MHz sample rate.

Signals were collected via 2-channel PCI boards and uploaded to the software program AEwin (PCI-2, AEwin E4.70, Mistras Group BV, Schiedam, The Netherlands). A 20-1000 kHz electronic band pass filter was applied, and only waveforms above the noise level of 28 dB_{AE} were retained as described in Vergeynst et al. (2016).

Xylem water potential (ψ_{xylem}, MPa) was measured on wrapped excised leaves using the pressure chamber (PMS Instrument Company, Corvalis, OR, USA) (Figure 4.3). When the frequency of new AE signals became higher, monitored live with the AEwin software program, the time between consecutive pressure bomb readings was shortened. At the start of dehydration, measurements were frequent with a mean time interval of approximately 5 minutes. This interval increased for the subsequent measurement days to between 0.5 to 2 hours, ending with maximum three readings from day three onwards. For generating the stress strain relation, only the xylem water potential values that changed compared to the previous were used.

4.3.4   Processing acoustic emission data

Following Vergeynst et al. (2015b) we translated the measured AE into meaningful percentage loss of hydraulic conductivity (PLC) by first cumulating the AE signals over the entire dehydration period. From the cumulative AE, the first derivative was calculated to produce the AE activity curve, after which second and third derivatives were calculated. The definition of Vergeynst et al. (2016) was used to determine the endpoint of the VC (ψ_{100}). AE activity was calculated numerically over a time interval of 5 min, while second and third derivatives were quantified over 24 hours due to the slow dehydration process. Translation to PLC (%) was obtained by re-scaling the cumulated AE signals from zero to ψ_{100}. Values corresponding with the onset of cavitation (ψ_{xylem} at 12%; ψ_{12}), 50% loss of conductivity (ψ_{xylem} at 50%; ψ_{50}) and at full embolism (ψ_{xylem} at 88%; ψ_{88}) were calculated as well.

4.3.5   Volumetric water content

Prior to the start of dehydration, a wood sample of ~5 cm of length was taken from each of the cut ends of the branches of set 2. At the end of the bench-top dehydration, similar sampling was performed (Vergeynst et al. 2015a). The samples were weighed (Sartorius precision balance with 0.001g accuracy, Sartorius Weighing Technology GmBH, Goettingen, Germany) and both diameter and length were determined via an automated caliper. These were then placed in brown paper bags and oven-dried at 80°C for two weeks, after which the weight, length and diameter of the samples were re-determined. Sample volume was estimated assuming a cylindrical form after which initial and final water mass fraction and initial basic wood density (ρ_b, kg m^{-3}) (oven dry mass/green volume) were calculated following Vergeynst et al. (2015b). Volumetric water content (VWC, kg m^{-3}) was calculated by multiplying mass fraction with ρ_b, whilst the actual change in VWC was

obtained by re-scaling the continuous weight data to the range of water contents between initial and final water content of the samples (Vergeynst et al. 2015b).

4.3.6   Stress-strain relation, modulus of elasticity and hydraulic capacitance

Relative radial xylem shrinkage ($\Delta d/d_i$) was determined using the initial diameter (d_i) prior to dehydration and the continuous diameter change (Δd; difference between the diameter after each five minute consecutive time step (d_t) and the initial diameter (d_i)) monitored with the dendrometers (Irvine and Grace 1997; Eq. 1):

$$\frac{\Delta d}{d_i} = \left(\frac{d_t - d_i}{d_i} \right) \qquad \text{(Eq. 1)}$$

Point measurements of ψ_{xylem} of the five branches (set 1) were plotted versus their corresponding relative radial xylem shrinkage to produce a pooled stress-strain curve, from which the apparent modulus of elasticity in the radial direction (E'_r, MPa) was obtained as the slope of the linear regression between pooled ψ_{xylem} and $\Delta d/d_i$ (Irvine and Grace 1997). This stress-strain relation was used to obtain continuous xylem water potential data that was used to produce the x-axis of the vulnerability and volumetric water content curve (Vergeynst et al. 2015a). Plotting VWC against xylem water potential showed two regions of interest, separated by two distinct breakpoints. The first and second breakpoint indicate the start and end of phase I, or the elastic shrinkage phase, and were calculated via the segmented R package (Muggeo 2008). The third breakpoint corresponds with ψ_{100} of the PLC curve and the region between second and third breakpoint is known as the cavitation or inelastic shrinkage phase, or phase II (Figs. 1 and 3, Vergeynst et al., 2015b). Following the procedure of Vergeynst et al. (2015b), hydraulic capacitance for both phases was determined as follows (Eq. 2):

$$C = \frac{dVWC}{d\psi_{xylem}} = \frac{dVWC}{d\left(\Delta d/d_i \right)} \left(\frac{d\psi_{xylem}}{d\left(\Delta d/d_i \right)} \right)^{-1} = \frac{dVWC}{d\left(\Delta d/d_i \right)} (E'_r)^{-1} \qquad \text{(Eq. 2)}$$

In addition, we calculated overall hydraulic capacitance as the slope of the linear regression fitted through the entire data set.

4.3.7   Microscopic analysis

In order to visualize the origin of *M. eminii*'s hydraulic capacitance and to decipher wood anatomical traits, the anatomy of six additional branches with similar dimensions as the branches used for vulnerability assessment, were analyzed. Branch samples, which were excised at a 40 cm

distance from branch tip to mimic sensor positioning during the bench-top dehydration test, were marked with white wash and preserved in separate labeled Ø54 mm containers containing a 20/40/40 ratio of ethanol (70% concentration), glycerin and distilled water (Figure 4.4A). These were then taken to the wood lab of the Royal Museum for Central Africa, Tervuren-Belgium (50° 49.855'N, 4° 31.098'E) for microscopic analysis.

At the wood lab, samples were resized by cutting cross-sections of the branches with a miniature saw until a point near the 40 cm mark was reached. The six cut samples were then placed in ice trays and marked with paper tags. Hot polyethylene glycol (PEG) liquid was poured over the samples until the border of the tray was reached, and these were then placed in the oven at 80°C for a period of four days and then removed for a day to allow PEG solidification in order to mummify the branch segments. These segments were then reshaped using a sharp knife (Figure 4.4B) after a spirit-level positioning was done for all the branch wood samples clamped inside the semi-automated microtome (Microm HM 440 E, GMI, Ramsey, MN, USA) sample holder (Figure 4.4C). Microtome sectioning was done at a thickness of 12-16 µm. The obtained transverse sections were put on glass slides, covered with nylon and fastened into position using rubber bands. Residual PEG was washed off by dipping the sections in water after which they were placed in a zigzag manner in a custom-made holder (Figure 4.4D). They were stained by placing them for 5 minutes in a container with a solution mix of 0.35 g Safranin in 35 ml 50 % ethanol and 0.65 g Alcian blue in 65 ml DI water. The sample was then rinsed by dipping in distilled water and thereafter consecutively dehydrated for 3 minutes each, following the ethanol-concentration gradient of 50%, 75%, 96% and finally 100% ethanol (Figure 4.4E). Once the dehydration process was done, the thin sections were transferred onto new cut-colour-frosted microscope slides (W x D x H; 76 x 26 x 1 mm; VWR International Ltd, UK), excess ethanol was drained by tilting the slides after which a microscopy mounting agent Euparal was added and the entire setup covered using microscope cover glasses to make permanent slides (Figure 4.4F). This completed setup was then labeled; weights were placed on them, allowed to dry for three days and thereafter analyzed microscopically (Figure 4.4G).

Figure 4.4 Illustratively from top to bottom and from left to right: the storing of the wood samples in the concoction as described in the text at the tropical greenhouse at ILVO (A). The reshaping of the mummified branch (B) and making of thin sections (C). The thin sections secured with a rubber band between nylon and glass slide were dipped in water to rinse off excess PEG (D). These were then dipped in alcohol of varying concentrations in the trash bin-like containers (E). Excess alcohol was drained by tilting the slides, Euparal added and setup covered using microscope cover glasses (F). Weights were placed on them and allowed to dry (G).

Complete transverse sections were transformed into images using an automated OLYMPUS BX60 microscope (NRI-MCDB, Microscopy facility, UC, Santa Barbara, USA) with a motorized positioning stage (Märzhäuser GmbH & Co. KG, Germany; 100 x 100 mm travel range; ball screw pitch of 1 mm) that allowed complete capture of the sections. These were visualized

using the OLYMPUS Stream Motion 1.8 software, for which a 10x magnification was used. To allow for more detail, cross-sections were also divided into four quadrants and visualised by a 20x magnification. Images were then processed with ArcGIS 10.2.2 (ESRI, Redlands, Ca, USA). Entire transverse sections were further analyzed for vessel grouping index (V_G (-), the ratio of the total number of vessels to the total number of vessel groupings (sum of solitary vessels + vessel clusters + radial multiples)) and solitary vessel index (V_S (-), the ratio of total number of solitary vessels to the total number of vessel grouping including solitary and grouped vessels) (Scholz et al. 2013). The average vessel area (μm^2) was determined, from which mean conduit diameter (μm) was obtained by assuming a circular vessel shape. In addition, ratios of total vessel area to xylem wood area were determined. Conduit wall thickness t (μm) and conduit wall span b (μm) were measured manually using the ImageJ 1.47v software. Conduit wall reinforcement $(t/b)^2$ (-) was calculated and averaged over the four separate quadrants following Hacke et al. (2001b).

4.4 Results

M. eminii branches had a basic wood density (ρ_b) of 302±21 kg m^{-3} and an initial volumetric water content (VWC$_{init}$) of 751±12 kg m^{-3}. They were completely desiccated within four days.

The averaged VC curve of *M. eminii* with standard error bands was sigmoidal shaped (Figure 4.5) and resulted in a ψ_{12} of -1.8±0.2 MPa (23.75 hrs., PLC: 12%), a ψ_{50} of -2.1±0.1 MPa (48.6 hrs., PLC: 50%), a ψ_{88} of -2.3 ±0.1 MPa (76.6 hrs., PLC: 88%) and a ψ_{100} of -2.6±0.0 MPa (104 hrs., PLC: 100%).
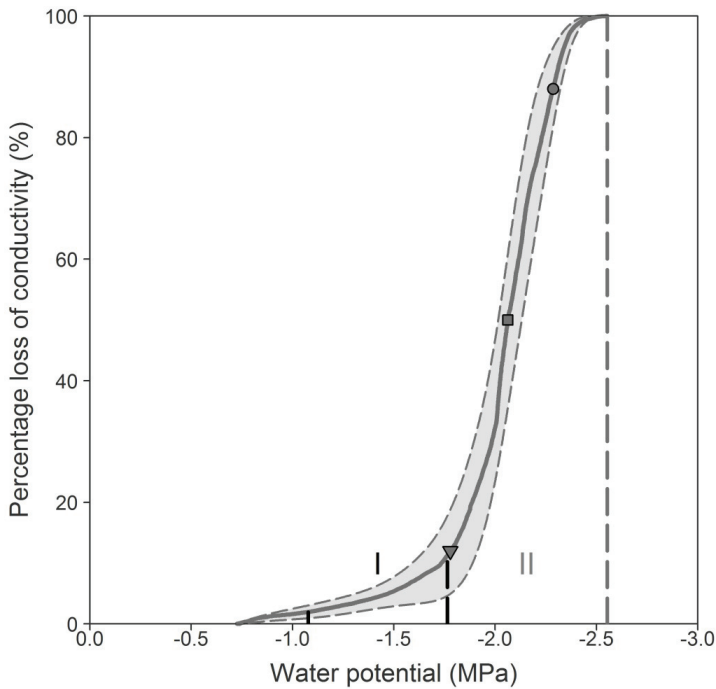
Figure 4.5 Illustration of *Maesopsis eminii*'s average vulnerability curve with standard error margins obtained by plotting converted cumulative acoustic emission values as percentage loss of hydraulic conductivity against xylem water potential. Phases I and II are delimited by vertical lines and the vulnerability thresholds ψ_{12} ($\triangledown$), ψ_{50} ($\square$), ψ_{88} ($\bigcirc$) and ψ_{100} (dashed line) are indicated as well.

Even though this illustrates that *M. eminii* required a small decrease in xylem pressure to shift from onset of cavitation (ψ_{12}) to fully embolized (ψ_{88}), the timespan for this transition expanded beyond two days. As branch dehydration progressed, we noted for all five branches of set 1 that some leaves on the same branch sampled at the same time had much lower water potentials values (more negative) while others had values that approached 0 MPa. This is reflected in the stress-strain curve by the large variability in ψ_{xylem} for similar values of $\Delta d/d_i$ during the entire dehydration process (Figure 4.6).
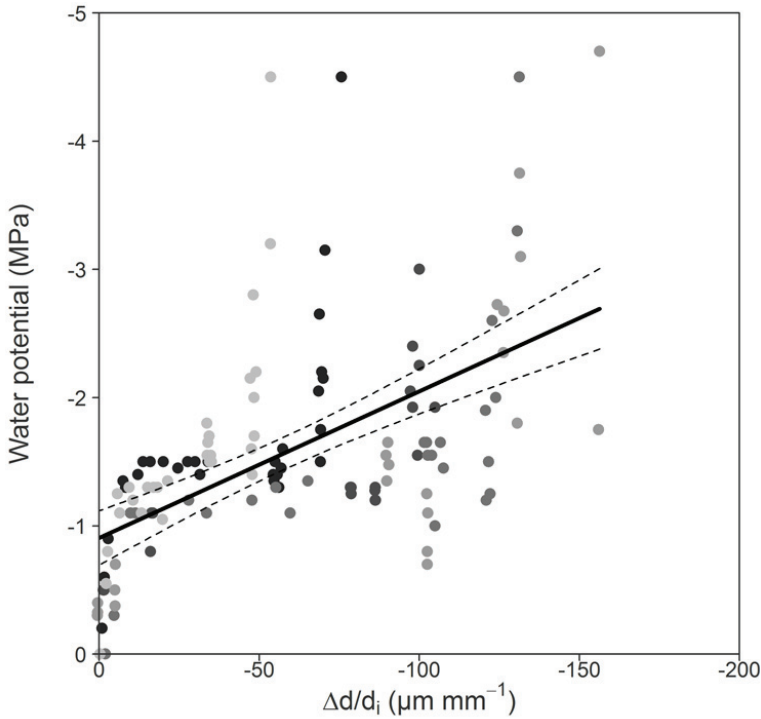
Figure 4.6 Stress-strain relationship of the examined *Maesopsis eminii* samples (○) was obtained by plotting measured xylem water potential against corresponding relative radial xylem diameter shrinkage ($\Delta d/d_i$). The different shade colours indicate the five different branches. The linear regression was calculated for the pooled stress-strain relationship ($\psi = 0.011\ \Delta d/d_i - 0.91$; R = 0.33). The dashed lines indicate a 95% confidence interval (P-value: $3.0e^{-12}$). The variability between the samples and resulting low R of the pooled relationship indicate how xylem water potential values varied due to internal leaf-water redistribution as branches dehydrated.

.

The apparent modulus of elasticity in the radial direction (E'_r) was calculated as the slope of the linear regression fitted to the pooled stress-strain curve ($R^2 = 0.41$) and was 15 MPa. In Figure 4.7, the relationship between xylem water potential and volumetric water content (VWC) is shown. The elastic hydraulic capacitance ($C_{elastic}$, capacitance of phase I) was 251 ± 16 kg m^{-3} MPa^{-1} ($R^2=0.998$) and the inelastic capacitance ($C_{inelastic}$, capacitance of Phase II) was 516 ± 44 kg m^{-3} MPa^{-1} ($R^2=0.999$). The overall hydraulic capacitance was 408 ± 30 kg m^{-3} MPa^{-1} ($R^2=0.967$). VWC decreased by 25% during the elastic phase and in total by 82% at the end of the inelastic phase (Figure 4.7).
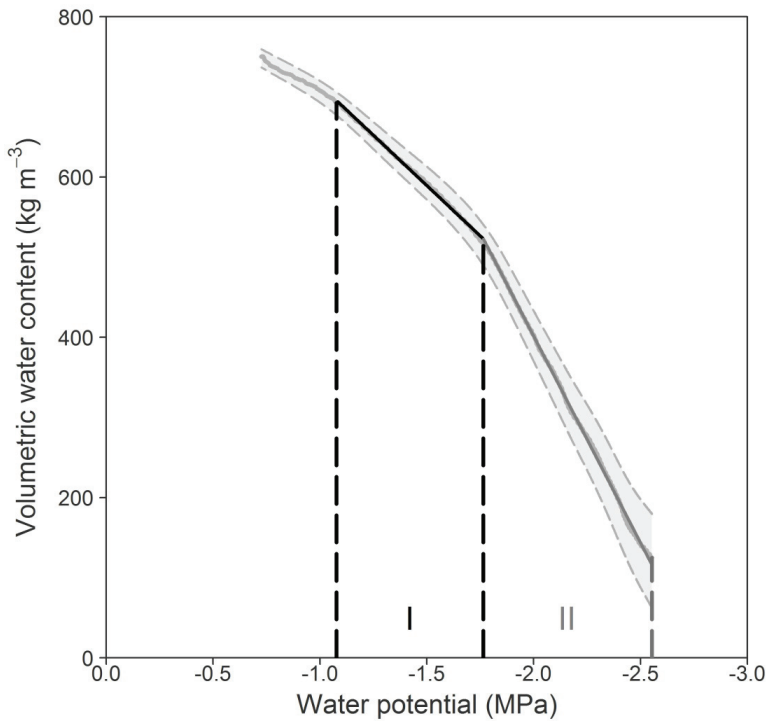
Figure 4.7 *Maesopsis eminii*'s average volumetric water content (VWC) with standard error margins plotted against xylem water potential during the bench dehydration experiment. Phases I and II are delimited by vertical lines and the slopes within these phases represent elastic ($C_{elastic}$) and inelastic ($C_{inelastic}$) hydraulic capacitance, respectively.

Results from the branch wood anatomical analysis showed an average vessel area of 1359 ± 767 µm^2, ranging between 300 and 5000 µm^2. The average vessel diameter was 40 ± 12 µm. Conduit walls were on average 5.2 ± 1.1 µm thick. Only 8.3% of the entire xylem wood area was occupied by vessels, with the remaining area occupied by fibres and parenchyma, also around hydraulic conduits (Figure 4.8).

Figure 4.8 Optical micrographs of an entire stained thin section of a branch of the tropical diffuse-porous *Maesopsis eminii*, with the bark still intact, and stained with Saf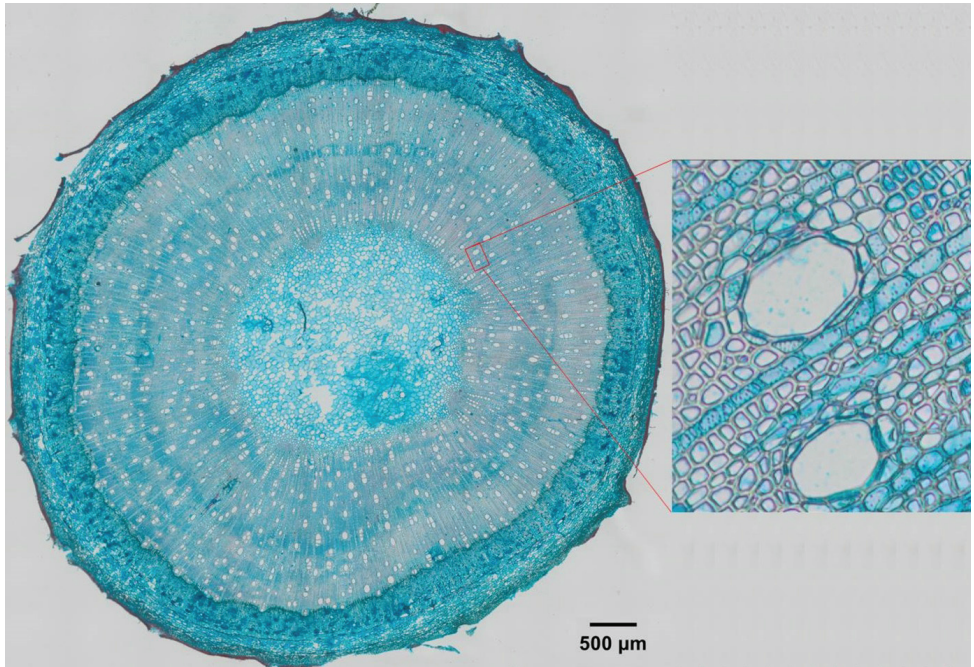ranin and Alcian blue. Regions coloured blue are associated with parenchyma and tension wood, the red portions are strongly lignified cell walls, vessels and fibres. Vessel grouping is also visible. The inset to the right depicts *M. eminii* hydraulic conduits being surrounded by parenchymatous cells.

Conduit wall reinforcement $(t/b)^2$ (-) was 0.02 ± 0.01. Vessel grouping index V_G (-) and solitary vessel index V_S (-) were calculated from the micrograph (Figure 4.8) and were 1.52 and 0.61, respectively, indicating a high degree of solitary vessels.

4.5   Discussion

4.5.1   How vulnerable is *M. eminii* to drought-induced cavitation? Trade-off between safety and efficiency

The ψ_{50}-value is widely used as a relevant and useful metric to quantify drought resistance across species (Anderegg 2015). We compared *M. eminii*'s ψ_{50}-value of -2.1 ± 0.1 MPa that was similar to Markesteijn et al. (2011b) studied pioneer saplings (-1.8 ± 0.4 MPa) with Choat et al.'s values for other species to gauge *M. eminii*'s xylem vulnerability to drought-induced cavitation. Notwithstanding the fact that on average *M. eminii* achieved its ψ_{50} and ψ_{88} values respectively ~2 and ~3 days after the start of dehydration, our species was weighted vulnerable to drought-induced cavitation, because more than half of the species studied by Choat et al. (2012) had lower (more

negative) values. Further confirmation of *M. eminii*'s vulnerability was ascertained after juxtaposing its ρ_b and $(t/b)^2$ against the curvilinear relationship ψ_{50} vs ρ_b and the linear relationship ψ_{50} vs $(t/b)^2$, which both portrayed *M. eminii* as sensitive to drought-induced cavitation (Hacke et al. 2000, Hacke and Sperry 2001, Hacke et al. 2001, Pittermann et al. 2006, Hao et al. 2008, Rosner et al. 2013). Besides, despite *M. eminii*'s V_G and V_S values indicating low vessel connectivity and vessel grouping that signify high hydraulic conduit safety and low hydraulic efficiency (Loepfe et al. 2007), *M. eminii*'s high average vessel diameter might lower its hydraulic safety. As wide vessels have been observed e.g. in Acer species, to have a higher probability of leakier pits through which air-seeding can occur (Christman et al. 2009).

4.5.2   How vulnerable is vulnerable? Seeking desiccation-delay mechanisms

Reliance on these aforementioned parameters alone would lead to the wrong conclusion of how vulnerable *M. eminii*'s xylem is to drought-induced cavitation, because *M. eminii* seems to employ a desiccation-delay strategy (Figure 4.6). Ideally, as a branch dehydrates, one would expect the branch xylem water potential (ψ_{xylem}) value to linearly decline with time and diameter shrinkage (Figure 4.6). However, observation on dehydrating *M. eminii* branches defies the odds, as abnormally divergent ψ_{xylem} values were measured in all five dehydrating *M. eminii* branches. Per branch, some leaf values became more negative with drought as expected, while others in the same branch and at the same time tended towards 0 MPa values (Figure 4.6). These observations led us to speculate that as shrinkage and dehydration progressed, *M. eminii* progressively cut some leaves off from the water supply chain with the favoured ones remaining continuously supplied with "redistributed" water, hence, their water potential tending toward 0 MPa. This strategy may be a vital means of survival in the field where a few leaves are selected to support continued carbon fixation even during the dry season (Pearson et al. 2003b), allowing light-demanding trees like *M. eminii* (Eggeling 1947) to quickly grow to higher light levels.

M. eminii's general stress-strain pattern (Figure 4.6) shows that, regardless of this "redistribution" phenomenon, ψ_{xylem} values became more negative as shrinkage tended towards -70 µm mm^{-1}, which implies that xylem water became limiting. Between -70 and -125 µm mm^{-1} however, the water potentials unexpectedly increased towards 0 MPa again (Figure 4.6), suggesting that a certain amount of water must be expelled from cavitating vessel associated parenchyma localized around *M. eminii*'s hydraulic conduit that store water (Figure 4.8) to buffer the more negative water potentials. Once these relief waters ran out (>-125 µm mm^{-1}), water potentials became more negative again and this was irreversible (Figure 4.6). This internally stored water collectively contributes to the hydraulic capacitance (*C*) (Holbrook 1995). Therefore, *C* defined as the amount of water released from the tissue per unit decrease in water potential (Edwards and Jarvis 1982, Steppe and Lemeur 2007) undoubtedly constitutes part of *M. eminii*'s "redistribution" water. *M. eminii*'s *C* seems substantial as it delayed complete dehydration by 4 days and portrayed

M. eminii's unsafe safety margin safe (0.5 ± 0.1 MPa (Figure 4.5); difference between onset of cavitation (ψ_{12}) and full embolism (ψ_{88}) (Domec and Gartner 2001, Meinzer et al. 2009)). We could substantiate this C using indicators such as *M. eminii*'s low basic wood density values of 302 ± 21 kg m^{-3} and high initial VWC (Figure 4.7), which both indicate a notable amount of stored water within *M. eminii*'s wood structure. In addition, VWC curves can be used to quantify hydraulic capacitance values (e.g. Vergeynst et al. 2015b). For *M. eminii*, hydraulic capacitance values were computed for two distinct phases (elastic and inelastic) and also the overall pooled one was calculated (Figure 4.7). Phase computations and related hydraulic capacitance data seldom exist in literature, and if they do exist (e.g. Meinzer et al. (2003, 2009) and McCulloh et al. (2012)) study conditions of measured branches vary from ours. Measurements are usually performed on samples sourced from much older and taller trees thriving within tropical forests and not in tropical greenhouses like ours, making direct comparison of our $C_{elastic}$ (251 ± 16 kg m^{-3} MPa^{-1}), $C_{inelastic}$ (516 ± 44 kg m^{-3} MPa^{-1}) and pooled (408 ± 30 kg m^{-3} MPa^{-1}) values with these field study values difficult. In spite of that, our study has shown that *M. eminii* relies on the participatory contribution of C during drought in prolonging the life span of some of its leaves (ψ_{xylem} values tending towards 0 MPa; Figure 4.6) with a significant C supply coming from the inelastic phase that is twice as high as the elastic amount (Figure 4.7). This supports the observed VC curve (Figure 4.5) and stress-strain (Figure 4.6) patterns, and is in line with the findings of Vergeynst et al. (2015b) who confirmed that water released by cavitation may significantly contribute to C under conditions of drought stress (Hölttä et al. 2009). *M. eminii* may thus be able to survive periods of drought stress by allowing a certain degree of cavitation.

Vergeynst et al. (2015b) excluded the initial decline in VWC versus water potential from their C calculations as it was attributed to water loss from open vessels at the cut branch ends and thus considered negligible. We however noted for *M. eminii* that this gentle slope was substantial and contributed to a C of 147 ± 8 kg m^{-3} MPa^{-1} (Figure 4.7). Tyree and Yang (1990) postulated that capillary water, found in the lumens of inactive xylem elements and intracellular spaces, could be a possible source responsible for this initial drop in VWC and is usually released between -0.2 and -0.5 MPa (Tyree and Ewers 1991). The initial decline in VWC for *M. eminii* took place between -0.7 and -1.1 MPa (Figure 4.7) and with this increase in xylem tension, PLC increased from 0 to 2 % (Figure 4.5). The small change in PLC led us to presume that release of capillary water was the cause for this initial drop, which is considered to be a reversible process (Tyree and Ewers 1991). Furthermore, a high apparent modulus of elasticity (E'_r) implies that a small decrease in water content is associated with a large decrease in cell water potential and turgor pressure (Kozlowski et al. 1991). *M. eminii* with an E'_r of 15 MPa that falls right in the middle of Bartlett et al.'s (2012) studied tropical species (between 5-30 MPa, except an outlier with an E'_r of about 75 MPa) has elastic cell walls that allows room for a greater water storage capacity (Sanchez-Diaz and Kramer

1971, Lambers et al. 1998) and justifies the observed delay in declining water potential values (Figure 4.5 and Figure 4.6) and its bendability.

Conclusively, this study highlights that reliance on one sole commonly used parameter to assess how vulnerable a species' xylem is to drought-induced cavitation may be misleading. This study therefore calls for the combined use of percentage loss of hydraulic conductivity, hydraulic capacitance, wood structural and anatomical features, and leaf strategies in the interpretation of a species' vulnerability to drought. More important also, this pioneering work on *M. eminii* has echoed scarcity of studies within Africa's tropical terrestrial species' that seems to be endowed with novel unexplored traits that may ward off drought momentarily.

5 General conclusions and future perspectives

The findings of this PhD study are the first proof of how seedlings of the exemplified African light-demanding deciduous tree species *M. eminii* might cope under non-drought and drought conditions. Based on the integrated ecophysiological assessment of its characteristics (Chapters 1, 2, 3 and 4), we can confidently say that *M. eminii* uses a number of strategies to cope with drought. Since measurements throughout this PhD study were centralized on potted seedlings because of their importance for successful regeneration in dry areas we can, for now, only theoretically extrapolate our findings to seedlings and adult *M. eminii* trees within a natural tropical forest ecosystem, and assume that they will employ most of these traits that make them less drought vulnerable. The lack of replicates and ground truthing on juveniles and adult trees within *M. eminii*'s natural environment is clearly one of the weakest points of this PhD study. However, since all findings from separate measurements (Chapters 1, 2, 3 and 4) corroborated each other, the findings of this PhD study will not be far from actual field measurements. To fully appreciate the relevance of strategies evoked by *M. eminii* to cope with drought, a comparison with other tropical forest tree species is needed. Therefore, this final chapter uses information reflected in the four main research chapters to assess *M. eminii*'s drought performance by comparing it to other drought-related studies performed on seedlings with a similar ecological strategy. Additionally, loopholes in this study that require extended research attention are also pointed out.

During drought, species-specific traits and mechanisms (Engelbrecht et al. 2005, Slot and Poorter 2007) are more important than species origin (Engelbrecht and Kursar 2003, Engelbrecht et al. 2005) when it comes to assessing how long a species can tolerate drought (Figure 5.1). Drought tolerance is the ability to survive drought while minimizing reductions in growth, and ultimately fitness (Engelbrecht and Kursar 2003).
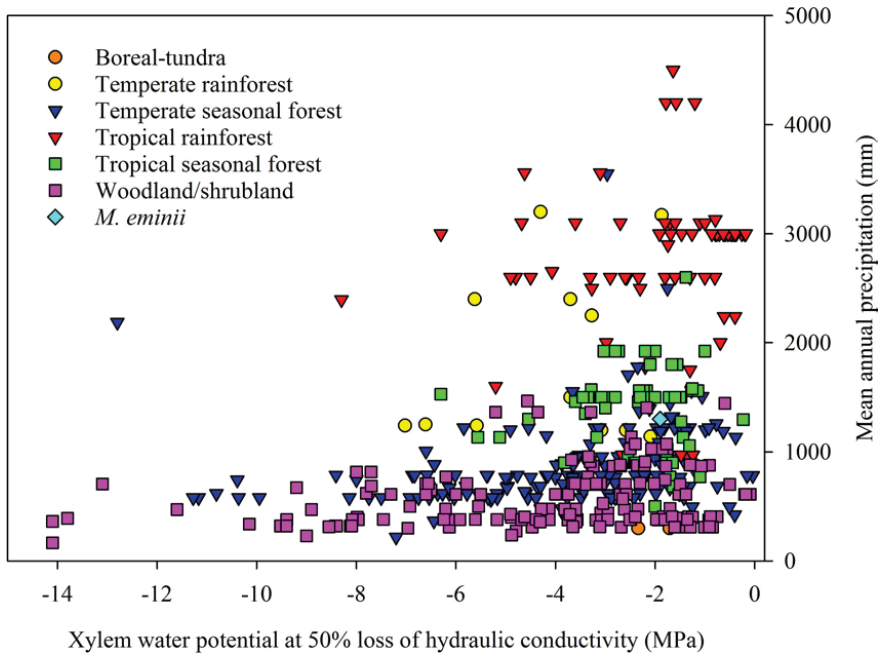
Figure 5.1 Illustration of the diversity in global tree species drought tolerance using the xylem water potential value at which 50% loss of xylem hydraulic conductivity (ψ_{50}) occurs, and the mean annual precipitation received at the locations the plants or seeds were sourced (drawn from data sourced from Choat et al. (2012)).

Figure 5.1 emphasizes the statement made in the previous paragraph, and also points out that at times the ψ_{50} index might be misleading when assessing drought tolerance of a species. Based on Figure 5.1, *M. eminii* is comparatively unable to tolerate drought stress due to its low ψ_{50} value. This value is misleading as has been explained in Chapter 4. Species-specific functional traits are known to provide a more comprehensive overview of how a plant would cope with drought. Borchert's (1994) classification based on an extensive overview of species thriving in a "tropical dry forest, moist province transition" is a good starting point to forecast *M. eminii*'s drought performance. It categorizes different species based on their traits (i.e., leaf phenology, wood density, wood type (softwood or hardwood), wood water content, and leaf type) into different "functional type" groups. *M. eminii* falls under Borchert's D_{light} group: a semi-deciduous tree (becoming deciduous during drought) with low density wood, shallow roots, extensive wood parenchyma, mesomorphic leaves of low drought tolerance and high stem water storage. However, because they never actually mechanistically assessed how the traits are used to cope with drought, other drought-related studies were sought to gauge *M. eminii*'s performance.

It is important to note already that despite several studies existing, differences in experimental set-up (e.g., Engelbrecht et al. 2006), conditioning and plant age present hurdles when it comes to comparing species' drought performance. Moreover, different ecological strategies exist. Therefore, for *M. eminii*'s drought performance assessment, focus will be made on the traits evoked to cope with drought. Since *M. eminii* is a pioneer species it is only fitting to firstly assess it performance within its ecological strategy cohort (pioneer), and here and there, if needed, compare it to species with different ecological niches.

5.1   Leaf traits based on ecophysiological assessments

A comparison between *M. eminii* and three 15 cm tall tropical forest Bolivian pioneer tree species obtained from Slot et al.'s (2007) study is tabled below (Table 5.1).

Table 5.1 Illustrative overview of mean values (± SE) of physiological parameters of seedlings of four tropical pioneer tree species (N = 10 per species). Species family, forest type where seeds were sources and leaf phenology pattern (deciduousness) are also included. A_{max} is the maximum photosynthetic rate, R_d is the dark respiration rate, g_s is the stomatal conductance, and WUE is the water use efficiency. Species were sourced from Slot et al.'s (2007) study. Information on *M. eminii* is extracted from Chapters 2 and 3.

Species	Family	A_{max} (μmol m^{-2} s^{-1})	R_d (μmol m^{-2} s^{-1})	g_s (mmol m^{-2} s^{-1})	WUE (mmol mol^{-1})	Deciduousness	Forest
***Maesopsis eminii* Engl.**	**Rhamnaceae**	**5.00 ± 2.20**	**1.50 ± 0.60**	**39.0 ± 30.0**	**-**	**Seedlings & adults**	**moist**
Astronium urundeuva (Allemao) Engl.	Anacardiaceae	2.52 ± 0.25	0.32 ± 0.03	50.1 ± 3.1	0.050 ± 0.003	Adult	dry
Ceiba samauma (Mart.) K. Schum	Bombacaceae	2.69 ± 0.25	0.27 ± 0.02	42.5 ± 5.4	0.066 ± 0.003	Seedlings & adults	dry & moist
Triplaris amaricana L.	Polygonaceae	3.45 ± 0.20	0.27 ± 0.03	81.3 ± 5.5	0.043 ± 0.003	None	moist

The species diversity mirrored through measured variables (Table 5.1) as suggested by Slot et al. (2007) might prove useful under non-water limiting conditions (e.g., higher photosynthetic rates imply faster growth). But during drought the opposite might be true. Fast-growing and light-demanding early successional species (i.e., *Triplaris* (9) and *Astronium* (9)) (Table 5.1) succumbed to drought within a short time compared to *Ceiba* (12 days) (Slot and Poorter 2007). *M. eminii* is a fast grower, and based on the 15-month-old seedling experiment in Uganda, *M. eminii* survived drought for longer than the 12 days. Because *M. eminii*'s g_s rates are relatively low compared to Slot et al.'s (2007) fast growers (Table 5.1), it might suggest that *M. eminii*'s low rates are important in coping with drought as less water is lost (conservative water user). Additionally, since *M. eminii* sheds its leaves as seedlings, its leaf loss habit momentarily plays a role in drought delay as was found for *Ceiba* (see Slot et al. 2007) and *Dipteryx panamensis* (Pittier) Record & Mell (see Engelbrecht and Kursar 2006). Moreover, this drought avoidance mechanism (leaf shedding) has been supposed by Poorter and Markesteijn (2008) to be a costly initiative as only 22% of the deciduous species in their study were deciduous as seedlings. Implicitly, this

costly initiative might explain why like *Ceiba*, *M. eminii* naturally occurs in both dry and moist forest. Nonetheless, this shedding strategy does not always guarantee drought tolerance. Engelbrecht and Kursar (2003), using 2 to 9-month-old tropical seedlings of five different species with leaf phenology similar to *Maesopsis* and *Ceiba* (Table 5.1), demonstrated that deciduous species' drought tolerance varied remarkably when subjected to a 24 week long drought: *Tabebuia rosea* (Bertol.) A. DC. < *Pterocarpus rohrii* Vahl < *Cordia alliodora* (Ruiz & Pav.) Oken < *Pseudobombax septenatum* (Jacq.) Dugand < *Dipteryx panamensis* (Pittier) Record & Mell. Furthermore, as opposed to Slot et al.'s (2007) fast-growing species, *M. eminii* has tap roots. Even though we never assessed *M. eminii*'s tap root water content, root water storage capacity was found to play a significant role in delaying drought stress effects in *Ceiba*. The combined drought avoiding functional traits (tap rooting and deciduous leaf loss) have been found to enhance species drought survival when evergreens were compared to deciduous species in a study where drought stress effects were monitored on 36 tropical tree species in Bolivia (see Poorter and Markesteijn 2008).

Fast-growing pioneers are usually associated with high photosynthetic rates as is attested by Ellis et al. (2010) for their Panamanian (2.5 year old saplings) pioneers (i.e., 21-34.6 $\mu mol\ CO_2\ m^{-2}\ s^{-1}$) as well as by Meir et al. (2007) for the tropical pioneer *Musanga cecropioides* R.Br. (Mc) (i.e., 13.9 $\mu mol\ CO_2\ m^{-2}\ s^{-1}$). The loading mechanism evoked by *M. eminii* that involves increasing fixed sugar concentration around its veins in mature leaves indicates a species that invests a lot of energy in such a mechanism to most likely compensate for its low photosynthetic rates (Chapter 3). Because autoradiographs have not been generated for the majority of species, it is hard to discern whether this type of mechanism exists in all pioneers. However, what is certain is that (i) global vegetation model parameter need to be reassessed and (ii) *M. eminii* has unique leaf traits that are not only mirrored through autoradiographs, but is reflected in (i) the stress-strain relation that shows hydraulic redistribution within the leaf (Chapter 4), and (ii) its nocturnal sap flow (Chapter 2). Evidence of other plants that redistribute sap between leaves is yet to be found. Nocturnal sap loss is however a leaf trait that has been recorded for several plant species (Caird et al. 2007). The overview for trees as documented by Caird et al. (2007) and Zeppel et al. (2012) with the exception of *M. eminii* is tabled below (Table 5.2). Comparatively, the overview indicates that *M. eminii*'s nocturnal water contribution to daily water loss is not far from most of the documented trees.

Table 5.2 Overview of tree species known to conduct nocturnal sap flow. Besides nocturnal stomatal conductance (g_s) leaf lifespan (D = deciduous and E = evergreen) is mentioned. For forest type a '-' is used when not mentioned in the cited paper.

Species	Leaf lifespan	Forest type	Nocturnal g_s (mol m^{-2} s^{-1})
Maesopsis eminii	**D**	**Moist**	**0.011±0.004**
Acer rubrum[1,3]	D	Mixed deciduous[3]	<0.050
Betula papyrifera[1,3]	D	Mixed deciduous[3]	0.170
Betula pendula[1,4]	D	-[4]	0.090
Blepharocalyx salicifolius[1,5]	E	Savanna[5]	0.081
Dacrydium cupressinum[1,6]	E	-[6]	0.005
Eucalyptus grandis[1,7]	-	-[7]	0.104
Fraxinus pennsylvanica Marshall's Seedless[1,8]	D	-[8]	0.0-0.001
Larix occidentalis[1,9]	D	Mixed confer[9]	0.042
Picea abies[1,10]	E	-[10]	0.006
Pinus ponderosa[1,6,11]	E	Mixed conifer[6,11]	0.003-0.019
Pinus radiata[1,6]	E	-[6]	0.009
Populus angustifolia[1,12]	D	-[12]	0.051
Populus balsamifera ssp. *Trichocarpa*[1,12,13]	D	Great Basin and Mojave desert[12,13]	0.120-0.153
Populus koreana x *P. trichocarpa* Peace[1,14]	D	-[14]	0.23
Pseudotsuga menziesii[1,9]	E	Mixed confer[9]	0.029
Qualea grandiflora[1,5]	D	Savanna[5]	0.158
Quercus laevis[1,12]	D	-[12]	0.053
Quercus rubrav[1,3,6]	D	Mixed deciduous[3,6]	<0.050-0.011
Quintinia acutifolia[1,6]	E	-[6]	0.015
Styrax ferrugineus[1,15]	D	Savanna[15]	0.05-0.1
Thuja plicata[1,9]	E	Mixed confer[9]	0.010
Tilia cordata Greenspire[1,8]	D	-[8]	0.0-0.001
Tsuga heterophylla[1,9]	E	Mixed confer[9]	0.020
Eucalyptus sideroxylon[2]	-	-[2]	0-0.060

Values are taken from Caird et al. (2007)[1], Zeppel et al. (2012)[2], Daley and Phillips 2006[3], Matyssek et al. 1995[4], Scholz et al. 2007[5], Barbour et al. 2005[6], Benyon 1999[7], Whitlow et al. 1992[8], Kavanagh et al. 2007[9], Keller and Häsler 1984[10], Grulke et al. 2004[11], Howard and Donovan 2007[12], Synyder et al. 2003[13], Furukawa et al. 1990[14], Bucci et al. 2004[15].

Nocturnal water fluxes may provide several advantages for plants, including refilling of capacitance, embolism removal at night when there is less evaporative demand, transport of nutrients or oxygen supply (see review by Zeppel et al. 2014). This trait may be advantageous for *M. eminii* during water-limiting conditions, because processes such as refilling of capacitance, embolism removal and nutrient transport are adventitious, providing benefit to the sub-optimal loss of water at night when no carbon is gained (Zeppel et al. 2014). Further research is needed for this nocturnal phenomenon, which evidently is not simply a consequence of incomplete stomatal closure. However, based on our drought study (Chapter 2), we can assume that this nocturnal water loss was detrimental to *M. eminii*'s survival under prolonged drought stress.

5.2   Wood hydraulic traits based on ecophysiological assessments

Comparison of *M. eminii*'s hydraulic traits with other species is not easy, because in this PhD a very thorough examination of the effects of drying on *M. eminii* seedlings was strived for. In many ways,

this study goes far beyond routine studies of xylem vulnerability with the aim to set a new standard for investigating xylem vulnerability, capacitive water release, hydraulic relocation, and anatomy to create a comprehensive study of the effects of drying in woody plants. In the few routine studies that exist, they vastly include species of different ages, analysis on different parts of the plants (e.g., branch, stem, roots) or different experimental conditions (e.g. this PhD study deals with greenhouse-grown seedlings while others use trees thriving in natural forests), which results in marked differences of hydraulic properties (Table 5.3). Moreover, the ψ_{50} value as already found for *M. eminii* is non-conclusive (see Chapter 4), making a comparative assessment of how drought-tolerance *M. eminii* is difficult. However, what stands out is that the hydraulic capacitance (*C*) will play an important buffering role in delaying drought stress effects as was illustrated for *M. eminii* (Chapter 4). It can be correlated to wood density (Table 5.3). Based on *C*, *M. eminii* falls in the middle of the pioneer drought tolerance spectrum. Moreover, this illustration (Table 5.3) again confirms that classification according to forest type alone is insignificant when it comes to assessing a species' drought performance, but that species-specific traits are pivotal for coping with drought.

Table 5.3 Overview of hydraulic traits of several tropical pioneer species sourced from various studies: McCulloh et al. (2012)[1], Chapter 3[2], Markesteijn et al. (2011b)[3], Meinzer et al. (2003)[4] and Markesteijn et al. (2011a)[5]. WD is wood density, SD is stem diameter, D is deciduous, E is evergreen, C is hydraulic capacitance, ψ_{50} is the xylem water potential at 50% loss of hydraulic conductivity, SDT is seasonally dry tropical and TLDD is Tropical lowland dry deciduous. Stem refers to complete stems of saplings.

Species	WD (kg m⁻³)	Ψ50 (-MPa)	Height (m)	C (kg m⁻³ MPa⁻¹)	SD (mm)	Leaf lifespan	Forest type	Study subjects
Maesopsis eminii Engl.[2]	**302±21**	**2.1±0.1**	**2.3±0.4**	**408±30**	**28.3±5.4**	**D**	**Moist**	**Branches**
Miconia. argentea (SW.) DC.[1]	590	1.6	4.4±0.8	212	-	-	SDT	Stems
Anacardium excelsum (Bentero & Balb. Ex Kunth) Skeels[1]	380	0.9	4.0±1.1	610	-	D[4]	SDT	Stems
Anacardium excelsum[3]	390±30	1.56	38	~310	980	D	TLDD	Branches
Cordia alliodora[3]	520±30	3.00	26	83	340	D	TLDD	Branches
Astronium urundeuva[3]	-	1.8	1.5-2	-	-	E	TLDD	Branches
Bougainvillea modesta[3]	-	3.7	1.5-2	-	-	E	TLDD	Branches
Cecropia concolor[3]	-	0.8	1.5-2	-	-	E	TLDD	Branches
Ceiba speciosa[3]	-	1.4	1.5-2	-	-	D	TLDD	Branches
Centrolobium microchaete[3]	-	1.2	1.5-2	-	-	D	TLDD	Branches
Solanum riparium[3]	-	2.1	1.5-2	-	-	E	TLDD	Branches
Cecropia concolor[5]	201±20	0.2 ± 0.02	1.5-2	---	-	E	TLDD	Stem & leaves
Ceiba samaura[4]	240±20	0.9 ± 0.11	1.5-2	-	-	D	TLDD	Stem & leaves
Ceiba speciosa[5]	240±20	0.8 ± 0.06	1.5-2	-	-	D	TLDD	Stem & leaves
Centrolobium microchaete[5]	300±30	1.4 ± 0.38	1.5-2	-	-	D	TLDD	Stem & leaves
Combretum leprosum[5]	430±30	1.3 ± 0.04	1.5-2	-	-	E	TLDD	Stem & leaves
Astronium urundeuva[5]	380±20	0.5 ± 0.04	1.5-2	-	-	D	TLDD	Stem & leaves
Bougainvillea modesta[5]	420±20	1.0 ± 0.09	1.5-2	-	-	E	TLDD	Stem & leaves
Machaerium scleroxylon[5]	490±20	1.4 ± 0.13	1.5-2	-	-	D	TLDD	Stem & leaves
Manihot guaranatica[5]	190±10	0.8 ± 0.04	1.5-2	-	-	D	TLDD	Stem & leaves
Pterogyne nitens[5]	350±10	1.8 ± 0.05	1.5-2	-	-	E	TLDD	Stem & leaves
Schinopsis brasiliensis[5]	510±20	1.1 ± 0.07	1.5-2	-	-	D	TLDD	Stem & leaves
Solanum riparium[5]	250±20	0.4 ± 0.03	1.5-2	-	-	E	TLDD	Stem & leaves
Spondias mombin[5]	220±20	0.7 ± 0.10	1.5-2	-	-	D	TLDD	Stem & leaves
Tabebuia impetiginosa[4]	430±30	1.1 ± 0.08	1.5-2	-	-	E	TLDD	Stem & leaves

5.3 *M. eminii* for enrichment planting

Doucet et al.'s (2016) study on enrichment planting in Cameroon showed that fast-growing and light-demanding tropical pioneer timber species of low wood density (i.e., *Terminalia superba* Engl. & Diels and *Triplochiton scleroxylon* K. Schum) performed best in terms of survival and growth rates. As implied by Doucet et al. (2016) enrichment planting is a strategy of enhancing a natural forest's economic and diversity value through sowing seeds or planting seedlings of commercially important indigenous tree species. The indicator used was wood density, which was weekly correlated with growth, maximum growth and survival. The correlation was only significant between wood density and maximum growth (Doucet et al. 2016). Accordingly, *M. eminii* with these attributes (fast growth, low wood density, timber species, and traits included in the thesis introduction) might be a good enrichment planting option especially in degraded environments (owed to its found drought tolerance traits). Moreover, Chazdon (2008) supports the use of indigenous trees that ensure sustainable rural livelihoods and community participation, in addition to the tree species being able to withstand stresses of climate change. Chapter 1 indicates that the successful establishment of indigenous *M. eminii* is plausible as long as its growth conditions are met. However, the associated costs are unknown as it was not the goal of this PhD. Still, since Doucet et al.'s (2016) study found that species performance (growth, maximum growth and survival) was weakly correlated to functional traits (i.e., seed mass, tree diameter and height, ecological strategy, deciduousness, dispersal and wood density), planting of *M. eminii* seedlings in degraded forests needs to be practically assessed to increase certainty of its suitability as an enrichment option.

5.4 **Future research**

The 2013 protracted dry season in Uganda resulted in no rain and thus affected the planned rain-fed treatment (Chapter 2). This hindered the observation of potential effects of seasonal rains on *M. eminii* seedlings' response to drought. Therefore, a large-scale study following rainfall seasonality should be done under natural tropical setting, with replicates, and with resilience-oriented theme, on both seedlings and adult trees of not only *M. eminii* but also other economically important African tree species. This would enable a comprehensive assessment to gauge whether there are other African tree species aside from *M. eminii* with advanced drought-coping strategies. Field campaign measurements encompassing gas exchange (i.e., photosynthesis, transpiration), stomatal conductance, sap flow, stem diameter variations, leaf and stem water potential, drought-induced vulnerability to cavitation, capacitive water release, hydraulic relocation, and anatomy on intact adult and juvenile trees, and linking these to environmental variables of radiation, vapour

pressure deficit, temperature, relative humidity and soil water potential, would give a clear drought response picture of these tree species.

Equally important is the classification of *M. eminii* under the continuum of stomatal responses to drought as either isohydric (carbon starved) or anisohydric (hydraulic failure) (Allen et al. 2010) that was never addressed during this PhD study. This should be done by carrying out predawn and midday leaf g_s and leaf water potential measurements of unmanipulated control (well-watered) and drought-threated plants. Determination of the grouping under which *M. eminii* falls will not only add to the archive of species classified under either grouping, but it will help connect the dots between the traits discovered during this PhD study to *M. eminii*'s drought-coping capabilities, thereby increasing the drought response predictions of this species.

Another interesting suggestion would be to quantify the actual amount of sap lost daily (day + night) by *M. eminii* during drought and non-drought cases, and under natural setting to determine its potential contribution to the global water budget which seems rather significant as *M. eminii* seem to have naturally leaky stomata or leaky cuticle, or both. Assumptions in process-based ecophysiological models and dynamic global vegetation models that propose g_s is zero when solar radiation is zero are likely to be incorrect. Consequently, failure to adequately consider nocturnal water loss may lead to substantial under-estimation of total plant water use and inaccurate estimation of ecosystem level water balance (Zeppel et al. 2014).

As echoed from Chapter 1, dominance or abundance percentage and ecophysiological, morphological and phenological characteristics of *M. eminii* trees at mapped sites were not tackled. *M. eminii*'s observed ecophysiological behaviour suggests some unique traits that allow it to delay and/or avoid drought impacts. It would be nice to have an idea on its percentage representation (dominance) and gap size preference within Africa's tropical forests. This should be done by using GPS to map point locations where it exists, make counts, assess climatic conditions where they are present, absent or planted, wood coring to determine age, investigate if interbreeding occurs to better explain the height differences of *M. eminii* subspecies, follow their phenology throughout all seasons, basal area determination, assess their competition with other surrounding tree species and see under which niche it generally occurs.

In conclusion, plant science is now more than ever relying on model predictions to gauge how forest tree species will respond to climate-induced drought. However, this PhD study has shown that understanding individual tree species' functional traits needs to take centre stage if model prediction certainty is to increase.

References

Achard, F., R. Ébeuchle, P. Mayaux, H.-J. Stibig, C. Bodart, A. Brink, S. Carboni, B. Declee, F. Donnay, H. D. Eva, A. Lupi, R. Rasi, R. Seliger, and D. Simonetti. 2014. Determination of tropical deforestation rates and related carbon losses from 1990 to 2010. Global Change Biology **20**:2540-2554.

Allen, C. D., A. K. Macalady, H. Chenchouni, D. Bachelet, N. McDowell, M. Vennetier, T. Kitzberger, A. Rigling, D. D. Breshears, E. H. T. Hogg, P. Gonzalez, R. Fensham, Z. Zhang, J. Castro, N. Demidova, J.-H. Lim, G. Allard, S. W. Running, A. Semerci, and N. Cobb. 2010. A global overview of drought and heat-induced tree mortality reveals emerging climate change risks for forests. Forest Ecology and Management **259**:660-684.

Anderegg, W. R. 2015. Spatial and temporal variation in plant hydraulic traits and their relevance for climate change impacts on vegetation. New Phytologist **205**:1008-1014.

Anderegg, W. R., J. A. Berry, D. D. Smith, J. S. Sperry, L. D. Anderegg, and C. B. Field. 2012. The roles of hydraulic and carbon stress in a widespread climate-induced forest die-off. Proceedings of the National Academy of Sciences **109**:233-237

Anderegg, W. R., T. Klein, M. Bartlett, L. Sack, A. F. Pellegrini, B. Choat, and S. Jansen. 2016. Meta-analysis reveals that hydraulic traits explain cross-species patterns of drought-induced tree mortality across the globe. Proceedings of the National Academy of Sciences **113**:5024-5029.

Anfodillo, T., V. Carraro, M. Carrer, C. Fior, and S. Rossi. 2006. Convergent tapering of xylem conduits in different woody species. New Phytologist **169**:279-290.

Ani, S. and H. Aminah. 2006. Plantation Timber of *Maesopsis eminii*. Journal of Tropical Forest Science **18**.

Asefi-Najafabady, S. and S. Saatchi. 2013. Response of African humid tropical forests to recent rainfall anomalies. Philosophical Transactions of the Royal Society B: Biological Sciences **368**:20120306.

Atkin, O. K., K. J. Bloomfield, P. B. Reich, M. G. Tjoelker, G. P. Asner, D. Bonal, G. Bönisch, M. G. Bradford, L. A. Cernusak, E. G. Cosio, D. Creek, K. Y. Crous, T. F. Domingues, J. S. dukes, E. J. J.G., J. R. Evans, G. D. Farquhar, N. M. Fyllas, P. P. G. Gauthier, E. Gloor, T. E. Gimeno, K. L. Griffin, R. Guerrieri, M. A. Heskel, C. Huntingford, F. Y. Ishida, J. Kettge, H. Lambers, M. J. Liddell, J. Lloyd, C. H. Lusk, R. E. Martin, A. P. Maksimov, T. C. Maximov, Y. Malhi, B. E. Medlyn, P. Meir, L. Mercado, M., M. Nicholas, D. Ng, U. Niinemets, O. O'Sullivan, O. L. Phillips, L. Poorter, P. Poot, I. C. Prentice, N. Salinas, L. M. Rowland, M. G. Ryan, S. Sitch, M. Slot, N. G. Smith, M. H. Turnbull, M. C. VanderWel, F. Valladares, E. J. Veneklaas, L. K. Weerasinghe, Wirth Christian, I. J.

Wright, K. R. Wythers, J. Xiang, S. Xiang, and J. Zaragoza-Castells. 2015. Global variability in leaf respiration in relation to climate, plant functional types and leaf traits. New Phytologist **206**:614-636.

Avila, J. M., A. Gallardo, B. Ibáñez, and L. Gómez‑Aparicio. 2016. Quercus suber dieback alters soil respiration and nutrient availability in Mediterranean forests. Journal of Ecology.

Barbour, M. M., L. A. Cernusak, D. Whitehead, K. L. Griffin, M. H. Turnbull, D. T. Tissue, and G. D. Farquhar. 2005. Nocturnal stomatal conductance and implications for modelling δ18O of leaf-respired CO2 in temperate tree species. Functional Plant Biology **32**:1107-1121.

Barnard, D. M., F. C. Meinzer, B. Lachenbruch, K. A. McCulloh, D. M. Johnson, and D. R. Woodruff. 2011. Climate‑related trends in sapwood biophysical properties in two conifers: avoidance of hydraulic dysfunction through coordinated adjustments in xylem efficiency, safety and capacitance. Plant, Cell & Environment **34**:643-654.

Bartlett, M. K., C. Scoffoni, and L. Sack. 2012. The determinants of leaf turgor loss point and prediction of drought tolerance of species and biomes: a global meta‑analysis. Ecology Letters **15**:393-405.

Bazzaz, F. A. and S. T. A. Pickett. 1980. Physiological ecology of tropical succession: a comparative review. Annual review of ecology and systematics **11**:287-310.

Begg, J. E. and N. C. Turner. 1970. Water potential gradients in field tobacco. Plant Physiology **46**:343-346.

Beier, C., C. Beierkuhnlein, T. Wohlgemuth, J. Penuelas, B. Emmett, C. Körner, H. Boeck, J. H. Christensen, S. Leuzinger, I. A. Janssens, and K. Hansen. 2012. Precipitation manipulation experiments–challenges and recommendations for the future. Ecology Letters **15**:899-911.

Benyon, R. G. 1999. Nighttime water use in an irrigated Eucalyptus grandis plantation. Tree Physiology **19**:853-859.

Berdanier, A. B. and J. S. Clark. 2016. Multiyear drought‑induced morbidity preceding tree death in southeastern US forests. Ecological Applications **26**:17-23.

Berry, P. M., S. Brown, M. Chen, A. Kontogianni, O. Rowlands, G. Simpson, and M. Skourtos. 2014. Cross-sectoral interactions of adaptation and mitigation measures. Climatic change:1-13.

Binggeli, P. 1989. The ecology of *Maesopsis* invasion and dynamics of the evergreen forest of the East Usambaras and their implications for forests conservation and forestry practices. Pages 269-300 *in* A. C. Hamilton and R. Bensted-Smith, editors. Forest conservation in the East Usambara Mountains Tanzania. IUCN, Gland.

Binggeli, P. and A. C. Hamilton. 1990. Tree species invasions and sustainable forestry in the East Usambaras. Pages 39-47 *in* I. Hedberg and E. Persson, editors. Research for conservation of Tanzanaian catchment forests. Uppsala Universitet Reprocentralen HSC, Uppsala.

Binggeli, P. and A. C. Hamilton. 1993. Biological invasion by *Maesopsis eminii* in the East Usambara forests, Tanzania. Opera Botanica **121**:229-235.

Binggeli, P., C. Ruffo, D. Taylor, and A. Hamilton. 1989. Seed Banks in the Forest Soils. Pages 307-309 *in* G. IUCN, editor. Forest Conservation in the East Usambara Mountains, Tanzania. IUCN, Gland Switzerland and Cambridge.

Bishaw, B., H. Neufeldt, J. Mowo, A. Abdelkadir, J. Muriuki, G. Dalle, T. Assefa, K. Guillozet, H. Kassa, and I. K. Dawson. 2013. Farmers' Strategies for Adapting to and Mitigating Climate Variability and Change through Agroforestry in Ethiopia and Kenya.*in* C. M. Davis, B. Bernart, and A. Dmitriev, editors. Forestry Communications Group, Corvallis, Oregon.

Black, E., J. Slingo, and K. R. Sperber. 2003. An observational study of the relationship between excessively strong short rains in coastal East Africa and Indian Ocean SST. Monthly Weather Review **131**:74-94.

Bloemen, J., I. Bauweraerts, F. De Vos, C. Vanhove, S. Vandenberghe, P. Boeckx, and K. Steppe. 2015. Fate of xylem-transported ^{11}C-and ^{13}C-labeled CO_2 in leaves of poplar. Physiologia plantarum **153**:555-564.

Borchert, R. 1994. Soil and stem water storage determine phenology and distribution of tropical dry forest trees. Ecology:1437-1449.

Bosu, P. P., M. M. Apetorgbor, and A. Refera. 2009. Ecology and management of tropical Africa's forest invaders. In: Invasive Plants and Forest Ecosystems. Page 357 *in* R. K. Kohli, S. Jose, H. P. Singh, and D. R. Batish, editors. Invasive Plants and Forest Ecosystems CRC Press 2008, Florida, USA.

Bouche, P. S., M. Larter, J.-C. Domec, R. Burlett, P. Gasson, S. Jansen, and S. Delzon. 2014. A broad survey of hydraulic and mechanical safety in the xylem of conifers. Journal of experimental botany:eru218.

Bragg, T., N. Webb, R. Spencer, J. Wood, C. Nicholl, and E. Potter. 1991. User Manual for the Porometer type AP4. Delta-T Devices Ltd., Cambridge, England.

Bréda, N., R. Huc, A. Granier, and E. Dreyer. 2006. Temperate forest trees and stands under severe drought: a review of ecophysiological responses, adaptation processes and long-term consequences. Annals of Forest Science **63**:625-644.

Brodribb, T. J., D. J. Bowman, S. Nichols, S. Delzon, and R. Burlett. 2010. Xylem function and growth rate interact to determine recovery rates after exposure to extreme water deficit. New Phytologist **188**:533-542.

Bucci, S. J., F. G. Scholz, G. Goldstein, F. C. Meinzer, J. A. Hinojosa, W. A. Hoffmann, and A. C. Franco. 2004. Processes preventing nocturnal equilibration between leaf and soil water potential in tropical savanna woody species. Tree Physiology **24**:1119-1127.

Buchholz, T., T. Tennigkeit, and A. Weinreich. 2010a. Single tree management models: *Maesopsis eminii*. Pages 247-266 *in* F. Bongers and T. Tennigkeit, editors. Degraded forests in Eastern Africa: management and restoration. Earthscan, London, UK and Washington, DC, USA.

Buchholz, T., A. Weinreich, and T. Tennigkeit. 2010b. Modeling heliotropic tree growth in hardwood tree species—A case study on *Maesopsis eminii*. Forest Ecology and Management **260**:1656-1663.

References

Bulafu, C., D. Baranga, P. Mucunguzi, R. J. Telford, and V. Vandvik. 2013. Massive structural and compositional changes over two decades in forest fragments near Kampala, Uganda. Ecology and evolution **3**:3804-3823.

CABI. 2016. *Maesopsis eminii* (umbrella tree).

Caird, M. A., J. H. Richards, and L. A. Donovan. 2007. Nighttime stomatal conductance and transpiration in C3 and C4 plants. Plant Physiology **143**:4-10.

Calama, R., J. Puértolas, G. Madrigal, and M. Pardos. 2013. Modeling the environmental response of leaf net photosynthesis in Pinus pinea L. natural regeneration. Ecological Modelling **251**:9-21.

Cannell, M. G. R. and J. H. M. Thornley. 1998. Temperature and CO2responses of leaf and canopy photosynthesis: a clarification using the non-rectangular hyperbola model of photosynthesis. Annals of Botany **82**:883-892.

Cao, M., Q. Zhang, and H. H. Shugart. 2001. Dynamic responses of African ecosystem carbon cycling to climate change. Climate Research **17**:183-193.

Carlquist, S. 1984. Vessel grouping in dicotyledon wood: significance and relationship to imperforate tracheary elements. Aliso **10**:505-525.

Chapotin, S. M., J. H. Razanameharizaka, and N. M. Holbrook. 2006. Baobab trees (Adansonia) in Madagascar use stored water to flush new leaves but not to support stomatal opening before the rainy season. The New phytologist **169**:549.

Chave, J., D. Coomes, S. Jansen, S. L. Lewis, N. G. Swenson, and A. E. Zanne. 2009. Towards a worldwide wood economics spectrum. Ecology Letters **12**:351-366.

Chave, J., M. Réjou-Méchain, A. Búrquez, E. Chidumayo, M. S. Colgan, W. B. C. Delitti, A. Duque, T. Eid, P. M. Fearnside, R. C. Goodman, M. Henry, A. Martínez-Yrízar, W. A. Mugasha, H. C. Muller-Landau, M. Mencuccini, B. W. Nelson, A. Ngomanda, E. M. Nogueira, E. Ortiz-Malavassi, R. Pélissier, P. Ploton, C. M. Ryan, J. G. Saldarriaga, and G. Vieilledent. 2014. Improved allometric models to estimate the aboveground biomass of tropical trees. Global Change Biology **20**:3177-3190.

Chazdon, R. L. 2008. Beyond deforestation: restoring forests and ecosystem services on degraded lands. Science **320**:1458-1460.

Choat, B., S. Jansen, T. J. Brodribb, H. Cochard, S. Delzon, R. Bhaskar, S. J. Bucci, T. S. Feild, S. M. Gleason, U. G. Hacke, A. L. Jacobsen, F. Lens, H. Maherali, J. Martinez-Vilalta, S. Mayr, M. Mencuccini, P. J. Mitchell, A. Nardini, Pittermann, Jarmila, B. R. Pratt, J. S. Sperry, M. Westboy, I. J. Wright, and A. E. Zanne. 2012. Global convergence in the vulnerability of forests to drought. Nature **491**:752-755.

Christman, M. A., J. S. Sperry, and F. R. Adler. 2009. Testing the 'rare pit'hypothesis for xylem cavitation resistance in three species of Acer. New Phytologist **182**:664-674.

Ciais, P., A. Bombelli, M. Williams, S. L. Piao, J. Chave, C. M. Ryan, M. Henry, P. Brender, and R. Valentini. 2011. The carbon balance of Africa: synthesis of recent research studies. Philosophical Transactions of the Royal Society of London A: Mathematical, Physical and Engineering Sciences **369**:2038-2057.

Ciais, P., S.-L. Piao, P. Cadule, P. Friedlingstein, and A. Chédin. 2009. Variability and recent trends in the African terrestrial carbon balance. Biogeosciences **6**:1935-1948.

Clark, J. S., L. Iverson, C. W. Woodall, C. D. Allen, D. M. Bell, D. C. Bragg, A. W. D'Amato, F. W. Davis, M. H. Hersh, I. Ibanez, S. T. Jackson, S. Matthews, N. Pederson, M. Peters, M. W. Schwartz, K. M. Waring, and N. Zimmermann. 2016. The impacts of increasing drought on forest dynamics, structure, and biodiversity in the United States. Global Change Biology.

Clark, C., J. Poulsen, E. Connor, and V. Parker. 2004. Fruiting trees as dispersal foci in a semi-deciduous tropical forest. Oecologia **139**:66-75.

Cochard, H., E. Badel, S. Herbette, S. Delzon, B. Choat, and S. Jansen. 2013. Methods for measuring plant vulnerability to cavitation: a critical review. Journal of experimental botany **64**:4779.

Collins, M., R. Knutti, J. Arblaster, J.-L. Dufresne, T. Fichefet, P. Friedlingstein, X. Gao, W. J. Gutowski, T. Johns, G. Krinner, M. Shongwe, C. Tebaldi, A. J. Weaver, and M. Wehner. 2013. Long-term Climate Change: Projections, Commitments and Irreversibility.*in* T. F. Stocker, D. Qin, G.-K. Plattner, M. Tignor, S. K. Allen, J. Boschung, A. Nauels, Y. Xia, V. Bex, and P. M. Midgley, editors. Climate Change 2013: The Physical Science Basis. Contribution of Working Group I to the Fifth Assessment Report of the Intergovernmental Panel on Climate Change. Cambridge University Press, Cambridge, United Kingdom and New York, NY, USA.

Comita, L. S. and B. M. Engelbrecht. 2009. Seasonal and spatial variation in water availability drive habitat associations in a tropical forest. Ecology **90**:2755-2765.

Cordeiro, N. J., D. A. Patrick, B. Munisi, and V. Gupta. 2004. Role of dispersal in the invasion of an exotic tree in an East African submontane forest. Journal of Tropical Ecology **20**:449-457.

Couralet, C., J. Van den Bulcke, L. M. Ngoma, J. Van Acker, and H. Beeckman. 2013. Phenology in functional groups of Central African rainforest trees. Journal of Tropical Forest Science **25**:361-374.

Croat, T. B. 1978. Flora of Barro Colorado Island. Stanford University Press, Stanford, California.

Daley, M. J. and N. G. Phillips. 2006. Interspecific variation in nighttime transpiration and stomatal conductance in a mixed New England deciduous forest. Tree Physiology **26**:411-419.

Dawson, W., D. F. Burslem, and P. E. Hulme. 2011. The comparative importance of species traits and introduction characteristics in tropical plant invasions. Diversity and Distributions **17**:1111-1121.

Dawson, W., D. F. Burslem, and P. E. Hulme. 2015. Consistent Effects of Disturbance and Forest Edges on the Invasion of a Continental Rain Forest by Alien Plants. Biotropica **47**:27-37.

De Frenne, P., F. Rodríguez-Sánchez, D. A. Coomes, L. Baeten, G. Verstraeten, M. Vellend, M. Bernhardt-Römermann, C. D. Brown, J. Brunet, J. Cornelis, G. M. Decocq, H. Diershke, O. Eriksson, F. S. Gilliam, R. Hedl, T. Heinke, M. Hermy, P. Hommel, M. A. Jenkins, D. L. Kelly, K. J. Kirby, F. J. G. Mitchell, T. Naaf, M. Newman, G. Peterken, P. Petrik, J. Schiultz, G. Sonnier, H. Van Calster, D. M. Waller, G.-R. Walther, P. S. White, K. D. Woods, M. Wulf, B. J. Graae, and K. Verheyen. 2013. Microclimate moderates plant

responses to macroclimate warming. Proceedings of the National Academy of Sciences **110**:18561-18565.

De Roo, L., L. Vergeynst, N. J. F. De Baerdemaeker, and K. Steppe. 2016. Acoustic Emissions to Measure Drought-Induced Cavitation in Plants. Applied Sciences **6**:71.

De Schepper, V., J. Bühler, M. Thorpe, G. Roeb, G. Huber, D. van Dusschoten, S. Jahnke, and K. Steppe. 2013. 11C-PET imaging reveals transport dynamics and sectorial plasticity of oak phloem after girdling. Frontiers in Plant Science **4**.

De Swaef, T., K. Steppe, and R. Lemeur. 2009. Determining reference values for stem water potential and maximum daily trunk shrinkage in young apple trees based on plant responses to water deficit. Agricultural Water Management **96**:541-550.

Dixon, H. H. and J. Joly. 1895. On the ascent of sap. Philosophical Transactions of the Royal Society of London. B **186**:563-576.

Domec, J.-C. and B. L. Gartner. 2001. Cavitation and water storage capacity in bole xylem segments of mature and young Douglas-fir trees. Trees **15**:204-214.

Domingues, T. F., P. Meir, T. R. Feldpausch, G. Saiz, E. M. Veenendaal, F. Schrodt, M. Bird, G. Djagbletey, F. Hien, H. Compaore, A. Diallo, J. Grace, and J. Llyoyd. 2010. Co‐limitation of photosynthetic capacity by nitrogen and phosphorus in West Africa woodlands. Plant, Cell & Environment **33**:959-980.

dosAnjos, L., M. A. Oliva, K. N. Kuki, M. S. Mielke, M. C. Ventrella, M. F. Galvão, and L. R. Pinto. 2015. Key leaf traits indicative of photosynthetic plasticity in tropical tree species. Trees **29**:247-258.

Doucet, J.-L., K. Daïnou, G. Ligot, D.-Y. Ouédraogo, N. Bourland, S. E. Ward, P. Tekam, P. Lagoute, and A. Fayolle. 2016. Enrichment of Central African logged forests with high-value tree species: testing a new approach to regenerating degraded forests. International Journal of Biodiversity Science, Ecosystem Services & Management **12**:83-95.

Doughty, C. E., D. B. Metcalfe, C. A. J. Girardin, F. F. Amezquita, D. G. Cabrera, W. H. Huasco, J. E. Silva-Espejo, A. Araujo-Murakami, M. C. da Costa, W. Rocha, T. R. Feldpausch, A. L. M. Mendoza, A. C. L. da Costa, P. Meir, O. L. Phillips, and Y. Malhi. 2015. Drought impact on forest carbon dynamics and fluxes in Amazonia. Nature **519**:78-82.

Dunn, O. J. 1964. Multiple Comparisons Using Rank Sums. Technometrics **6**:241-252.

Eamus, D. 1999. Ecophysiological traits of deciduous and evergreen woody species in the seasonally dry tropics. Trends in Ecology & Evolution **14**:11-16.

Edwards, W. R. N. and P. G. Jarvis. 1982. Relations between water content, potential and permeability in stems of conifers. Plant Cell and Environment **5**:271-277.

Eggeling, W. 1947. Observations on the ecology of the Budongo rain forest, Uganda. The Journal of Ecology:20-87.

Eggeling, W. J. and C. M. Harris. 1939. Forest trees and Timbers of the British Empire IV: Fifteen Uganda Timbers. Page 120pp. Clarendon Press, Oxford.

Ellis, A. R., S. P. Hubbell, and C. Potvin. 2000. In situ field measurements of photosynthetic rates of tropical tree species: a test of the functional group hypothesis. Canadian journal of botany **78**:1336-1347.

Engelbrecht, B. M. J., L. S. Comita, R. Condit, T. A. Kursar, M. T. Tyree, B. L. Turner, and S. P. Hubbell. 2007. Drought sensitivity shapes species distribution patterns in tropical forests. Nature **447**:80-82.

Engelbrecht, B. M. J., J. W. Dalling, T. R. H. Pearson, R. L. Wolf, D. A. Galvez, T. Koehler, M. T. Tyree, and T. A. Kursar. 2006. Short dry spells in the wet season increase mortality of tropical pioneer seedlings. Oecologia **148**:258-269.

Engelbrecht, B. M. J. and T. A. Kursar. 2003. Comparative drought-resistance of seedlings of 28 species of co-occurring tropical woody plants. Oecologia **136**:383-393.

Engelbrecht, B. M. J., T. A. Kursar, and M. T. Tyree. 2005. Drought effects on seedling survival in a tropical moist forest. Trees **19**:312-321.

Engler, A. 1906. Über *Maesopsis eminii* Engl., einen wichtigen Waldbaum des nordwestlichen Deutsch-Ostafrika, und die Notwendigkeit einer gründlichen forstbotanischen Erforschung der Wälder dieses Gebietes. . Notizblatt des Königl. botanischen Gartens und Museums zu Berlin. **38**:240-242.

Epila, J., N. J. F. De Baerdemaeker, L. L. Vergeynst, W. H. Maes, H. Beeckman, and K. Steppe. 2016. Capacitive water release and internal leaf water relocation delay drought-induced cavitation in African *Maesopsis eminii*. Tree Physiology (accepted).

Epila, J., H. Verbeeck, T. Otim-Epila, P. Okullo, E. Kearsley, and K. Steppe. 2016. The ecology of *Maesopsis eminii* Engl. in tropical Africa. Journal of African Ecology (accepted).

Epron, D., M. Bahn, D. Derrien, F. A. Lattanzi, J. Pumpanen, A. Gessler, P. Högberg, P. Maillard, M. Dannoura, D. Gérant, and Buchmann, Nina. 2012. Pulse-labelling trees to study carbon allocation dynamics: a review of methods, current knowledge and future prospects. Tree Physiology **32**:776-798.

Évrard, C. M. 1960. Rhamnaceae. Pages 429-452 Flore du Congo Belge et du Ruanda-Urundi. Institut National pour l'Étude Agronomique du Congo Belge, Brussels, Belgium.

Exell, A. W. and F. A. Mendonça. 1954. Conspectus florae Angolensis. Ministerio DoUltramar Lisboa.

Fang, L., S. Zhang, G. Zhang, X. Liu, X. Xia, S. Zhang, W. Xing, and X. Fang. 2015. Application of Five Light-Response Models in the Photosynthesis of Populus× Euramericana cv.'Zhonglin46'Leaves. Applied biochemistry and biotechnology:1-15.

FAO. 1977. FAO-UNESCO Soil Map of the World, 1:5.000.000. Paris.

FAO. 1978. Report on the Agro-Ecological Zones Project, World Soil Resources Report n. 48. Rome.

Fatichi, S., S. Leuzinger, and C. Körner. 2014. Moving beyond photosynthesis: from carbon source to sink‐driven vegetation modeling. New Phytologist **201**:1086-1095.

Fauset, S., T. R. Baker, S. L. Lewis, T. R. Feldpausch, K. Affum‐Baffoe, E. G. Foli, K. C. Hamer, and M. D. Swaine. 2012. Drought‐induced shifts in the floristic and functional composition of tropical forests in Ghana. Ecology Letters **15**:1120-1129.

References

Ferrer-Paris, J. R., A. Y. Sánchez-Mercado, C. Lozano, L. Zambrano, J. Soto, J. Baettig, and M. Leal. 2014. A compilation of larval host-plant records for six families of butterflies (Lepidoptera: Papilionoidea) from available electronic resources.

Filella, I., J. Llusia, J. Piñol, and J. Peñuelas. 1998. Leaf gas exchange and fluorescence of Phillyrea latifolia, Pistacia lentiscus and Quercus ilex saplings in severe drought and high temperature conditions. Environmental and Experimental Botany **39**:213-220.

Fisher, J. B., M. Sikka, S. Sitch, P. Ciais, B. Poulter, D. Galbraith, J.-E. Lee, C. Huntingford, N. Viovy, N. Zeng, A. Ahlstrom, M. R. Lomas, P. E. Levy, C. Frankenberg, S. Saatchi, and Y. Malhi. 2013. African tropical rainforest net carbon dioxide fluxes in the twentieth century. Philosophical Transactions of the Royal Society of London B: Biological Sciences **368**:20120376.

Flexas, J., J. Bota, J. Galmes, H. Medrano, and M. Ribas‐Carbó. 2006. Keeping a positive carbon balance under adverse conditions: responses of photosynthesis and respiration to water stress. Physiologia plantarum **127**:343-352.

Flexas, J., J. Galmes, M. Ribas-Carbo, and H. Medrano. 2005. The effects of water stress on plant respiration. Pages 85-94 Advances in Photosynthesis and Respiration. Springer.

Ford, C. R., C. E. Goranson, R. J. Mitchell, R. E. Will, and R. O. Teskey. 2004. Diurnal and seasonal variability in the radial distribution of sap flow: predicting total stem flow in Pinus taeda trees. Tree Physiology **24**:951-960.

Fu, Q., L. Cheng, Y. Guo, and R. Turgeon. 2011. Phloem Loading Strategies and Water Relations in Trees and Herbaceous Plants. Plant Physiology **157**:1518-1527.

Furukawa, A., S.-Y. Park, and Y. Fujinuma. 1990. Hybrid poplar stomata unresponsive to changes in environmental conditions. Trees **4**:191-197.

Gallé, A., P. Haldimann, and U. Feller. 2007. Photosynthetic performance and water relations in young pubescent oak (*Quercus pubescens*) trees during drought stress and recovery. New Phytologist **174**:799-810.

GFEPAFCC. 2009. Adaptation of forests and people to climate change-a global assessment report. International Union of Forest Research Organizations (IUFRO).

Gleason, S. M., M. Westoby, S. Jansen, B. Choat, U. G. Hacke, R. B. Pratt, R. Bhaskar, T. J. Brodribb, S. J. Bucci, K.-F. Cao, H. Cochard, S. Delzon, J.-C. Domec, Z.-X. Fan, T. S. Feild, A. L. Jacobsen, D. M. Johnson, F. Lens, H. Maherali, J. Martinez-Vilalta, S. Mayr, K. A. McCulloh, M. Mencuccini, P. J. Mitchell, H. Morris, A. Nardini, J. Pittermann, L. Plavcova, S. G. Schreiber, J. S. Sperry, and I. J. Wright. 2016. Weak tradeoff between xylem safety and xylem‐specific hydraulic efficiency across the world's woody plant species. New Phytologist **209**:123-136.

Gliniars, R., G. S. Becker, D. Braun, and H. Dalitz. 2013. Monthly stem increment in relation to climatic variables during 7 years in an East African rainforest. Trees **27**:1129-1138.

Goldstein, G., J. Andrade, F. Meinzer, N. Holbrook, J. Cavelier, P. Jackson, and A. Celis. 1998. Stem water storage and diurnal patterns of water use in tropical forest canopy trees. Plant, Cell & Environment **21**:397-406.

Greer, D. H. and M. M. Weedon. 2012. Modelling photosynthetic responses to temperature of grapevine (*Vitis vinifera* cv. Semillon) leaves on vines grown in a hot climate. Plant, Cell & Environment **35**:1050-1064.

Griffiths, H., G. Weller, L. F. M. Toy, and R. J. Dennis. 2013. You're so vein: bundle sheath physiology, phylogeny and evolution in C3 and C4 plants. Plant, Cell & Environment **36**:249-261.

Grulke, N., R. Alonso, T. Nguyen, C. Cascio, and W. Dobrowolski. 2004. Stomata open at night in pole-sized and mature ponderosa pine: implications for O3 exposure metrics. Tree Physiology **24**:1001-1010.

Guada, G., J. J. Camarero, R. Sánchez-Salguero, and R. M. N. Cerrillo. 2016. Limited growth recovery after drought-induced forest dieback in very defoliated trees of two pine species. Frontiers in Plant Science **7**.

Gustafson, E. J., A. M. G. De Bruijn, R. E. Pangle, J.-M. Limousin, N. G. McDowell, W. T. Pockman, B. R. Sturtevant, J. D. Muss, and M. E. Kubiske. 2015. Integrating ecophysiology and forest landscape models to improve projections of drought effects under climate change. Global Change Biology **21**:843-856.

Hacke, U. G. and J. S. Sperry. 2001. Functional and ecological xylem anatomy. Perspectives in Plant Ecology, Evolution and Systematics **4**:97-115.

Hacke, U. G., J. S. Sperry, and J. Pittermann. 2000. Drought experience and cavitation resistance in six shrubs from the Great Basin, Utah. Basic and Applied Ecology **1**:31-41.

Hacke, U. G., J. S. Sperry, W. T. Pockman, S. D. Davis, and K. A. McCulloh. 2001. Trends in wood density and structure are linked to prevention of xylem implosion by negative pressure. Oecologia **126**:457-461.

Hacke, U. G., J. S. Sperry, J. K. Wheeler, and L. Castro. 2006. Scaling of angiosperm xylem structure with safety and efficiency. Tree Physiology **26**:689-701.

Hall, J. B. 1995. *Maesopsis eminii* and its status in the East Usambara Mountains. Forestry and Beekeeping Division and Metsähallitus Consulting, Dar es Salaam, Tanzania and Vantaa, Finland.

Hall, J. B. 2010. Future options for *Maesopsis*: agroforestry asset or conservation catastrophe. Pages 221-246 *in* F. Bongers and T. Tenningkeit, editors. Degraded forests in Eastern Africa: Management and restoration. Earthscan, London.

Hampe, A. and F. Bairlein. 2000. Modified dispersal‑related traits in disjunct populations of bird‑dispersed Frangula alnus (Rhamnaceae): a result of its Quaternary distribution shifts? Ecography **23**:603-613.

Hanssens, J., T. De Swaef, N. Nadezhdina, and K. Steppe. 2013. Measurement of Sap Flow Dynamics through the Tomato Peduncle Using a Non-Invasive Sensor Based on the Heat Field Deformation Method. Pages 409-416 *in* IX International Workshop on Sap Flow 991.

Hao, G.-Y., W. A. Hoffmann, F. G. Scholz, S. J. Bucci, F. C. Meinzer, A. C. Franco, K.-F. Cao, and G. Goldstein. 2008. Stem and leaf hydraulics of congeneric tree species from adjacent tropical savanna and forest ecosystems. Oecologia **155**:405-415.

References

Hardy, O. J., C. Born, K. Budde, K. Daïnou, G. Dauby, J. Duminil, E.-E. B. K. Ewédjé, C. Gomez, M. Heuertz, G. K. Koffi, A. J. Lowe, C. Micheneau, D. Ndoade-Bourobou, R. Pineiro, and V. Poncet. 2013. Comparative phylogeography of African rain forest trees: a review of genetic signatures of vegetation history in the Guineo-Congolian region. Comptes Rendus Geoscience **345**:284-296.

Hepper, F. N. 1979. Second edition of the map showing the extent of floristic exploration in Africa south of the Sahara.*in* G. Kunkel, editor. Taxonomic aspects of African economic botany. AETFAT, Bentham-Moxon Trust, Royal Botanic Gardens, Kew.

Herault, B., B. Bachelot, L. Poorter, V. Rossi, F. Bongers, J. m. Chave, C. Paine, F. Wagner, and C. Baraloto. 2011. Functional traits shape ontogenetic growth trajectories of rain forest tree species. Journal of Ecology **99**:1431-1440.

Hiernaux, P., E. Mougin, L. Diarra, N. Soumaguel, F. Lavenu, Y. Tracol, and M. Diawara. 2009. Sahelian rangeland response to changes in rainfall over two decades in the Gourma region, Mali. Journal of Hydrology **375**:114-127.

Hijmans, R. J., S. E. Cameron, J. L. Parra, P. G. Jones, and A. Jarvis. 2005. Very high resolution interpolated climate surfaces for global land areas. International journal of climatology **25**:1965-1978.

Holbrook, N. M. 1995. Stem water storage. Pages 151-174 *in* B. L. Gartner, editor. Plant stems: physiology and functional morphology. Academic Press, San Diego, California.

Hölttä, T., M. Mencuccini, and E. Nikinmaa. 2009. Linking phloem function to structure: analysis with a coupled xylem–phloem transport model. Journal of Theoretical Biology **259**:325-337.

Howard, A. R. and L. A. Donovan. 2007. Helianthus nighttime conductance and transpiration respond to soil water but not nutrient availability. Plant Physiology **143**:145-155.

Howard, P. C. 1991. Nature conservation in Uganda's tropical forest reserves. IUCN, Gland Switzerland and Cambridge, UK with the financial support of WWF-International.

Hsiao, T. C. 1973. Plant responses to water stress. Annual review of plant physiology **24**:519-570.

Hubeau, M. and K. Steppe. 2015. Plant-PET Scans: In Vivo Mapping of Xylem and Phloem Functioning. Trends in plant science **20**:676-685.

Hulme, P. E., D. F. R. P. Burslem, W. Dawson, E. Edward, J. Richard, and R. Trevelyan. 2013. Aliens in the Arc: Are Invasive Trees a Threat to the Montane Forests of East Africa? Pages 145-165 *in* C. L. Foxcroft, P. Pyšek, M. D. Richardson, and P. Genovesi, editors. Plant Invasions in Protected Areas: Patterns, Problems and Challenges. Springer Netherlands, Dordrecht.

Humair, F., P. J. Edwards, M. Siegrist, and C. Kueffer. 2014. Understanding misunderstandings in invasion science: why experts don't agree on common concepts and risk assessments. NeoBiota **20**:1-30.

IPCC. 2007. Climate change 2007-the physical science basis: Working group I contribution to the fourth assessment report of the IPCC. Cambridge University Press.

Irvine, J. and J. Grace. 1997. Continuous measurements of water tensions in the xylem of trees based on the elastic properties of wood. Planta **202**:455-461.

James, R., R. Washington, and D. P. Rowell. 2013. Implications of global warming for the climate of African rainforests. Philosophical Transactions of the Royal Society B: Biological Sciences **368**:20120298.

Jenkin, R. N., W. Howard, T. Thomas, and G. Deane. 1977. Forestry development prospects in the Imatong Central Forest Reserve, southern Sudan. Land Resources Division.

Jensen, K. H., J. A. Savage, and N. M. Holbrook. 2013. Optimal concentration for sugar transport in plants. Journal of The Royal Society Interface 10: 20130055.

Johnston, M. C. 1972. Rhamnaceae. Pages 36-38 *in* E. Milne-Redhead and R. M. Polhill, editors. Flora of tropical East Africa. Crown Agents for Oversea Governments and Administrations, London, United kingdom.

Jøker, D. 2000. *Maesopsis eminii* Engl. Seed Leaflet-Danida Forest Seed Centre.

Kavanagh, K. L., R. Pangle, and A. D. Schotzko. 2007. Nocturnal transpiration causing disequilibrium between soil and stem predawn water potential in mixed conifer forests of Idaho. Tree Physiology **27**:621-629.

Kearsley, E., T. de Haulleville, K. Hufkens, A. Kidimbu, B. Toirambe, G. Baert, D. Huygens, Y. Kebede, P. Defourny, J. Bogaert, H. Beeckman, K. Steppe, P. Boeckx, and H. Verbeeck. 2013. Conventional tree height–diameter relationships significantly overestimate aboveground carbon stocks in the Central Congo Basin. Nature Communications **4**.

Keller, T. and R. Häsler. 1984. The influence of a fall fumigation with ozone on the stomatal behavior of spruce and fir. Oecologia **64**:284-286.

Kiser, M. R., C. D. Reid, A. S. Crowell, R. P. Phillips, and C. R. Howell. 2008. Exploring the transport of plant metabolites using positron emitting radiotracers. HFSP journal **2**:189-204.

Kolari, P., T. Chan, A. Porcar-Castell, J. Bäck, E. Nikinmaa, and E. Juurola. 2014. Field and controlled environment measurements show strong seasonal acclimation in photosynthesis and respiration potential in boreal Scots pine. Frontiers in Plant Science **5**:717.

Koller, S., V. Holland, and W. Brüggemann. 2013. Effects of drought stress on the evergreen Quercus ilex L., the deciduous Q. robur L. and their hybrid Q. × turneri Willd. Photosynthetica **51**:574-582.

Kozlowski, T. T., P. J. Kramer, and S. G. Pallardy. 1991. The Physiological Ecology of Woody Plants. Academic Press, Inc., New York.

Kruskal, W. H. and W. A. Wallis. 1952. Use of Ranks in One-Criterion Variance Analysis. Journal of the American Statistical Association **47**:583-621.

Lambers, H., F. S. Chapin III, and T. L. Pons. 1998. Plant physiological ecology Springer New York.

Larcher, W. 2003. Physiological plant ecology: ecophysiology and stress physiology of functional groups. Springer Science & Business Media.

Lawton, R. M. 1969. A new record, *Maesopsis eminii* Engl., for Zambia. Kirkia, Salisbury **7**:145-146.

Leegood, R. C. 2008. Roles of the bundle sheath cells in leaves of C3 plants. Journal of experimental botany **59**:1663-1673.

Lewis, J. D., N. G. Phillips, B. A. Logan, C. R. Hricko, and D. T. Tissue. 2011. Leaf photosynthesis, respiration and stomatal conductance in six Eucalyptus species native to mesic and xeric environments growing in a common garden. Tree Physiology **31**:997-1006.

Lewis, S. L., B. Sonké, T. Sunderland, S. K. Begne, G. Lopez-Gonzalez, G. M. van der Heijden, O. L. Phillips, K. Affum-Baffoe, T. R. Baker, L. Banin, J.-F. Bastin, H. Beeckman, P. Boeckx, J. Bogaert, C. De Canniere, E. Chezeaux, C. J. Clark, M. Collins, G. Djagbletey, M. Noel, K. Djuikouo, V. Droissart, J.-L. Doucet, C. E. N. Ewango, S. Fauset, T. R. Feldpausch, E. G. Foli, J.-F. Gillet, A. C. Hamilton, D. J. Harris, T. B. Hart, T. de Haulleville, A. Hladik, K. Hufkens, D. Huygens, P. Jeanmart, K. J. Jeffery, E. Kearsley, M. E. Leal, J. Lloyd, J. C. Lovett, J.-R. Makana, Y. Malhi, A. Marshall, R., L. O. Ojo, K. S.-H. Peh, G. Pickavance, J. R. Poulsen, J. M. Reitsma, D. Sheil, M. Simo, K. Steppe, H. E. Taedoumg, J. Talbot, J. R. D. Talpin, D. Taylor, S. C. Thomas, B. Toirambe, H. Verbeeck, J. Vleminckx, L. J. T. White, S. Wilcock, H. Woell, and L. Zemagho. 2013. Above-ground biomass and structure of 260 African tropical forests. Philosophical Transactions of the Royal Society B: Biological Sciences **368**:20120295.

Lieth, J. and J. Reynolds. 1987. The nonrectangular hyperbola as a photosynthetic light response model: geometrical interpretation and estimation of the parameter. Photosynthetica **21**:363-365.

Lloret, F., A. Escudero, J. M. Iriondo, J. Martínez‐Vilalta, and F. Valladares. 2012. Extreme climatic events and vegetation: the role of stabilizing processes. Global Change Biology **18**:797-805.

Loepfe, L., J. Martinez-Vilalta, J. Pinol, and M. Mencuccini. 2007. The relevance of xylem network structure for plant hydraulic efficiency and safety. Journal of Theoretical Biology **247**:788-803.

Loustalot, A. J. 1945. Influence of soil moisture conditions on apparent photosynthesis and transpiration of peacan leaves. J. Agr. Research **71**:519-532.

Maes, W. H., W. M. J. Achten, B. Reubens, and B. Muys. 2011. Monitoring stomatal conductance of *Jatropha curcas* seedlings under different levels of water shortage with infrared thermography. Agricultural and Forest Meteorology **151**:554-564.

Maes, W. H., W. M. J. Achten, B. Reubens, D. Raes, R. Samson, and B. Muys. 2009. Plant–water relationships and growth strategies of *Jatropha curcas* L. seedlings under different levels of drought stress. Journal of Arid Environments **73**:877-884.

Maharjan, S. K., L. Poorter, M. Holmgren, F. Bongers, J. J. Wieringa, and W. D. Hawthorne. 2011. Plant functional traits and the distribution of West African rain forest trees along the rainfall gradient. Biotropica **43**:552-561.

Maley, J. 1996. The African rain forest–main characteristics of changes in vegetation and climate from the Upper Cretaceous to the Quaternary. Proceedings of the Royal Society of Edinburgh. Section B. Biological Sciences **104**:31-73.

Malhi, Y., S. Adu-Bredu, R. A. Asare, S. L. Lewis, and P. Mayaux. 2013a. African rainforests: past, present and future. Philosophical Transactions of the Royal Society B: Biological Sciences **368**:20120312.

Malhi, Y., S. Adu-Bredu, R. A. Asare, S. L. Lewis, and P. Mayaux. 2013b. The past, present and future of Africa's rainforests. Philosophical Transactions of the Royal Society of London B: Biological Sciences **368**:20120293.

Malhi, Y., C. E. Doughty, G. R. Goldsmith, D. B. Metcalfe, C. A. J. Girardin, T. R. Marthews, J. del Aguila-Pasquel, L. E. O. C. Aragão, A. Araujo-Murakami, P. Brando, A. C. L. da Costa, J. E. Silva-Espejo, F. F. Amezquita, D. R. Galbraith, C. A. Quesada, W. Rocha, N. Salinas-Revilla, D. Silverio, and P. Meir. 2015. The linkages between photosynthesis, productivity, growth and biomass in lowland Amazonian forests. Global Change Biology **21**:2283-2295.

Markesteijn, L. and L. Poorter. 2009. Seedling root morphology and biomass allocation of 62 tropical tree species in relation to drought‐ and shade‐tolerance. Journal of Ecology **97**:311-325.

Markesteijn, L., L. Poorter, F. Bongers, H. Paz, and L. Sack. 2011a. Hydraulics and life history of tropical dry forest tree species: coordination of species' drought and shade tolerance. New Phytologist **191**:480-495.

Markesteijn, L., L. Poorter, H. Paz, L. Sack, and F. Bongers. 2011b. Ecological differentiation in xylem cavitation resistance is associated with stem and leaf structural traits. Plant, Cell & Environment **34**:137-148.

Martin, P. A., A. C. Newton, E. Cantarello, and P. Evans. 2015. Stand dieback and collapse in a temperate forest and its impact on forest structure and biodiversity. Forest Ecology and Management **358**:130-138.

Matías, L., J. L. Quero, R. Zamora, and J. Castro. 2012. Evidence for plant traits driving specific drought resistance. A community field experiment. Environmental and Experimental Botany **81**:55-61.

Matyssek, R., M. S. Günthardt-Goerg, S. Maurer, and T. Keller. 1995. Nighttime exposure to ozone reduces whole-plant production in Betula pendula. Tree Physiology **15**:159-165.

Mayaux, P., J.-F. Pekel, B. Desclée, F. Donnay, A. Lupi, F. Achard, M. Clerici, C. Bodart, A. Brink, R. Nasi, and A. Belward. 2013. State and evolution of the African rainforests between 1990 and 2010. Philosophical Transactions of the Royal Society of London B: Biological Sciences **368**:20120300.

McCulloh, K. A., D. M. Johnson, F. C. Meinzer, S. L. Voelker, B. Lachenbruch, and J.-C. Domec. 2012. Hydraulic architecture of two species differing in wood density: opposing strategies in co-occurring tropical pioneer trees. Plant, Cell & Environment **35**:116-125.

McCulloh, K. A., F. C. Meinzer, J. S. Sperry, B. Lachenbruch, S. L. Voelker, D. R. Woodruff, and J.-C. Domec. 2011. Comparative hydraulic architecture of tropical tree species representing a range of successional stages and wood density. Oecologia **167**:27-37.

McDowell, N., W. T. Pockman, C. D. Allen, D. D. Breshears, N. Cobb, T. Kolb, J. Plaut, J. Sperry, A. West, D. G. Williams, and E. A. Yepez. 2008. Mechanisms of plant survival and mortality during drought: why do some plants survive while others succumb to drought? New Phytologist **178**:719-739.

McDowell, N. G. and S. Sevanto. 2010. The mechanisms of carbon starvation: how, when, or does it even occur at all? New Phytologist **186**:264-266.

McGuire, A. D., S. Sitch, J. S. Clein, R. Dargaville, G. Esser, J. Foley, M. Heimann, F. Joos, J. Kaplan, D. W. Kicklighter, R. A. Meier, J. M. Melillo, B. Moore III, I. C. Prentice, N. Ramankutty, T. Reichenau, A. Schloss, H. Tian, L. J. Williams, and U. Wittenberg. 2001. Carbon balance of the terrestrial biosphere in the twentieth century: Analyses of CO2, climate and land use effects with four process-based ecosystem models. Global Biogeochemical Cycles **15**:183-206.

McKee, T. B., N. J. Doesken, and J. Kleist. 1993. The relationship of drought frequency and duration to time scales. Pages 179-183 *in* Proceedings of the 8th Conference on Applied Climatology. American Meteorological Society Boston, MA.

Meinzer, F. C., S. A. James, G. Goldstein, and D. Woodruff. 2003. Whole‑tree water transport scales with sapwood capacitance in tropical forest canopy trees. Plant, Cell & Environment **26**:1147-1155.

Meinzer, F. C., D. M. Johnson, B. Lachenbruch, K. A. McCulloh, and D. R. Woodruff. 2009. Xylem hydraulic safety margins in woody plants: coordination of stomatal control of xylem tension with hydraulic capacitance. Functional Ecology **23**:922-930.

Meir, P., P. E. Levy, J. Grace, and P. G. Jarvis. 2007. Photosynthetic parameters from two contrasting woody vegetation types in West Africa. Plant Ecology **192**:277-287.

Meir, P. and I. Woodward. 2010. Amazonian rain forests and drought: response and vulnerability. New Phytologist **187**:553-557.

Mencuccini, M. 2014. Temporal scales for the coordination of tree carbon and water economies during droughts. Tree Physiology **34**:439-442.

Metz, B. 2001. Climate change 2001: mitigation: contribution of Working Group III to the third assessment report of the Intergovernmental Panel on Climate Change. Cambridge University Press.

Mori, S. A. and J. L. Brown. 1994. Report on wind dispersal in a lowland moist forest in central French Guiana. Brittonia **46**:105-125.

Mugasha, A. G. 1981. The silviculture of Tanzanian indigenous tree species.II. *Maesopsis eminii* Engl. Tanzania Silviculture Technical Note **52**:14pp.

Muggeo, V. M. R. 2008. Segmented: an R package to fit regression models with broken-line relationships. R News **8**:20–25.

Nadezhdina, N., M. W. Vandegehuchte, and K. Steppe. 2012. Sap flux density measurements based on the heat field deformation method. Trees **26**:1439-1448.

Niinemets, Ü. 2010. Responses of forest trees to single and multiple environmental stresses from seedlings to mature plants: past stress history, stress interactions, tolerance and acclimation. Forest Ecology and Management **260**:1623-1639.

O'Grady, A. P., D. Eamus, and L. Hutley. 1999. Transpiration increases during the dry season: patterns of tree water use in eucalypt open-forests of northern Australia. Tree Physiology **19**:591-597.

Oksanen, J. and P. R. Minchin. 2002. Continuum theory revisited: what shape are species responses along ecological gradients? Ecological Modelling **157**:119-129.

O'Leary, M. H. 1988. Carbon Isotopes in Photosynthesis. BioScience **38**:328-336.

Orwa, C., A. Muta, R. Kindt, R. Jamnadass, and S. Anthony. 2009. Agroforestree Database: A tree reference and selection guide version 4.0 (http://www.worldagroforestry.org/sites/treedbs/treedatabases.asp).

Oslisly, R., L. White, I. Bentaleb, C. Favier, M. Fontugne, J.-F. Gillet, and D. Sebag. 2013. Climatic and cultural changes in the west Congo Basin forests over the past 5000 years. Philosophical Transactions of the Royal Society B: Biological Sciences **368**:20120304.

Otto, F. E. L., R. G. Jones, K. Halladay, and M. R. Allen. 2013. Attribution of changes in precipitation patterns in African rainforests. Philosophical Transactions of the Royal Society B: Biological Sciences **368**:20120299.

Ouédraogo, D.-Y., F. Mortier, S. Gourlet-Fleury, V. Freycon, and N. Picard. 2013. Slow‐growing species cope best with drought: evidence from long‐term measurements in a tropical semi‐deciduous moist forest of Central Africa. Journal of Ecology **101**:1459-1470.

Owiunji, I. and A. Plumptre. 1998. Bird communities in logged and unlogged compartments in Budongo Forest, Uganda. Forest Ecology and Management **108**:115-126.

Padilla, F. M. and F. I. Pugnaire. 2007. Rooting depth and soil moisture control Mediterranean woody seedling survival during drought. Functional Ecology **21**:489-495.

Pammenter, N. W. and C. Van der Willigen. 1998. A mathematical and statistical analysis of the curves illustrating vulnerability of xylem to cavitation. Tree Physiology **18**:589-593.

Pantin, F., T. Simonneau, and B. Muller. 2012. Coming of leaf age: control of growth by hydraulics and metabolics during leaf ontogeny. New Phytologist **196**:349-366.

Parks, C. G. and P. Bernier. 2010. Adaptation of forests and forest management to changing climate with emphasis on forest health: A review of science, policies and practices. Forest Ecology and Management **259**:657-659.

Parmentier, I., Y. Malhi, B. Senterre, R. J. Whittaker, A. Alonso, M. P. B. Balinga, A. Bakayoko, F. Bongers, C. Chatelain, J. A. Comiskey, R. Cortay, M.-N. D. Kamdem, J.-L. Doucet, L. Gautier, W. D. Hawthrone, Y. A. Issembe, F. N. Kouame, L. A. Kouka, M. E. Leal, J. Lejoly, S. L. Lewis, L. Nusbaumer, M. P. E. Parren, K. S.-H. Peh, O. L. Phillips, D. Sheil, B. Sonke, M. S. M. Sosef, T. C. H. Sunderland, J. Stropp, H. T. Steege, e. M. D. Swai, M. G. P. Tchouto, B. S. Van Gemerden, J. L. C. H. Van Valkenburg, and H. Woll. 2007. The odd man out? Might climate explain the lower tree α‐diversity of African rain forests relative to Amazonian rain forests? Journal of Ecology **95**:1058-1071.

Pearson, T. R., D. F. Burslem, R. E. Goeriz, and J. W. Dalling. 2003a. Interactions of Gap Size and Herbivory on Establishment, Growth and Survival of Three Species of Neotropical Pioneer Trees. Journal of Ecology:785-796.

Pearson, T. R., D. F. Burslem, R. E. Goeriz, and J. W. Dalling. 2003b. Regeneration niche partitioning in neotropical pioneers: effects of gap size, seasonal drought and herbivory on growth and survival. Oecologia **137**:456-465.

Pelling, M. 2010. Adaptation to climate change: from resilience to transformation. Routledge.

References

Pellizzari, E., J. J. Camarero, A. Gazol, G. Sangüesa‑Barreda, and M. Carrer. 2016. Wood anatomy and carbon‑isotope discrimination support long‑term hydraulic deterioration as a major cause of drought‑induced dieback. Global Change Biology.

Phillips, N. G., M. G. Ryan, B. J. Bond, N. G. McDowell, T. M. Hinckley, and J. Čermák. 2003. Reliance on stored water increases with tree size in three species in the Pacific Northwest. Tree Physiology **23**:237-245.

Picard, N., M. Henry, N. H. Fonton, J. Kondaoulé, A. Fayolle, L. Birigazzi, G. Sola, A. Poultouchidou, C. Trotta, and H. Maïdou. 2015. Error in the estimation of emission factors for forest degradation in central Africa. Journal of Forest Research:1-8.

Pietragalla, J. and A. Pask. 2012. Stomatal conductance.

Pineda-Garcia, F., H. Paz, and F. C. Meinzer. 2013. Drought resistance in early and late secondary successional species from a tropical dry forest: the interplay between xylem resistance to embolism, sapwood water storage and leaf shedding. Plant, Cell & Environment **36**:405-418.

Pittermann, J., J. S. Sperry, J. K. Wheeler, U. G. Hacke, and E. H. Sikkema. 2006. Mechanical reinforcement of tracheids compromises the hydraulic efficiency of conifer xylem. Plant, Cell & Environment **29**:1618-1628.

Plumptre, A. J. 1996. Changes following 60 years of selective timber harvesting in the Budongo Forest Reserve, Uganda. Forest Ecology and Management **89**:101-113.

Pockman, W. T., J. S. Sperry, and J. W. O'Leary. 1995. Sustained and significant negative water pressure in xylem. Nature **378**:715-716.

Poorter, L. and L. Markesteijn. 2008. Seedling Traits Determine Drought Tolerance of Tropical Tree Species. Biotropica **40**:321-331.

Porporato, A., F. Laio, L. Ridolfi, and I. Rodriguez-Iturbe. 2001. Plants in water-controlled ecosystems: active role in hydrologic processes and response to water stress: III. Vegetation water stress. Advances in Water Resources **24**:725-744.

Prabhakar, M. 2004. Structure, delimitation, nomenclature and classification of stomata. Acta Botanica Sinica **46**:242-252.

Rao, K. and K. S. Rajput. 1999. Seasonal behaviour of vascular cambium in teak (*Tectona grandis*) growing in moist deciduous and dry deciduous forests. IAWA Journal **20**:85-93.

Raunkier, C. 1934. The life forms of plants and plant geography. Oxford University Press, New York.

Raven, P. H. and D. I. Axelrod. 1974. Angiosperm biogeography and past continental movements. Annals of the Missouri Botanical Garden **61**:539-673.

Ravindranath, N. H. 2007. Mitigation and adaptation synergy in forest sector. Mitigation and Adaptation Strategies for Global Change **12**:843-853.

Richardson, D. M., P. Pyšek, M. Rejmánek, M. G. Barbour, F. D. Panetta, and C. J. West. 2000. Naturalization and invasion of alien plants: concepts and definitions. Diversity and Distributions **6**:93-107.

Richardson, J., L. Chatrou, J. Mols, R. Erkens, and M. Pirie. 2004. Historical biogeography of two cosmopolitan families of flowering plants: Annonaceae and Rhamnaceae. Philosophical Transactions of the Royal Society B: Biological Sciences **359**:1495-1508.

Roman, D. T., K. A. Novick, E. R. Brzostek, D. Dragoni, F. Rahman, and R. P. Phillips. 2015. The role of isohydric and anisohydric species in determining ecosystem-scale response to severe drought. Oecologia **179**:641-654.

Rosner, S., B. Karlsson, J. Konnerth, and C. Hansmann. 2009. Shrinkage processes in standard-size Norway spruce wood specimens with different vulnerability to cavitation. Tree Physiology **29**:1419-1431.

Rosner, S., J. Světlík, K. Andreassen, I. Børja, L. Dalsgaard, R. Evans, B. Karlsson, M. M. Tollefsrud, and S. Solberg. 2013. Wood density as a screening trait for drought sensitivity in Norway spruce 1. Canadian Journal of Forest Research **44**:154-161.

RStudio, T. 2015. RStudio: Integrated Development for R. RStudio, Inc., Boston, MA.

Ryan, M. G., R. M. Hubbard, S. Pongracic, R. J. Raison, and R. E. McMurtrie. 1996. Foliage, fine-root, woody-tissue and stand respiration in Pinus radiata in relation to nitrogen status. Tree Physiology **16**:333-343.

Saatchi, S., J. Mascaro, L. Xu, M. Keller, Y. Yang, P. Duffy, F. Espírito-Santo, A. Baccini, J. Chambers, and D. Schimel. 2015. Seeing the forest beyond the trees. Global Ecology and Biogeography **24**:606-610.

Sala, A., D. R. Woodruff, and F. C. Meinzer. 2012. Carbon dynamics in trees: feast or famine? Tree Physiology **32**:764-775.

Sanchez-Diaz, M. F. and P. J. Kramer. 1971. Behavior of corn and sorghum under water stress and during recovery. Plant Physiology **48**:613-616.

Sass-Klaassen, U., P. Fonti, P. Cherubini, J. Gričar, E. M. R. Robert, K. Steppe, and A. Bräuning. 2016. A Tree-Centered Approach to Assess Impacts of Extreme Climatic Events on Forests. Frontiers in Plant Science **7**.

Saugier, B., A. Granier, J. Pontailler, E. Dufrene, and D. Baldocchi. 1997. Transpiration of a boreal pine forest measured by branch bag, sap flow and micrometeorological methods. Tree Physiology **17**:511-519.

Schabel, H. G. and A. Latiff. 1997. *Maesopsis eminii* Engler. Pages 184-187 *in* I. Faridah Hanum and L. J. G. van der Maesen, editors. Plant resources of South-East Asia No. 11: Auxiliary plants. Backhuys, Leiden, The Netherlands.

Scheiter, S., L. Langan, and S. I. Higgins. 2013. Next‐generation dynamic global vegetation models: learning from community ecology. New Phytologist **198**:957-969.

Schenk, H. J., K. Steppe, and S. Jansen. 2015. Nanobubbles: a new paradigm for air-seeding in xylem. Trends in plant science **20**:199-205.

Schindelin, J., I. Arganda-Carreras, E. Frise, V. Kaynig, M. Longair, T. Pietzsch, S. Preibisch, C. Rueden, S. Saalfeld, B. Schmid, J.-Y. Tinevez, D. J. White, V. Hartenstein, K. Eliceiri, P. Tomancak, and A. Cardona. 2012. Fiji: an open-source platform for biological-image analysis. Nat Meth **9**:676-682.

References

Schippers, P., F. Sterck, M. Vlam, and P. A. Zuidema. 2015. Tree growth variation in the tropical forest: understanding effects of temperature, rainfall and CO2. Global Change Biology **21**:2749-2761.

Scholz, A., M. Klepsch, Z. Karimi, and S. Jansen. 2013. How to quantify conduits in wood. Frontiers in Plant Science **4**:1-11.

Scholz, F. G., S. J. Bucci, G. Goldstein, F. C. Meinzer, A. C. Franco, and F. Miralles-Wilhelm. 2007. Removal of nutrient limitations by long-term fertilization decreases nocturnal water loss in savanna trees. Tree Physiology **27**:551-559.

Sevanto, S. 2014. Phloem transport and drought. Journal of experimental botany.

Sevanto, S., N. G. McDowell, L. T. Dickman, R. Pangle, and W. T. Pockman. 2014. How do trees die? A test of the hydraulic failure and carbon starvation hypotheses. Plant, Cell & Environment **37**:153-161.

Shaw, E., N. Sewankambo, F. Lisk, K. J. David, O. C. Garimoi, I. J. Baanabe, S. Irene, and H. Besada. 2009. CIGI Speacial Report Climate change in Africa: Adaptation, mitigation and governance challenges. The Centre for International Governance Innovation (CIGI), Waterloo, Ontario, Canada.

Shen, F., R. Gao, W. Liu, and W. Zhang. 2002. Physical analysis of the process of cavitation in xylem sap. Tree Physiology **22**:655-659.

Shongwe, M. E., G. J. van Oldenborgh, B. van den Hurk, and M. van Aalst. 2011. Projected changes in mean and extreme precipitation in Africa under global warming. Part II: East Africa. Journal of Climate **24**:3718-3733.

Slewinski, T. L. and D. M. Braun. 2010. Current perspectives on the regulation of whole-plant carbohydrate partitioning. Plant Science **178**:341-349.

Slik, J. W. F., V. Arroyo-Rodríguez, S.-I. Aiba, P. Alvarez-Loayza, L. F. Alves, P. Ashton, P. Balvanera, M. L. Bastian, P. J. Bellingham, E. van den Berg, L. Bernacci, P. d. C. Bispo, L. Blanc, K. Böhning-Gaese, P. Boeckx, F. Bongers, B. Boyle, M. G. Bradford, F. Q. Brearley, M. B.-N. Hockemba, S. Bunyavejchewin, D. C. L. Matos, M. Castillo-Santiago, E. L. M. Catharino, S.-L. Chai, Y. Chen, R. K. Colwell, R. L. Chazdon, C. J. Clark, D. B. Clark, D. A. Clark, H. Culmsee, K. Damas, H. S. Dattaraja, G. Dauby, P. Davidar, S. J. DeWalt, J.-L. Doucet, A. Duque, G. Durigan, K. A. O. Eichhorn, P. V. Eisenlohr, E. Eler, C. Ewango, N. Farwig, K. J. Feeley, L. Ferreira, R. Field, A. d. O. Filho, C. Fletcher, O. Forshed, G. Franco, G. Fredriksson, T. Gilespie, J.-F. Gillet, G. Amarnath, D. M. Griffith, J. Grogan, N. Gunatilleke, D. Harris, R. Harrison, A. Hector, J. Homeier, N. Imai, A. Itoh, P. A. Jansen, C. A. Joly, B. H. J. de Jong, K. Kartawinata, E. Kearsley, D. L. Kelly, D. Kenfack, M. Kessler, K. Kitayama, R. Kooyman, E. Larney, Y. Laumonier, S. G. Laurance, W. F. Laurance, M. J. Lawes, I. Leao do Amaral, S. G. Letcher, J. Lindsell, X. Lu, A. Mansor, A. Marjokorpi, E. H. Martin, H. Meilby, F. P. L. Melo, D. J. Metcalfe, V. P. Medjobe, J. P. Metzger, J. Millet, D. Mohandass, J. C. Montero, M. de Morisson Valeriano, B. Mugerwa, H. Nagamasu, Nilus, Reuben, S. Ochoa-Gaona, N. O. Page, P. Parolin, M. P. E. Parren, N. Parthasarathy, E. Paudel, A. Permana, M. T. F. Piedade, N. C. A. Pitman, L. Poorter, A. D. Poulsen, J. Poulsen, J. Powers, R. C. Prasad, J.-P. Puyrvavaud, J.-C. Razafimahaimodison, J. Reitsma, d. S. J. Roberto, W. R. Spironello, H. Romero-Saltos, F. Rovero, A. H. Rozak, K. Ruokolainen, E. Rutishauser, F. Saiter, P. Saner, B. A. Santos, F. Santos, S. K. Sarker, M. Satdichanh, C. B. Schmitt, J. Schöngart, M. Schulze, M. S. Suganuma, D. Sheil, E. da Silva Pinheiro, P. Sist, T. Stevart, R. Sukumar, I.-F. Sun, T. Sunderland, H. S. Suresh, E. Suzuki, M. Tabarelli, J. Tang, N. Targhetta, I. Theilade, D. W.

Thomas, P. Tchouto, J. Hurtado, R. Valencia, J. L. C. H. Van Valkenburg, T. Van Do, R. Vasquez, H. Verbeeck, V. Adekunle, S. A. Vieira, C. O. Webb, T. Whitfeld, S. A. Wich, J. Williams, F. Wittmann, H. Woll, X. Yang, C. Y. A. Yao, S. L. Yap, T. Yoneda, R. A. Zahawi, R. Zakaria, R. Zang, R. L. de Assis, B. G. Luize, and E. M. Venticinque. 2015. An estimate of the number of tropical tree species. Proceedings of the National Academy of Sciences **112**:7472-7477.

Slot, M. and L. Poorter. 2007. Diversity of tropical tree seedling responses to drought. Biotropica **39**:683-690.

Snyder, K., J. Richards, and L. Donovan. 2003. Night-time conductance in C3 and C4 species: do plants lose water at night? Journal of experimental botany **54**:861-865.

Somorin, O. A. 2010. Climate impacts, forest-dependent rural livelihoods and adaptation strategies in Africa: A review. African Journal of Environmental Science and Technology **4**:903-912.

Sperry, J. S., F. C. Meinzer, and K. A. McCulloh. 2008. Safety and efficiency conflicts in hydraulic architecture: scaling from tissues to trees. Plant, Cell & Environment **31**:632-645.

Steppe, K., H. Cochard, A. Lacointe, and T. Améglio. 2012. Could rapid diameter changes be facilitated by a variable hydraulic conductance? Plant, Cell & Environment **35**:150-157.

Steppe, K., D. J. De Pauw, T. M. Doody, and R. O. Teskey. 2010. A comparison of sap flux density using thermal dissipation, heat pulse velocity and heat field deformation methods. Agricultural and Forest Meteorology **150**:1046-1056.

Steppe, K., D. J. De Pauw, R. Lemeur, and P. A. Vanrolleghem. 2006. A mathematical model linking tree sap flow dynamics to daily stem diameter fluctuations and radial stem growth. Tree Physiology **26**:257-273.

Steppe, K. and R. Lemeur. 2004. An experimental system for analysis of the dynamic sap-flow characteristics in young trees: results of a beech tree. Functional Plant Biology **31**:83-92.

Steppe, K. and R. Lemeur. 2007. Effects of ring-porous and diffuse-porous stem wood anatomy on the hydraulic parameters used in a water flow and storage model. Tree Physiology **27**:43-52.

Steppe, K., F. Sterck, and A. Deslauriers. 2015. Diel growth dynamics in tree stems: linking anatomy and ecophysiology. Trends in plant science **20**:335-343.

Steppe, K., J. von der Crone, and D. De Pauw. 2016. TreeWatch.net: a tree water and carbon monitoring network to assess instant tree hydraulic functioning and stem growth. Frontiers in Plant Science, http://dx.doi.org/10.3389/fpls.2016.00993.

Struhsaker, T. T. 1987. Forestry issues and conservation in Uganda. Biological Conservation **39**:209-234.

Tanaka, A. and A. Makino. 2009. Photosynthetic research in plant science. Plant and cell physiology **50**:681-683.

Taylor, D. 1989. Root distribution in relation to vegetation and soil type in the forests of the East Usambaras. Pages 313-330 *in* A.C.Hamilton and R. Bensted-Smith, editors. Forest Conservation in the East Usambara Mountains, Tanzania. IUCN, Gland, Switzerland and Cambridge, UK.

Thornley, J. H. M. 1998. Dynamic model of leaf photosynthesis with acclimation to light and nitrogen. Annals of Botany **81**:421-430.

Tihurua, E. F. d. S. 2012. Studi anatomi daun dan batang *Maesopsis eminii* (Rhamnaceae). Berkala Penelitian Hayati **17**:193-196.

Tomlinson, K. W., L. Poorter, F. J. Sterck, F. Borghetti, D. Ward, S. de Bie, and F. van Langevelde. 2013. Leaf adaptations of evergreen and deciduous trees of semi‐arid and humid savannas on three continents. Journal of Ecology **101**:430-440.

Tsakiris, G. and H. Vangelis. 2005. Establishing a drought index incorporating evapotranspiration. European Water **9**:3-11.

Turgeon, R. 2010. The Role of Phloem Loading Reconsidered. Plant Physiology **152**:1817-1823.

Tyree, M. T., S. D. Davis, and H. Cochard. 1994. Biophysical perspectives of xylem evolution: is there a tradeoff of hydraulic efficiency for vulnerability to dysfunction? IAWA Journal **15**:335-360.

Tyree, M. T., B. M. J. Engelbrecht, G. Vargas, and T. A. Kursar. 2003. Desiccation tolerance of five tropical seedlings in Panama. Relationship to a field assessment of drought performance. Plant Physiology **132**:1439-1447.

Tyree, M. T. and F. W. Ewers. 1991. The hydraulic architecture of trees and other woody plants. New Phytologist **119**:345-360.

Tyree, M. T. and J. S. Sperry. 1989. Vulnerability of xylem to cavitation and embolism. Annual review of plant biology **40**:19-36.

Tyree, M. T., G. Vargas, B. M. J. Engelbrecht, and T. A. Kursar. 2002. Drought until death do us part: a case study of the desiccation‐tolerance of a tropical moist forest seedling‐tree, Licania platypus (Hemsl.) Fritsch. Journal of experimental botany **53**:2239-2247.

Tyree, M. T. and S. Yang. 1990. Water-storage capacity ofThuja, Tsuga andAcer stems measured by dehydration isotherms. Planta **182**:420-426.

UNEP/ISSS/ISRIC/FAO. 1993. Global and national soils and terrain database (SOTER): Procedures manual. FAO, Rome.

Upchurch, R. P., M. L. Peterson, and R. M. Hagan. 1955. Effect of Soil-Moisture Content on the Rate of Photosynthesis and Respiration in Ladino Clover (*Trifolium Repens* L.). Plant Physiology **30**:297.

Van den Bilcke, N., S. De Smedt, D. J. Simbo, and R. Samson. 2013. Sap flow and water use in African baobab (*Adansonia digitata* L.) seedlings in response to drought stress. South African Journal of Botany **88**:438-446.

van der Molen, M. K., A. J. Dolman, P. Ciais, T. Eglin, N. Gobron, B. E. Law, P. Meir, W. Peters, O. L. Phillips, M. Reichstein, T. Chen, S. C. Dekker, M. Doubková, M. A. Friedl, M. Jung, B. J. J. M. van den Hurk, R. A. M. de Jeu, B. Kruijt, T. Ohta, K. T. Rebel, S. Plummer, S. I. Seneviratne, S. Sitch, A. J. Teuling, G. R. van der Werf, and G. Wang. 2011. Drought and ecosystem carbon cycling. Agricultural and Forest Meteorology **151**:765-773.

Vandegehuchte, M. W. and K. Steppe. 2012. Interpreting the Heat Field Deformation method: Erroneous use of thermal diffusivity and improved correlation between temperature ratio and sap flux density. Agricultural and Forest Meteorology **162**:91-97.

Vandegehuchte, M. W. and K. Steppe. 2013. Corrigendum to: Sap-flux density measurement methods: working principles and applicability. Functional Plant Biology **40**:1088-1088.

Varone, L. and L. Gratani. 2015. Leaf respiration responsiveness to induced water stress in Mediterranean species. Environmental and Experimental Botany **109**:141-150.

Veenendaal, E., M. Swaine, D. Newbery, H. Prins, and N. Brown. 1998. Limits to tree species distributions in lowland tropical rainforest. Pages 163-191 *in* Dynamics of tropical communities: the 37th symposium of the British Ecological Society, Cambridge University, 1996. Blackwell Science Ltd.

Verchot, L. V., M. Van Noordwijk, S. Kandji, T. Tomich, C. Ong, A. Albrecht, J. Mackensen, C. Bantilan, K. V. Anupama, and C. Palm. 2007. Climate change: linking adaptation and mitigation through agroforestry. Mitigation and Adaptation Strategies for Global Change **12**:901-918.

Vergeynst, L. L., M. Dierick, J. A. N. Bogaerts, V. Cnudde, and K. Steppe. 2015a. Cavitation: a blessing in disguise? New method to establish vulnerability curves and assess hydraulic capacitance of woody tissues. Tree Physiology **35**:400-409.

Vergeynst, L. L., M. G. Sause, M. A. Hamstad, and K. Steppe. 2015b. Deciphering acoustic emission signals in drought stressed branches: the missing link between source and sensor. Frontiers in Plant Science **6**:494.

Vergeynst, L. L., M. G. R. Sause, N. J. F. De Baerdemaeker, L. De Roo, and K. Steppe. 2016. Clustering reveals cavitation-related acoustic emission signals from dehydrating branches. Tree Physiology under revision.

Viisteensaari, J., S. Johansson, V. Kaarakka, and O. Luukkanen. 2000. Is the alien tree species Maesopsis eminii Engl.(Rhamnaceae) a threat to tropical forest conservation in the East Usambaras, Tanzania? Environmental Conservation **27**:76-81.

Wang, K., S. Kellomäki, and K. Laitinen. 1995. Effects of needle age, long-term temperature and CO2 treatments on the photosynthesis of Scots pine. Tree Physiology **15**:211-218.

Washington, R., R. James, H. Pearce, W. M. Pokam, and W. Moufouma-Okia. 2013. Congo Basin rainfall climatology: can we believe the climate models? Philosophical Transactions of the Royal Society B: Biological Sciences **368**:20120296.

Wheeler, J. K., B. A. Huggett, A. N. Tofte, F. E. Rockwell, and N. M. Holbrook. 2013. Cutting xylem under tension or supersaturated with gas can generate PLC and the appearance of rapid recovery from embolism. Plant, Cell & Environment **36**:1938-1949.

Whitlow, T. H., N. L. Bassuk, and D. L. Reichert. 1992. A 3-year study of water relations of urban street trees. Journal of Applied Ecology:436-450.

Wilhite, D. A. and M. H. Glantz. 1985. Understanding: the drought phenomenon: the role of definitions. Water international **10**:111-120.

Williams, C. A., N. P. Hanan, J. C. Neff, R. J. Scholes, J. A. Berry, A. S. Denning, and D. F. Baker. 2007. Africa and the global carbon cycle. Carbon Balance and Management **2**:1-13.

Willis, K., K. D. Bennett, S. Burrough, M. Macias-Fauria, and C. Tovar. 2013. Determining the response of African biota to climate change: using the past to model the future. Philosophical Transactions of the Royal Society B: Biological Sciences **368**:20120491.

Xu, J. Z., Y. M. Yu, S. Z. Peng, S. H. Yang, and L. X. Liao. 2014. A modified nonrectangular hyperbola equation for photosynthetic light-response curves of leaves with different nitrogen status. Photosynthetica **52**:117-123.

Ye, Z.-P. 2007. A new model for relationship between irradiance and the rate of photosynthesis in *Oryza sativa*. Photosynthetica **45**:637-640.

Ye, Z.-P., D. J. Suggett, P. Robakowski, and H.-J. Kang. 2013. A mechanistic model for the photosynthesis–light response based on the photosynthetic electron transport of photosystem II in C3 and C4 species. New Phytologist **199**:110-120.

Zeppel, M. J. B., J. D. Lewis, B. Chaszar, R. A. Smith, B. E. Medlyn, T. E. Huxman, and D. T. Tissue. 2012. Nocturnal stomatal conductance responses to rising [CO2], temperature and drought. New Phytologist **193**:929-938.

Zeppel, M., J. Lewis, N. Phillips, and D. Tissue. 2014. Consequences of nocturnal water loss: a synthesis of regulating factors and implications for capacitance, embolism and use in models. Tree Physiology **34**:1047-1055.

Zhou, L., Y. Tian, R. B. Myneni, P. Ciais, S. Saatchi, Y. Y. Liu, S. Piao, H. Chen, E. F. Vermote, C. Song, and T. Hwang. 2014. Widespread decline of Congo rainforest greenness in the past decade. Nature **509**:86-90.

Zimmermann, M. 1983. Xylem structure and the ascent of sap. Springer, Berlin.

Zuidema, P. A., P. J. Baker, P. Groenendijk, P. Schippers, P. van der Sleen, M. Vlam, and F. Sterck. 2013. Tropical forests and global change: filling knowledge gaps. Trends in plant science **18**:413-419.

Zwieniecki, M. A. and N. M. Holbrook. 2009. Confronting Maxwell's demon: biophysics of xylem embolism repair. Trends in plant science **14**:530-534.

Curriculum Vitae

Personal information
Name: Jackie Epila
Date of birth: 18th January 1983
Place of birth: Apala (Uganda)
Tel: +32483103116
Email: Jackie.Epila@UGent.be or epilajackie@yahoo.co.uk

Education and training
• October 2012-December 2016: PhD student, Ghent University, Belgium. PhD thesis: Ecophysiological assessment of drought vulnerability of the African tropical tree species *Maesopsis eminii* Engl..
• 2012-2015: Doctoral school specialist and transferable skills training programs in: Tropical forestry, Land information systems, Meteorology and climatology, effective oral presentations, creative thinking, report writing, communication skills basics and conflict handling.
• 2010-2012: MSc. Environmental Sanitation (Great Distinction), Ghent University, Belgium.
• 2004-2007: BSc. Industrial Chemistry (2nd Class Honors-Upper Division), Makerere University, Uganda.
• 2006: Industrial training at National Water and Sewerage Corporation, Kampala, Uganda.
• 1998-2003: Secondary School, Nabisunsa Girls' S.S., Kampala Uganda.
• 1997: Lira Parents Primary School, Lira, Uganda.
• 1990-1996: Apia lower, Middle and Upper Schools and, Leififi Intermediate School, Apia, Western Samoa.
• 1989-1990: Buganda Road Primary School, Kampala Uganda.

Scholarships and grants
• October 2016-December 2016: UGent PhD Scholarship, Belgium; PhD in Applied Biological Sciences.
• October 2012-mid-July 2016: VLIR-UOS ICP PhD Scholarship, Belgium; PhD in Applied Biological Sciences.
• 2013: Research fund for pre-doctoral researchers (CWO-fund) to travel to London, UK.
• 2013: Parkyn Bursary, British Ecological Society, United Kingdom.
• 2011: VLIR-UOS South to South travel grant (declined).
• 2010-2012: VLIR-UOS ICP Masters' Scholarship, Belgium.
• 2004-2007: Government Scholarship, Uganda.
• 2002: Nabisunsa Girls' School best performer bursary UCE-UNEB, Uganda.

Scientific output (peer-reviewed journals)
• Reyer C, Brouwers N, Rammig A, Brook B, **Epila J**, Grant RF, Holmgren M, Langerwisch F, Leuzinger S, Lucht W, Medlyn B, Pfeiffer M, Steinkamp J, Vanderwel M, Verbeeck H, Villela D (2015). Forest resilience and tipping points at different spatio-temporal scales: approaches and challenges. Journal of Ecology 103: 5-15.

• **Epila J**, Maes WH, Verbeeck H, Van Camp J, Okullo JBL, Steppe K (2016). Plant measurements on African tropical *Maesopsis eminii* seedlings contradict pioneering water use behaviour. Journal of Environmental and Experimental Botany (accepted).

• **Epila J**, Hubeau M, Steppe K (2016). Photosynthesis and photoassimilate distribution in ^{11}C-labelled leaves reveal an unexpected carbon strategy in the African tropical tree species *Maesopsis eminii* Engl. (written).

• **Epila J**, Verbeeck H, Otim-Epila T, Okullo P, Kearsley E, Steppe K (2016). The ecology of *Maesopsis eminii* Engl. in tropical Africa. Journal of African Ecology (accepted).

• **Epila J**, De Baerdemaeker NJF, Vergeynst LL, Maes WH, Beeckman H, Steppe K (2016). Capacitive water release and internal leaf water relocation delay drought-induced cavitation in African *Maesopsis eminii*. Tree Physiology (accepted).

Participations and presentations at conferences, symposia, workshops or briefings

• **Epila J**, Verbeeck H, Okullo JBL, Steppe K. 2013. Drought vulnerability and resilience of *Maesopsis eminii*. 11th INTECOL Congress 2013, British Ecological Society. Excel London, UK. 18-23 August 2013 (oral presentation).

• **Epila J**, Maes WH, Verbeeck H, Van Camp J, Okullo JBL, Steppe K. 2015. Physio-morphological growth dynamics of equatorial *Maesopsis eminii* seedlings indicate drought stress vulnerability and resilience. Wood science underpinning tropical forest ecology and management: International closing symposium of the XYLAREDD project. Royal Museum for Central Africa (Tervuren, Belgium). 26- 29 May 2015 (oral presentation).

• **Epila J**, Hubeau M, De Baerdemaeker NJF, Verbeeck H, Okullo JBL, Steppe K. 2015. The non-food tree crop *Maesopsis eminii* Engl. investigated with PET and AE: A case of technology transfer. 9th Belgian Plant Biotechnology Association symposium (BPBA), Royal Library Brussels, Belgium. 13th November 2015 (poster presentation).

• **Epila J**, De Baerdemaeker NJF, Hubeau M, Beeckman H, Verbeeck H, Okullo JBL, Steppe K. 2015. Combining AE, PET and Microscopy to understand drought-stress responses of Africa's tropical forests: A case study of Ugandan *Maesopsis eminii* Engl. seedlings. 9th Symposium of the Ghent Africa Platform, Koninklijke Academie voor Nederlandse Taal en Letterkunde, Koningstraat Gent, Belgium. 17th December 2015 (poster presentation).

Educational activities

• 2013-2014: Tutor of a Master's student, Janne van Camp. Thesis title: Linking plant-water relations to wood anatomical features of *Maesopsis eminii* under different water conditions to assess its drought resilience.

• 2013: Participated in proposal write up for the North to South VLIR-UOS travel grant Janne van Camp received to travel to Uganda to conduct her Master Thesis: Linking plant-water relations to wood anatomical features of *Maesopsis eminii* under different water conditions to assess its drought resilience.

• 2010: Use of natural coagulants in domestic and industrial effluent treatment, Uganda.

• 2008-2010: Research and Development of *Jatropha carcus* biodiesel in Uganda.

• 2009: Data collection of waste oil use and recycle, disposal, treatment, capacity generated annually, possible spillages, consulting waste oil handlers in Uganda and data analysis.

• 2008-2009: Physiochemical analysis and life cycle assessment of *Jatropha carcus*.

Professional experiences

• 09/03/2015: Participated in overseeing an exercise on climates of the earth group work for Physical Land Resources and Environmental Sanitation Master's students.

• 26/01/2015: Supervision of Terrestrial Ecology Examinations.

• 2010-2012: Student representative and core group member at the Centre for Environmental Science and Technology (CES&T) Ghent University, Belgium.
• 2008-2010: Research Scientist at African Power Initiative Ltd (API), Uganda.
• 2007-2008: Data Clerk at the United Nations High Commissioner for Refugees (UNHCR), Uganda.
• 2007: Chemist at Kampala Pharmaceuticals Industries Ltd, Uganda.

Skills
• Microsoft Office (Word, Excel and PowerPoint), Plant Eco-physiology, basic GIS and R-statistics, EIA, ERA and abatement of air and water pollution, Languages (English, basic French, Basic Dutch and Luo), Effective communication and leadership skills.

Memberships
• 2010-2016: Member of Ghent Student's Network (GSN) and International Students at Gent (ISAG)
• 2015-2016: Member of the Belgian Plant Biotechnology Association (BPBA).
• 2012-2016: Member of the Gent University's Faculty of Bioscience Engineering Academic Club.
• 2012-2016: Member of OBSG
• 2013-2014: Member of the British Ecological Society (BES).